

Mass Properties Testing and Evaluation for the Multi-Mission Radioisotope Thermoelectric Generator

Frank S. Felicione

December 2009



The INL is a U.S. Department of Energy National Laboratory
operated by Battelle Energy Alliance

Mass Properties Testing and Evaluation for the Multi-Mission Radioisotope Thermoelectric Generator

Frank S. Felicione

December 2009

**Idaho National Laboratory
Idaho Falls, Idaho 83415**

<http://www.inl.gov>

**Prepared for the
U.S. Department of Energy
Office of Nuclear Energy
Under DOE Idaho Operations Office
Contract DE-AC07-05ID14517**

DISCLAIMER

This information was prepared as an account of work sponsored by an agency of the U.S. Government. Neither the U.S. Government nor any agency thereof, nor any of their employees, makes any warranty, expressed or implied, or assumes any legal liability or responsibility for the accuracy, completeness, or usefulness, of any information, apparatus, product, or process disclosed, or represents that its use would not infringe privately owned rights. References herein to any specific commercial product, process, or service by trade name, trade mark, manufacturer, or otherwise, does not necessarily constitute or imply its endorsement, recommendation, or favoring by the U.S. Government or any agency thereof. The views and opinions of authors expressed herein do not necessarily state or reflect those of the U.S. Government or any agency thereof.


INTENTIONALLY BLANK

Mass Properties Testing and Evaluation for the Multi-Mission Radioisotope Thermoelectric Generator

INL/EXT-09-17458
Revision 0

December 2009


Approved by:



Frank S. Felicione
Subject Matter Expert

01/06/2010

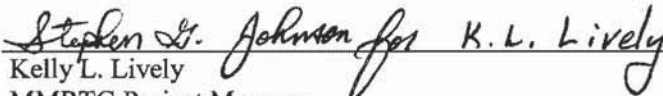
Date



Drake C. Kirkham
Quality Assurance

1/6/10

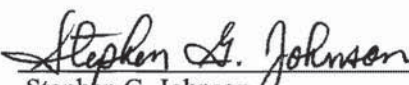
Date



Kelly L. Lively
MMRTG Project Manager

1/6/10

Date



Stephen G. Johnson
RPS Program Manager

1/6/10

Date

INTENTIONALLY BLANK

CONTENTS

ACRONYMS.....	x
1. SUMMARY	1
2. INTRODUCTION AND BACKGROUND	2
3. MOUNTING CONSIDERATIONS	3
4. LEVELING THE MP INSTRUMENT	5
5. CALIBRATION OF THE MP INSTRUMENT	5
6. MOUNTING FIXTURE INSTALLATION/ALIGNMENT	5
7. BALANCING THE MOUNTING FIXTURES	6
8. METROLOGICAL MEASUREMENTS TO RELATE THE MP INSTRUMENT AND TEST ARTICLE COORDINATE SYSTEMS.....	7
8.1 Alignment Measurements Along the X Axis	7
8.2 Alignment Measurements Along the Y Axis	8
8.3 Alignment Measurements Along the Z Axis	9
8.4 Tilt Considerations	9
8.4.1 Linear Offsets of the MP Instrument and Test Article Coordinates	10
8.4.2 Rotational Offsets	11
9. CG MEASUREMENTS	13
9.1 Accuracy and Repeatability	14
9.2 Measurement Sensitivity	17
9.3 Moment Measurements Using the Space Electronics Instrument.....	18
9.4 Test article Weight and CG Uncertainty	20
9.5 Measurement Results	22
10. TEMPERATURE CHANGES IN THE MOUNTING FIXTURES	22
10.1 General Thermal Considerations.....	23
10.2 Evaluation of Fixture Temperature Variation	24
11. COORDINATES TRANSLATION	27
12. SUMMARY AND CONCLUSIONS	28
12.1 Uncertainties Summary	29
12.2 Conclusions	29
13. REFERENCES	29

Appendix A INL Mass Properties Testing System Drawings List	71
Appendix B Geometric Constructions for Determining Offsets of the Coordinate Systems	75
Appendix C Specific Measurement System Output – Mass Standard	85
Appendix D Fixture Temperature Maps	97
Appendix E Temperature Induced CG Corrections	105
Appendix F Geometry Calculations.....	109
Appendix G Metrology Data Sheets and Data Reduction	113
Appendix H Data Sheet – Weigh Scale Calibration Check	127
Appendix I Measurement System Output – MMRTG.....	129
Appendix J MMRTG Weighing Record.....	135

FIGURES

Figure 1. Leveling the MP instrument	41
Figure 2. Equipment setup for calibrating the MP instrument.....	41
Figure 3. MP instrument calibration report.....	42
Figure 4. MP Mark-II mounting fixtures (mass standard shown installed)	43
Figure 5. Mark-II (aluminum) adapter ring	44
Figure 6. Coordinate systems and test positions	45
Figure 7. Final level checking of the MP mounting fixtures	46
Figure 8. Precision transit setup for alignment determination	47
Figure 9. Determining offsets of coordinate systems.....	48
Figure 10. Typical view of lower alignment pin through precision transit.....	48
Figure 11. Determining offsets of test article relative to MP instrument.....	49
Figure 12. Auxiliary alignment flange (pin detail superimposed)	50
Figure 13. Rotational alignment of the test article and MP instrument	51
Figure 14. Oblique viewing angles to determine the Y offset of the test article coordinates	52
Figure 15. Oblique perspective to determine Y offset	53
Figure 16. Typical construction to determine ΔY	54
Figure 17. Tilt geometry model in X-Z view (exaggerated).....	55
Figure 18. Mass standard column	56
Figure 19. Mass standard base flange	57
Figure 20. Pro-E software determination of CG in the mass standard.....	58

Figure 21. Mk-II (aluminum) adapter ring alignment features	59
Figure 22. Measured CG location and confidence intervals for the mass standard	60
Figure 23. Thermal effects after mounting the MMRTG	61
Figure 24. Expansion/contraction changes after rotation to Position No. 2.....	62
Figure 25. Temperature distributions in the rotation fixture (see temperature maps, Appendix D)	63
Figure 26. Key dimensions for the mounting fixtures and the test article CG position	64
Figure 27. Alignment geometry, isometric views (see Figures 28 & 29)	65
Figure 28. Alignment geometry, overhead views, X-Y, Position No. 1	66
Figure 29. Alignment geometry, elevation views	67
Figure 30. Tilt Analysis: X-Z Elevation View.....	68
Figure 31. Tilt analysis: Y-Z Elevation View.....	69

TABLES

Table 1. Balancing the Mounting Fixtures.....	30
Table 2. Metrology Summary for the Mass Standard.....	31
Table 3. Measurement Calculations and Predicted Values	32
Table 4. Parametric Evaluation of CG Uncertainty Contributors	33
Table 5. Confidence Intervals for PART and TARE Measurements.....	34
Table 6. Mass Properties Data and Calculations.....	35
Table 7. Adjustments for Temperature Changes, (Spreadsheet E-1), Room Temp > Pre-test (Map K-2).....	36
Table 8. Adjustments for Temperature Changes, (Spreadsheet E-2), Room temp > Pre-tare (Map K-6).....	38
Table 9. Spreadsheet B-1 - Y Offset Constructions Characteristics	40

INTENTIONALLY BLANK

ACRONYMS

A	Designator
ASTM	American Society for Testing Materials
B	Designator
B209	ASTM material configuration designator
B211	ASTM material configuration designator
CG	Center of gravity
C	Fixture alignment hole designator
D	Fixture alignment hole designator
F	Fahrenheit
G	Fixture alignment hole designator
GPHS	General Purpose Heat Source
H	Fixture alignment hole designator; or overall length of the mass standard
I	Fixture alignment hole designator
INL	Idaho National Laboratory
L	Length, defined by Figure 26
M	Moment
Mk	Mark (version indicator)
MMRTG	Multi-Mission Radioisotope Thermoelectric Generator
MOI	Moment of inertia
MP	Mass properties
MS	Mass standard
MSL	Mars Science Laboratory (Mission)
N	Upper limit number
NIST	National Institute of Standards and Technology
NW	Northwest
P	Length of locating pin; or offset of MS locating pin from cradle pin, defined in Figures 14 and 16
PWR	Pratt&Whitney Rocketdyne Co.
R	Position measured from test article's origin
RTG	Radioisotope Thermoelectric Generator
s^2	Estimate variance of a population
SSPSF	Space and Security Power Systems Facility
SW	Southwest
S/N	Serial number

T	Temperature
t	Statistics distribution (a.k.a. Student's t)
V	View
W	Weight
X	Coordinate direction
Y	Coordinate direction
y	Data value
Z	Coordinate direction

Subscripts

AR	Adapter ring
a	Ancillary [items during weighing]
bar	Indicates arithmetic average
BE	Best estimate
C	Cradle
CG	Center of gravity (center of mass)
ex	Excess
g	Gross [weight]
i	Counting index
j	Counting index
L	Lower locating pin
MS	Mass Standard
O	Offset
p	Part
pin	Alignment pin
R	Rotation fixture
SE	Space Electronics (Co.)
t	Tare
TA	Test article
U	Upper locating pin

X	Coordinate direction
XY	Projection onto the X-Y plane
XZ	Projection onto the X-Z plane
YZ	Projection onto the Y-Z plane
0	Base measurement; or referenced to test article's coordinate system origin
2	Indicates measurement made while in Position No. 2 (see Figure 26)

Superscripts

+	Positive side
-	Negative side
'	Alternate value; or referenced to mounting fixtures' coordinates
"	Referenced to test article's coordinates

Greek Symbols

α	Coefficient of thermal expansion
β	Angle, defined by Figure 27
Δ	Difference indicator
δ	Difference indicator
η	Mean value of a distribution
θ	Angle, defined by Figure 27
Φ	Angle, defined by Figure 27
ν	Degrees of freedom (equals N-1)
ξ	Angle, defined by Figure 27

INTENTIONALLY BLANK

Mass Properties Testing and Evaluation for the Multi-Mission Radioisotope Thermoelectric Generator

1. SUMMARY

Mass properties (MP) measurements were performed for the Multi-Mission Radioisotope Thermoelectric Generator (MMRTG), serial number (S/N) 0X730401, the power system designated for the Mars Science Laboratory (MSL) mission. Measurements were made using new mounting fixtures at the mass properties testing station in the Idaho National Laboratory (INL) Space and Security Power Systems Facility (SSPSF). The objective of making mass properties measurements was to determine the generator's flight configured mass and center of mass or center of gravity (CG). Using an extremely accurate platform scale, the mass of the as-tested generator was determined to be 100.117 ± 0.007 lb. Weight accuracy was determined by checking the platform scale with calibrated weights immediately prior to weighing the MMRTG.^a

CG measurement accuracy was assessed by surrogate testing using an inert mass standard for which the CG could be readily determined analytically. Repeated testing using the mass standard enabled the basic measurement precision of the system to be quantified in terms of a physical confidence interval about the measured CG position. However, repetitious testing with the MMRTG itself was not performed in deference to the gamma and neutron radiation dose to operators and the damage potential to the flight unit from extra handling operations. Since the mass standard had been specially designed to have a total weight and CG location that closely matched the MMRTG, the uncertainties determined from its testing were assigned to the MMRTG as well. On this basis, and at the 99% confidence level, a statistical analysis found the direct, as-measured MMRTG-MSL CG to be located at 10.816 ± 0.0011 in. measured perpendicular from the plane of the lower surface of the generator's mounting lugs (Z direction), and offset from the generator's long axis centerline in the X and Y directions by 0.0968 ± 0.0040 in. and 0.0276 ± 0.0026 in., respectively.

These uncertainties are based simply on the statistical treatment of results from repetitive testing performed with the mass standard and included position variations that may have occurred during several mounting/dismounting operations of both the mass standard and mounting fixtures. Because of the limited data available, the computed uncertainty intervals reported are likely, although not assuredly, wider than the intervals that would have been found had more extensive data been available. However, these uncertainties do not account for other contributors to measurement uncertainty that might be applicable. These include potential weighing errors, possible tilt of the as-mounted test article, or translation of the measurement results from the MP instrument coordinates to those of the test article. Furthermore, when testing heat producing test articles such as the MMRTG, measurement degradation can occur from thermal expansion/contraction of the mounting fixtures as they heat up or cool and cause a subtle repositioning of the test article. Analyses for such impacts were made and additional uncertainty allowances were conservatively assigned to account for these. A full, detailed description is provided in this report.

^a A record of the weigh-scale calibration check is provided in Appendix H.

After taking into account all additional potential sources of uncertainties, the best estimated, as-tested CG, relative to the MMRTG-based coordinate system, was conservatively determined to be centered at the measured, mean position of

$$X = 0.0968 \text{ in.}$$

$$Y = 0.0276 \text{ in.}$$

$$Z = 10.816 \text{ in.}$$

within a spherical, overall confidence interval having a conservatively estimated radius of 0.018 in., i.e., 0.036 in. diameter. Although this overall confidence interval is not amenable to a definitive, quantitative evaluation, there remains a high expectation that these results continue to be at least at the 99% level. This confidence interval is more than an order of magnitude tighter than the 10 mm (0.394 in.) diameter, allowable spherical measurement uncertainty specified for the MSL mission (Ref. 1 and Ref. 2).

Adjustments to the CG position for certain hardware differences between the testing and MSL mission flight configurations will be made by the design agency, Pratt & Whitney Rocketdyne (PWR).

2. INTRODUCTION AND BACKGROUND

The MSL mission features a mobile platform (a surface-rover vehicle) that provides the support structure for various scientific experiments onboard. Electrical power for propulsion of the rover vehicle, as well as power for the experiments, is furnished by the MMRTG. The MMRTG is a ^{238}Pu powered thermoelectric generator, producing approximately 110 W of direct current, electrical power. Accurate knowledge of the mass properties of the spacecraft and all major equipment on board is important to ensure the flight dynamics of the spacecraft during its several months-long travel to the Mars surface are well understood so that adequate fuel for attitude control functions and maneuvering can be provided. The MMRTG weighs approximately 100 lb and is physically packaged a considerable distance from the spacecraft centerline. This is a significant mass whose mass properties need to be factored into the overall mass properties determination for the spacecraft. Because of the importance to the mission success, a quantitative assessment of the certainty of these properties was needed. This report provides a complete account of the measurements made and the methodology used to establish the confidence bounds on the mass properties data.

Measurement uncertainty contributors arise from the measurement repeatability and sensitivity characteristics of the MP instrument, mounting position errors and unavoidable mounting variation, mass determination, and data rounding errors. A statistical treatment of repeated measurement data from the mass standard was performed to determine the associated confidence interval. This document describes the alignment metrology, the determination of the final confidence intervals, and specifies the appropriate corrections required. The test data and analyses upon which the conclusions are based are also presented.

To fully deduce the mass properties of the MMRTG, two major support activities were undertaken. These activities were

1. determine the confidence interval associated with the mass properties measurement approach and equipment to ensure the data acceptability criterion specified by the prime contractor has been satisfied; and
2. determine the physical alignment of the test article relative to the MP instrument so as to accurately translate the measurement results from the MP instrument's reference frame to that of the MMRTG.

To address both of these topics a specially constructed, dead-weight simulator, herein referred to as the mass standard, whose total mass and CG location closely mimicked those of the MMRTG, was

constructed and tested. The simple geometry of the mass standard rendered its CG properties amenable to analysis. Favorable comparison of CG locations measured using the mass standard to those analytically determined provided a high degree of confidence in the ability of the MP instrument to accurately measure the basic mass properties of the flight generator.

An accurate knowledge of the physical position of the test article relative to the datum of the MP instrument is vital. This relationship is necessary because the MP instrument measures the CG (and moment of inertia, MOI, if it were to be performed) relative to its own datum and coordinates, whereas the spacecraft designers require these properties referenced to the mounting plane of the generator. The MMRTG does not have a handy, precision “target” from which an accurate physical relationship of the generator to the MP instrument could be readily measured. By equipping the mass standard with suitable locator features, the physical alignment could be conveniently and accurately measured.

Many close-in manipulations of the test article mounting are required to perform the multiple measurements needed to acquire a reasonable data population. Had the actual MMRTG been used to acquire the data these handling activities would have exposed personnel to significant gamma and neutron radiation doses. Instead, data gleaned from surrogate measurements on the mass standard were applied to the reduction of the actual MMRTG test data. These uncertainty estimates are, therefore, truly applicable only to static, rigid, room temperature items having a weight similar to the mass standard (approximately 100 lb). Application of the confidence intervals determined from the mass standard measurements to an elevated temperature test article such as the MMRTG cannot be assured off hand because of the potential for thermal expansion/contraction in the mounting fixtures. Special attention was paid to this issue to ensure the results remained valid. The measurements and analyses that provided this assurance are thoroughly described in this report.

The wider fins on the MMRTG and its bottom-only mounting configuration required fixtures that were entirely new and of a different design from those used previously. The primary motivation for developing the detailed uncertainty analyses reported herein was to establish the accuracy that could be anticipated using these new mounting fixtures in conjunction with MMRTG-sized and -configured test articles. The mounting fixtures used previously for MP testing were of an entirely different design and were about 100 lb. lighter than those for the MMRTG. The earlier test articles were also about 30% heavier than the MMRTG. Both weight aspects contributed to a more favorable “signal-to-noise” ratio for the earlier MP measurements as compared to testing with the current equipment. Many of the measurements reported in this document were only performed to assess the capabilities of the MP instrument to make accurate measurements under these new conditions.

Having established the quantitative confidence level reported here, future MP testing of similar weight test articles that use these same fixtures need not duplicate all of these checks; a much more streamlined assessment would suffice to confirm the continued confidence level of the measurements.

3. MOUNTING CONSIDERATIONS

The mounting configuration of the MMRTG differs from that of the General Purpose Heat Source Radioisotope Thermoelectric Generator (GPHS-RTG) series generators previously tested at the INL’s MP test station. The GPHS-RTG series generators included features that allowed them to be mounted at their mid-section during testing, although they were end mounted on the spacecraft. The MMRTG can only be end mounted via the four lugs (mounting feet) provided at the end opposite to the fueling access. The mounting fasteners comprise special socket-head machine screws inserted from underneath the fixture to which the generator is attached with washers and split, spring-loaded locking nuts installed on the generator side. Compared to the previous generators tested, this mounting configuration difference plus the wider dimensions of the heat rejection fins on the MMRTG necessitated the construction of new mounting fixtures to accommodate the MMRTG on the MP instrument. These new fixtures were designated the Mark-II (“Mk-II”) MP mounting fixtures to contrast those fixtures used with the GPHS-RTG series generators.

The MP instrument measures the CG and/or the MOI of all equipment, fixtures, fasteners, and test article(s) mounted on it relative to its own reference frame.^b The origin of the MP instrument's reference frame is centered on its axis of rotation and on the surface of the instrument's interface plate, a surface having features that allow attaching test specific hardware. A tare measurement made in the absence of the test article, but with all of the equipment other than the test article in their same positions enables the influence of these items alone to be measured and then analytically deducted by the Space Electronics Co. software. Thereafter, the results pertain only to the MP of the test article itself, but these properties are still referenced to the MP instrument's coordinate system. The design agency requires that these properties be referenced to the coordinate system established for the test article itself. For the MMRTG the coordinate system datum is at the center of an imaginary plane that contacts the bottom of its four mounting lugs. An accurate translation of the measurement data to this coordinate system was a major consideration of the MP testing.

Two alternate approaches could be employed to handle the coordinate system translation. Physical adjustment features can be included in the design of the fixtures that allow shifting the test article until the coordinate systems axes are coincident in one or more coordinate directions or the actual offsets can be measured and then analytically accounted for in the measurement translation. A combination of these two approaches was used with the mounting fixtures for the previously tested GPHS-RTG units, such as the F-8 generator, which provides electrical power for the Pluto/New-Horizons mission, launched in January, 2006 and is currently enroute to Pluto. A mechanism was provided in the GPHS-RTG fixtures that allowed shifting the test article's position along the X axis of the MP instrument until the origin of the test article, when projected onto the interface plate of the MP instrument, was coincident to that of the MP instrument. The Z coordinate (long axis) offset, however, was measured and then used to analytically translate the CG measurement along this axis to the reference plane of the test article. The fixed, small offset (2 to 3 thousandths of an inch) along the MP instrument's Y axis was, in principle, also analytically correctable, but in practice was simply accepted. Vertical tilt of the F-8 generator was carefully measured and the measured CG location was then analytically adjusted to account for any tilting.

Although adjustable positioning simplifies interpreting the test data, it requires a more complex mounting design and makes for more tedious, time consuming configuration. For the radioactive RTGs, manipulating adjustable mountings subjects personnel to considerable radiation dose. The Mk-II mounting fixtures for end-mounted RTGs were therefore designed without any field adjustable features. In order to analytically translate the measured mass properties to the test article's reference frame, the precise offset of the test article's origin relative to that of the MP instrument origin must be provided by the user. Furthermore, any angular or tilted orientation or physical shift of the test article's reference frame must be accounted for off-line and appended to the reported measurement results.

The test article's coordinate system must be orthogonal. Mounting the device such that two of its axes form a plane that is parallel to the surface of the MP instrument interface plate simplifies the measurement; otherwise orientation of the test article's axes is not restricted. The coordinate systems for both the MP instrument and for the test article may be expressed in either Cartesian or polar coordinates. Once the relationship of the coordinate systems has been specified, the MP instrument software can report the measurement results relative to both the MP instrument as well as to the test article. These results are expressed in both Cartesian and polar coordinate systems.

^b MOI properties for the MMRTG were to be estimated analytically by PWR therefore they were not measured by INL.

4. LEVELING THE MP INSTRUMENT

The MP instrument measures the offsets of the test article in the horizontal plane, i.e., perpendicular to the gravity field. The instrument can neither sense nor compensate for a vertical tilt of the test article; such corrections for any tilt require a manual correction to the measurement results. Providing a level instrument surface to ensure a plumb mounting to begin with simplifies any post-test data adjustments.

The MP instrument interface plate is the horizontal surface upon which the test article and/or mounting fixtures are attached, and is the surface to be leveled. Its level was checked with a Starrett Instruments precision, calibrated level. By making repetitive, very small adjustments to the MP instrument's leveling pads, a very high degree of leveling was achieved. The smallest markings on the precision level used represent 0.0005 in. over a 12 in. span, allowing a credible resolution of 0.00025 in. over this span. Final leveling of the leveling pads on the MP instrument was made to achieve the interface plate level to within 0.00025 in/ft. The photograph in Figure 1 shows the setup and typical level achieved.

5. CALIBRATION OF THE MP INSTRUMENT

Prior to using the MP instrument, a calibration is required. A process has been developed by the instrument manufacturer, Space Electronics Co., to accomplish this calibration in the field. A special calibration beam and two calibration weights are supplied by the instrument manufacturer for calibration. The beam has locating features for accurate positioning on the MP instrument and for placement of the calibration weights. The weights themselves carry a current National Institute of Standards and Technology (NIST)-traceable calibration. The process requires fastening the beam onto the interface plate, placing the weights on the beam according to a programmed schedule as instructed by software prompts, and executing the calibration routine. The measurement is then automatically compared to the theoretical value provided by the Space Electronics software to generate a calibration constant that is subsequently applied by the software to the measurements. An internal check compares the calibration constants to an acceptable range and indicates if the calibration is acceptable. Figure 2 depicts the calibration setup. A typical calibration report is included as Figure 3.

6. MOUNTING FIXTURE INSTALLATION/ALIGNMENT

The Mk-II MP mounting fixtures are comprised of three major components. The Cradle Assembly ("cradle") forms the base of the fixtures and is fastened directly to the MP instrument's interface plate. Pivoting on two upright members of the cradle is a second assembly, the Rotation Fixture. By attaching the test article to this fixture, the test article can be positioned either vertically or horizontally relative to the MP instrument. This is necessary to obtain the third component of the CG location. Position No. 1 refers to orienting the test article so that its long axis is vertical. Orientation of the test article with its long axis horizontal is referred to as Position No. 2. The test article is attached to the rotation fixture via a suitable adapter which, for the MMRTG, is the Mk-II Adapter Ring ("aluminum adapter ring"). Construction of all three mounting fixture components includes features intended to help ensure the precise, predictable, and highly repeatable positioning of the test article when mounted on the MP instrument. INL drawings 751208 and 751210, included in this report as Figures 4 and 5 respectively, depict these fixtures^c. Figure 6 depicts the configuration for Positions No. 1 and No. 2 during the testing.

^c Appendix A lists all of the INL drawings that pertain to the MP testing system.

Despite the utmost care in their fabrication and handling, minor distortions in the flatness of the cradle, rotation fixture, and adapter ring collectively degrade the overall level when stacked upon the MP instrument interface plate. Figure 7 shows the final level achieved at the top of the adapter ring mounting slides (see INL Drawing 751215 for mounting slide details). The majority of the non-level condition is traceable primarily to a very slight distortion in the flatness of the rotation fixture base.

The upper surfaces of the mounting slides provide the actual support surface for the test article. The high point is the northwest (NW) mounting slide, Slide C, while the low point is the adjacent, southwest (SW) mounting slide, Slide D, with an overall level gradient measured directly between these two mounting slides of 0.0015 in./ft. Since the span between these two mounting slides is nominally only 7.85 in., the actual elevation difference Δ is proportionately less, viz.,

$$\Delta = 0.0015 \text{ in./ft.} * \frac{7.85 \text{ in.}}{12 \text{ in./ft.}} = 0.000981 \text{ in.}$$

This elevation difference creates a slight, induced tilt of the test article toward the south and west. This tilt is in addition to whatever inherent non-perpendicularity may be present in the test article itself. It is noted from Figure 7 that the net height difference computed when tracked around from the SW mounting slide to the NW mounting slide by traversing the adapter ring counter-clockwise, as viewed from above, is also 0.0015 in./ft, or 0.000981 in. When compared to the measurements across the diagonals, however, there is an apparent discrepancy of 0.00025 in./ft. However, when the actual spans are taken into account, the comparison of these measurements shows the actual elevation discrepancy to be only 0.0000281 in. This is well within the limiting accuracy of the precision level. For the purposes of this report, the elevation difference of 0.000981 in. is used. The discussion in Section 8.4 addresses adjustments to the measured CG position to account for this small, induced tilt characteristic.

7. BALANCING THE MOUNTING FIXTURES

The effects of any imbalance in the fixtures and/or test article on the measurements are canceled when the tare is made and the final test article CG calculations are performed. However, the accuracy of the final computations is increasingly degraded as imbalances in the mounted equipment become larger. Although the mounting fixtures are symmetrical by design, small issues such as minor dimensional variation among corresponding components, members, or the variation in the sizes of weld beads, etc. can affect the balance. A small brass trim weight having a mass of 0.472 lb was fabricated to compensate for fixture imbalance. The trim weight was positioned by trial and error to minimize the residual imbalance.

Based on operational experience, a maximum imbalance acceptance criterion of 0.75 in.-lb for each of the X and Y axes was stipulated. Table 1 shows the progressive improvement in the balance of the fixtures during a typical balancing session. As typified by this record, the final balance achieved was always considerably better than the acceptance criterion.

8. METROLOGICAL MEASUREMENTS TO RELATE THE MP INSTRUMENT AND TEST ARTICLE COORDINATE SYSTEMS

Offset measurements of the test article coordinate system datum relative to the MP instrument datum are needed to translate the measurements from the MP instrument coordinates to those of the test article. The offsets were determined by metrological measurements using a precision optical transit equipped with a micrometer viewer, as shown in Figure 8 and sighting accurately located precision target points. The transit used was a Brunson Optical Transit, Model 76RH, equipped with a Model 160 optical micrometer viewer. The transit was set up approximately 8 ft from the MP instrument and carefully leveled. The setup is depicted in Figure 9. A measurement resolution of approximately 0.001 in. can be routinely detected over this viewing distance. Precision, conical alignment pins were accurately placed at various positions on the equipment, as depicted in Figure 9. The sharp tips of these pins were targeted in the eyepiece of the transit. Figure 10 shows a typical view of such a pin in the transit. The pin shown in the photograph has a 1.125 in. diameter and the as-viewed spacing between the double lubber lines corresponds to a span of about 0.001 in.

Alignment was determined by measuring the lateral distances between pairs of alignment pins with the transit micrometer. One such pin was placed in the center hole (hole D)^d of the cradle fixture and another pin along the Y coordinate (hole G)^e. These holes are the same ones used to properly locate the cradle on the MP instrument using very close tolerance T-handle locating pins (cf., Figure 4). These peripheral holes are nominally 10 in. from the center pin and on the principal axes. During the optical alignment operations the MP instrument precision locating pins (Figure 9) actually penetrated the locator holes in both the cradle base and the MP instrument's interface plate, confirming the continued alignment of the cradle fixture to the MP instrument. The transit was focused on the tip of the pin in the center of the cradle base. The MP instrument was rotated while the center pin was observed in the transit. The sharp pointed locating pin rotated without any visible wobble, appearing to be perfectly stationary when viewed in the transit. This established that the tip of the center pin was very accurately aligned with the axis of rotation.

8.1 Alignment Measurements Along the X Axis

The transit line of sight was aligned with the Y axis of the cradle by viewing both the center locating pin and the locating pin on the Y axis. This established that the view was truly parallel to the Y axis and perpendicular to the X axis of the cradle and MP instrument. Another precision pointed locating pin was placed in the tapped hole in the center of the mass standard base protruding downward, as depicted in Figure 9. The pin featured a deliberately loose, 1 in. diameter, 8 threads/in. screw thread for attaching the pin. Accurate centering of the locating pin was achieved by providing a very snug fit to the inner cylindrical surface of a precision countersink centered on the mass standard's axis. Comparing the position of the tip of this pin to the position of the tip of the upward protruding pin in the cradle base revealed any lateral offset of the aluminum adapter ring centerline from the MP instrument's centerline in the direction perpendicular to the viewing direction as shown in Figure 11.

^d Locations of all alignment holes are shown in Figure 11.

^e Locations of all alignment holes are shown in Figure 11.

The alignment described above does not ensure that the horizontal coordinates of the test article are also oriented parallel to those of the MP instrument. To check this, an auxiliary alignment flange, Figure 12 (ref. Drawing 760957), was manufactured and mounted onto the aluminum adapter ring using the same type of precision, snug-fitting titanium shoulder screws that were used to mount both the MMRTG and the mass standard. Two small, upward pointing, slip-fit alignment pins on either end of a diameter along the carefully laid out Y axis of this flange were provided. A central threaded countersunk hole allowed the same lower precision locating pin that was used with the mass standard to be attached, pointing downward. The transit was positioned to allow sighting along the cradle's Y axis, as described previously. The transit was then shifted laterally to sight the downward pointing alignment pin to compensate for whatever small X offset was measured in the centerlines of the mass standard and the MP instrument. The nearer of the two alignment pins protruding upward in the flange was then focused in the transit, the micrometer zeroed, and the view adjusted to measure any offset in the upward pointing pin on the opposite (far) side of the flange. This would reveal any rotational misalignment of the aluminum adapter ring and/or test article. A simple geometric construction, as shown in Figure 13, would quantify any angular misalignment relative to the MP instrument's horizontal axes. In fact, no angular misalignment of this flange was discernable.

8.2 Alignment Measurements Along the Y Axis

Determining the alignment between the MP instrument and test article along the X axis in both Positions No. 1 and No. 2 as described in the previous paragraphs is quite straightforward. In principle, determining the alignment along the Y axis can be performed similarly. However, when in Position No. 1 the construction of the cradle fixture causes the determination of the Y offset to be more complicated. The outrigger members of the cradle obscure the view of the axial locating pins when the transit view is directed along the X axis. A view somewhat oblique to the X axis is required. Figure 14 depicts the positions of the fixture and test article locating pins relative to the viewing direction during this measurement. There is only a narrow viewing angle, between about 16.5° and 19° off of the X axis, for which the cradle centerline locating pin and both the lower and upper locating pins in the mass standard can be viewed through the transit in a vertical plane. Using a trial and error process, the assembly was rotated until a suitable view was found. Figure 15 shows a photograph of this process underway.

Stopping at an acceptable angle is tedious and time consuming. The assembly is supported by a precision air bearing and driven by a thin torque tube so the rotation angle cannot be manually positioned. Instead, the unit must be put into a test mode and during the instrument's rotation to the next measurement quadrant and the power must be shut off at just the right moment to catch this narrow viewing window. However, when the unit is stopped, the torsion drive unloads, causing the unit to oscillate for several minutes. Since the tilt of the test article could change very slightly when the pressure to the air support bearing is interrupted, the pressure must be left on to ensure accurate alignment measurements. Unloading the torsion drive returns the rotating assembly to its neutral position so that when the mounting fixtures finally come to rest, more likely than not the viewing angle will have been found to be unsuitable, making it necessary to repeat the process. Each repeat of the rotation cycle requires 6 – 7 minutes and 4 – 5 cycles may be required.

A drafting protractor that had been placed on the cradle oriented with its zero mark aligned with a line along the X axis could be sighted through the transit to detect the measurement angle on the lubber line. When the oscillations ceased and a suitable view had finally been achieved, the offsets of the locating pins were measured with the transit micrometer, and recorded. The viewing angle was read on the protractor and entered onto the data sheet. A geometric construction from these measurements then allowed the Y offsets for both the lower and upper locating pins to be computed. Figure 16 depicts an example of this construction.

Only a single view (Figure 14) is ostensibly required to calculate ΔY offset. However, taking the arithmetic average from multiple measurements using several of the four possible views enhances the accuracy. Appendix B provides the detailed geometric constructions for all four viewing angles. The constructions cover all of the 16 potential configurations. Each of the four views shown in Figure 14 has four possibilities: two of these refer to the relative position of the cradle centerline pin either near the viewer or away, as determined from the ΔX offset measurements and two refer to the lateral positions of the target pin relative to the cradle centerline pin as viewed either to the left of the cradle pin - Red scale on the micrometer, or to the right - Black scale. For example, if the relative positions of the pins were as depicted in Figure 14 the cradle center pin would be near the viewer in Views V_2 and V_3 but away from the viewer in Views V_1 and V_4 . In Views V_2 and V_3 the target pin would be to the left of the cradle pin whereas the target is to the right in Views V_1 and V_4 . Note that in View V_3 , had the viewing angle Φ been somewhat greater, the target pin would have lain to the right of the cradle pin. Since each construction in Appendix D is applicable to two different views, viz., Views V_1 and V_3 , or Views V_2 and V_4 , these eight constructions cover all 16 possible combinations. These constructions are all necessary, since the particular combination cannot be anticipated.^f Table 2 summarizes the measured offsets of the centerline of the test article relative to the MP instrument as found during the metrology testing. Additional discussion of these measurements is provided in Section 8.4.1.

8.3 Alignment Measurements Along the Z Axis

Because of the setup and limited measurement range of the transit, it could not be used to determine the offset of the test article datum along the Z coordinate from the MP instrument. This offset, identified as Y_0 in Figure 26, was instead deduced from the as-built dimensional inspections of the mountings as shown in the legend on the figure. As depicted in the figures (e.g., Figures 9 or 17) relative to the MP instrument, the Z coordinate is upward from the surface of the interface plate. The primed axes are parallel to these but their origin is centered on the test article datum, i.e., the center of the upper surfaces of the mounting slides on the aluminum adapter ring. The Z'' coordinate shares the same datum but this coordinate is measured along the axis that lies on the test article's long axis centerline, which may be somewhat tilted from the vertical in Position No. 1 or angled from the MP instrument's Y axis in Position No. 2. These coordinates are also depicted in Figures 29-31.

The Z component of the CG is reported by the MP instrument from the measurement made while the test article is in Position No. 2. The MP instrument actually measures this coordinate along its own +Y axis although it is reported as the Z component when this designation is entered by the user during the calculation report setup. Figure 26 depicts this measured distance as Y_2 to emphasize the actual basis (Y direction, Position No. 2) for the measurement.

8.4 Tilt Considerations

Sections 8.1 and 8.2 discussed how the offset of the test article datum from the MP instrument datum along both horizontal axes was determined. After lining up the transit on the center locating pin in the cradle and ensuring the view perspective was as desired, i.e., perpendicular to the X axis or at the angle required to measure the Y offset, the transit was rotated upward to measure the offset of the locating pin on the upper end of the mass standard in both X and Y directions. In conjunction with the lower pin

^f The method described is awkward and time-consuming. In retrospect, orienting the mass standard so as to make metrology measurements on both the lower and upper pins at the same angle is not necessary as these could just as well have been made independently. However, in lieu of the oblique-view method described, it is recommended that a small viewing window be cut through the oblique members on the cradle and through the upper counterweight stanchions to obviate this complicated approach and improve the accuracy of the ΔY measurement at the same time. This would need to be done very carefully to avoid distorting any parts of the fixture.

offset, these measurements revealed any tilt of the relatively tall mass standard about the horizontal axes of the MP instrument. The tilt model is depicted, very exaggerated, in Figure 17. This figure actually applies to any situation where the long axis of the test article is not perfectly parallel to the corresponding axis of the MP instrument (i.e., its Z axis in Position No. 1 or Y axis in Position No. 2). So a view similar to Figure 17 could be applied to either an elevation view showing the vertical tilt of the mass standard or an overhead (plan) view showing the angular relationship of the two coordinate systems' axes. However, the X component of the CG found from the Position No. 2 measurement is inferior to that made in Position No. 1 because the test article is physically so far removed from the MP instrument datum and therefore more prone to be affected by a tilt in the mounting. Therefore, this measurement was consistently discarded and the construction shown in Figure 17 was only used to determine the tilt of the mass standard from the vertical, i.e. Position No. 1.

The symmetry of the mass standard should show both the X'' and Y'' components of the CG position as measured from the centerline axis of the mass standard to be extremely small, if not actually zero. However, in addition to any unavoidable measurement variation, any CG offset that results from a tilt of the mass standard while in Position No. 1 would be sensed by the MP instrument and the X and Y components of the CG would be reported as non-zero. The as-mounted offsets along both the X and Y axes were determined by sighting the upper locating pin similarly to that described in Sections 8.1 and 8.2 for the lower pin.

Knowing the tilt allows the CG position relative to the test article's (tilted) coordinates to be calculated offline from the X and Y values reported by the MP instrument. This is further clarified by the discussion below. In discussing this, it may be anticipated from the outset that because the tilt angle during MMRTG testing is very small it is not likely to have any material effect on the test results reported by the Space Electronics software. Nevertheless, the development is of potential interest to the testing of a future test article whose coordinates cannot be aligned to those of the MP instrument.

The MP instrument measures the test article's CG offset from the MP instrument's datum, which is at the top of the interface plate and on the axis of rotation. To be useful to the design agency, this offset needs to be translated to the test article's coordinates. There are three issues that could affect the translation:

- linear offset of the test article's datum relative to the MP instrument's datum;
- rotational alignment of the test article's X and Y coordinates to those of the MP instrument, i.e., any "twist" associated with the mountings; and
- non-parallelism of the test article's Z axis relative to the Z axis of the MP instrument.

These issues were the subject of extensive metrological investigations for the new mounting fixtures. The approaches used and the results found are described below.

8.4.1 Linear Offsets of the MP Instrument and Test Article Coordinates

X Axis Linear Offset

Measurement of the linear offset measurement along the X axis was described in Section 8.1. As indicated in that section, this measurement was straightforward. The results for the X offsets are summarized in Table 2.

Y Axis Linear Offset

The general approach to measure the offset along the Y axis was described in Section 8.2. The present discussion provides additional details as to the determination of this offset. The eight data sheets in Appendix G are the actual records for the metrology sessions performed to determine the offsets and other alignment features using the mass standard. The multiple measurements listed on the data sheets were performed to minimize measurement errors. The final offset values used in the calculations were the

arithmetic averages of these data. Calculations for the Y offsets (the ΔY values) are also included in Appendix G.

Figure 14 shows an overhead view of the mounting fixtures with the cradle centerline pin indicated in red and one of the mass standard pins (upper or lower) shown in light green. Because of the obstruction to the view along the X axis as described in Section 8.2, oblique views to the X axis are required. The four possible views are indicated in the figure. These are numbered by the quadrant through which the view first passes, the quadrants having been numbered in the conventional way, viz., counterclockwise from the +X axis, as shown in the boxed designations on the figure. So View No. 1 (V_1) first passes through quadrant I, View V_4 first passes through quadrant IV, etc.

The precision transit was aligned to and locked onto the cradle centerline pin and the micrometer was zeroed. For this measurement the actual viewing angle relative to the MP instrument coordinates was immaterial. The cradle centerline alignment pin was removed and the drafting protractor was carefully centered on the centerline hole, aligned with the X axis of the cradle. By trial and error, the MP instrument was then rotated and stopped such that both the lower and upper locating pins in the mass standard could be viewed in the transit by only adjusting the transit's vertical tilt but without rotating it left or right. Each of the upper and lower pins in the mass standard, of course, could be anywhere within any of the four quadrants. These pins are depicted in light green in Figure 14; the placement shown in this figure is markedly exaggerated, intended only for illustration. The viewing angle on the protractor could be sighted in the transit. The angle was read from the protractor and recorded on a Y measurement data sheet. The rotational position of the mounting fixture's X axis was indicated by circling the relevant axis nearer to the viewer on the data sheet. By rotating the transit up and down, the offsets of the mass standard's upper and lower locating pins from the cradle centerline pin were then measured with the micrometer head and recorded on the data sheet. Several readings were typically recorded and averaged to arrive at the best estimate of the positions for a given configuration.

The geometric construction for determining the pin's Y offsets from the cradle centerline pin depends on three characteristics, as were described in Section 8.2: (1) the view quadrant; (2) whether the cradle pin is "near" the viewer or "away"; and (3) whether the mass standard pin lies to the left (red side of the micrometer scale) or to the right (black side of the micrometer scale) from the cradle pin as viewed in the transit. There are 16 possible combinations of these characteristics ($4 \times 2 \times 2 = 16$). Examination of Figure 14 shows that the only difference between views V_1 and V_3 is whether the plus (+) or minus (-) side of the X axis is closer to the viewer. This, however, does cause the signs on the Y offset to reverse. Accordingly, a signed unit multiplier i is included in the ΔY equation shown on the construction (Figure 16), where $i = +1$ or -1 as indicated in the legend. Similarly, views V_2 and V_4 differ only in this same regard. By allowing for this axis side to be either positive or negative in a given construction, these 16 combinations can be condensed to the 8 constructions shown in Appendix B. The identification of each construction is described in the construction title. Although it may be possible to contract the 8 constructions still further, doing so could introduce considerable confusion into the quick interpretation the results.

8.4.2 Rotational Offsets

Rotation about the Vertical Axis (Twist)

Section 8.1 described the use of the auxiliary flange to determine if the projections of the test article's X and Y axes onto the MP instrument interface plate were parallel to the MP instrument axes. It is noted that a tilt on only one of the horizontal axes would not necessarily generate a twist; however a tilt on both horizontal axes would create a twist. Since no twist was observed, any twist would have had to be too small to be detected with the 1.56 in. tall pins used with the auxiliary flange (Figure 12). These pins could not sense the imposed twist that would have been induced by a very slight tilt in both horizontal axes.

Rotation about a Horizontal Axis (Tilt)

Non-parallelism of the Z axes of the test article and the MP instrument implies a tilt exists in the vertical position of the test article. This may include a rotation about either or both of the MP instrument's horizontal axes. By measuring the offsets of both the upper and lower locating pins in the mass standard from the cradle pin, any non-trivial tilt that is present can be determined. The 37.269 in. tall mass standard (including upper and lower locating pins) significantly amplifies any tilt, enhancing the ability to detect even rather minor tilt angles.

The three orthogonal CG coordinates are reported by the MP instrument from measurements in Position No. 1 as X_{CG} and Y_{CG} and in Position No. 2 as X_{CG} and Z_{CG} . The preferred value for X_{CG} was consistently taken from Position No. 1 for better accuracy. Metrological sessions determined the best estimated values for X_U , X_L , Y_U , and Y_L (see Figure 17). The CG measurements performed with the mass standard in Position No. 2 provided the value for Z_{CG} . In fact, since the Z_{CG} position is also predictable from the mass standard's geometry, a comparison of this analytical value to that from the measurement also yields useful information on the measurement accuracy. The X_U and X_L offsets were measured directly; however the Y_U and Y_L offsets had to be determined indirectly, as was described in Section 8.2. Hence, their use in the correction of the CG position, above, also sheds information on the uncertainties associated with the methods used to deduce the offsets from the Y axis using the Y_U and Y_L measurements.

The MP instrument reports the X, Y, and Z components of the CG position relative to its own datum and axes ("machine-referenced" CG position, as indicated in Appendix C for example, run numbers 001620 - 001624). The user must furnish the lateral offsets of the testarticle datum from the MP instrument datum in the X and Y directions in Position No. 1 and the X and Z offsets in Position No. 2, again as indicated in these same run-numbered calculation sheets. These offsets are then subtracted from the measurement in the MP instrument reference frame by the Space Electronics Co. software to yield the lateral position of the CG relative to the test article's datum. This user-referenced CG position is also reported on the Space Electronics Co. reports. However, tall objects can experience some small amount of tilt, even when carefully mounted. To ensure the most accurate CG position is found, the tilt effect should be taken into account. Since the MP instrument itself is oblivious to any tilt, a manual correction is required.

Figure 17 shows the applicable geometric configuration with the tilt greatly exaggerated and defines the symbols. As before, the unprimed coordinates are those of the MP instrument. The primed coordinates are those positioned at the origin of the mounted test article. All of the primed axes are parallel to the corresponding axes of the MP instrument with only a lateral offset of the origin. The double primed coordinates are aligned to the test article itself. The nearly perfect symmetry of the mass standard provides a high assurance that its actual CG position will lie very nearly along its long axis. The test article referenced CG position needs to be corrected from the mountings' coordinates to account for any tilt in the mountings or in the test item itself, if known). After the CG correction has been made, any residual offset of the CG from the mass standard's long axis indicates the measurement error that must be assumed to result from the mountings and/or measurement instrument and therefore, needs to be applied to the MMRTG test results as well.^g

^g All metrology work was carried out using the mass standard. The mass standard was fabricated specifically for this purpose. Provisions were included in its design for installing accurate locating pins at the top and base for use as targets to be sighted with a precision transit. The MMRTG did not include any similar features. In the absence of any definitive information to the contrary, the assumption was made that the long axis of the MMRTG was perfectly perpendicular to its own mounting pads. This assumption justified applying whatever mounting-induced tilt that was observed with the mass standard to the MMRTG test measurements.

The tilt is defined by the deviation from the vertical of the projection of the Z axis of the test article onto the X-Z and Y-Z elevations. Two angles define the tilt. These angles measure the extent to which the upper pin is rotated toward the positive sides of the X and Y axes from a vertical line that passes through the test article datum. In the X-Z elevation view the deviation from the vertical toward the +X axis is denoted by the angle ϕ ; in the Y-Z elevation view the deviation toward the +Y axis is denoted by the angle β . These angles are depicted in the constructions in Figures 27-29. Configurations in multiple views are provided in these figures, which define the dimensions and angles. More detailed constructions for the analysis are provided in Figures 30 and 31. The base of the mass standard has been omitted in these figures to reduce clutter. Lacking information to the contrary, it has been assumed that any tilt of the test article is simply a rotation about its own origin, 0", which remains centered on and located at the plane of its mounting surface(s). The equations that define the offsets are provided on each of the detailed figures. These equations must be solved simultaneously for the projections of X" and Z" in the X-Z view and Y" and Z" in the Y-Z view. The solutions are

$$X''_{CG-XZ} = \frac{(Z_{CG} - Z_0) \sin \phi - (X_{CG} - X_0) \cos \phi}{\sin^2 \phi - \cos^2 \phi}$$

$$Z''_{CG-XZ} = \frac{(X_{CG} - X_0) \sin \phi - (Z_{CG} - Z_0) \cos \phi}{\sin^2 \phi - \cos^2 \phi}$$

$$Y''_{CG-YZ} = \frac{(Z_{CG} - Z_0) \sin \beta - (Y_{CG} - Y_0) \cos \beta}{\sin^2 \beta - \cos^2 \beta}$$

and

$$Z''_{CG-YZ} = \frac{(Y_{CG} - Y_0) \sin \beta - (Z_{CG} - Z_0) \cos \beta}{\sin^2 \beta - \cos^2 \beta}$$

The metrology data are documented and reduced in Appendix G. A Microsoft Excel spreadsheet was developed to methodically perform the calculations. A program listing is provided in Appendix F. The key results from the calculation are summarized in Table 2.

Once the lateral offsets for the X, Y, and Z axes, any tilt, and the angular orientation of the mounted test article in the horizontal plane have been found, the test article geometry relative to the MP instrument is fully specified. This allows the MP measurements to be translated to the test article coordinate system, and enables offsets at any other position on the test article to be quickly proportioned geometrically. For example, the offset measured as described above at the tip of the lower locating pin can be corrected to the offset at the elevation of the pin's base, 3.405 in. above the lower pin tip (cf. INL drawing 751227). The offset at this elevation is the offset needed for a coordinate system, such as that of the MMRTG, whose origin is at the axial centerline of the generator and in the plane of the bottom of its mounting pads.

9. CG MEASUREMENTS

This section first discusses the characteristics of the measurement that are important to understanding the mechanisms by which uncertainties arise and then presents the measurement results as reported by the Space Electronics software.

9.1 Accuracy and Repeatability

To assess the accuracy and repeatability of the test setup, the MMRTG mass standard was used. The mass standard is fabricated from two parts, the base plate and the column (bar), as shown in INL drawings 751224 and 75125, included in this report as Figures 18 and 19. These two parts are fastened together by a coarse-threaded connection. A precision countersink in the upper side of the base plate assures a very accurate centering of the column. Since both parts are the same material (Type 304 stainless steel), presumably having equal and uniform mass densities, the CG location for the entire assembly depends only on the geometry. Its theoretical CG location can be found from the individual part volumes and the positions of their respective volume centroids.

Despite the apparent geometric simplicity of the mass standard, the coarse screw threads joining the two parts plus the female screw threads in both ends complicate a very accurate hand calculation of each part's individual CG. The theoretical CG position for the mass standard was therefore determined from the Pro-E software used to generate the engineering drawings for this item. A printout of these results is shown in Figure 20 (note that the Pro-E model has the Y coordinate oriented in the direction of the mass standard's long axis, whereas this axis is the Z axis for the physical part as well as for the vertical axis of the MP instrument). The Pro-E software shows the CG to be located directly on the long axis as expected by the part's symmetry and 11.230 in. from the mounting surface (the underside of the flange). This computed location provides a standard against which to compare the CG measurement results to evaluate their accuracy. A mismatch between calculated and measured CG locations indicates the error contribution that must be assigned to the overall CG measurement uncertainty from the performance of the MP instrument itself.

Of course, the theoretical CG calculation should be based on the as-built dimensions of the mass standard, which may differ somewhat from the nominal dimensions shown on the drawings. Inspection reports following fabrication of the mass standard showed all dimensions conformed to the rather tight tolerances that had been specified in the design. It would be difficult to make the many inspection measurements sufficiently accurately to definitively contradict the volume computed on the basis of the nominal dimensions. On the basis of these dimensions, the Pro-E software calculated a volume of 340.72535 in^3 , as shown in Figure 20. The actual measured weight of the mass standard was recorded at 97.198 lb. The scale calibration check against NIST-traceable standards prior to the weighing showed a measurement variation (measured minus the calibrated) of approximately -0.007 lb. (see the weigh scale calibration record, Appendix H) at the 100 lb. level that approximates the weight of the mass standard and MMRTG. With this weight, the implied mass density would be 0.28529 lb/in^3 . This number rounds to the 0.29 lb/in^3 materials handbook density value that was assigned by the draftsman for the Type 304 stainless steel as shown in Figure 20. However, use of this relatively crude (two decimal places) density value with the Pro-E computed volume caused the total weight in Figure 20 to be calculated at 98.81035 lb. Aside from the crude density value used, any further discrepancy would probably stem from a combination of the true as-built dimensions, uncertainty in the actual depth of the pilot holes drilled on both ends for the female tapped holes, actual thread profiles and their dimensions vs. those built into the Pro-E software, and/or rounding errors. Any error in the assigned material density would, in principle, not have any effect on the CG location, since both parts are ostensibly the same material (although not from the same stock: one part is from bar stock and one is from plate stock). However, the former errors could affect the CG location. Since these issues only affected the mass standard measurements, and even then only rather slightly, any further concerns were dismissed in favor of simply rolling any residual discrepancy into an uncertainty allowance in the statistical evaluation of the mass standard results, described later.

During the tare measurements, it is important that all fixtures and components be in exactly their same positions as during the test article measurements. This required that the mounting slides on the aluminum adapter ring and all fasteners be carefully located to replicate their test positions. Since the mounting slides need to be radially unrestrained when the elevated temperature MMRTG is mounted, a design feature and testing procedure to accurately reposition these for the tare was developed. The mounting slides were repositioned using fine-threaded locator screws and then locked in place.^h The technique used is fully described in Sections 5.9.9.4 and 5.12.1.2 of the mass properties test procedure, RPS/HS-OI-28220, Rev. 0. For operational consistency, the same procedure was also used for measurements conducted with the room temperature mass standard.

The titanium mounting screws were kept segregated and inserted into the same mounting slide on the aluminum adapter ring as during the PART measurement. Spacers, having negligible mass, were used to position the mounting screws and flat washers to compensate for the displacement of the fasteners by the thickness of the test article's mounting pads. Very thin-walled, aluminum tube spacers were used with the elevated temperature MMRTG whereas plastic spacers were used with the room temperature, mass standard to preserve the more delicate aluminum spacers.

The uncorrected CG calculation results using the mass standard CG PART and TARE measurements in both Position No. 1 and Position No. 2 (long axis horizontal, with the +Z axis in the direction of the MP instrument's +Y axis) are shown in Table 3 for the four measurement campaigns using the mass standard, viz., MS-1 through MS-4. The PART and TARE run numbers selected for the analyses are indicated and the calculation run numbers are also cited. These calculation output records, identified by their run numbers, are provided in Appendix I. Table 3 also summarizes the datum offsets of the mass standard from the MP instrument datum. This table shows that the measurement results compared very favorably to the analytical predictions. The largest mismatches in the X, Y, and Z directions were 0.0049 in. (MS-3), 0.0017 in. (MS-4), and -0.0042 in. (11.2258 in. - 11.230 in., MS-1), respectively.

Table 3 also provides a statistical analysis that reveals the confidence interval associated with the mean value of the computed CG position coordinates. An estimate of the true variance, σ^2 , was required since the data from these four tests are far too sparse to infer the data are normally distributed. The estimate of the variance is s^2 , where

$$s^2 = \frac{1}{N-1} \sum_{i=1}^N (y_i - \bar{y})^2$$

The y_i are the measured CG values for the N data points respectively and \bar{y} is their arithmetic average. The estimated confidence interval uses the t-statistic (a.k.a. Student's t). These comprise a family of distributions where each distribution, t_v , pertains to a specific value of v , the degrees of freedom, where $v = N - 1$. For all v , these distributions are symmetrical about $t_v = 0$ and have a profile similar to that of the normal, or Gaussian, distribution. They peak at $t_v = 0$ and have an inflexion point and approach zero on both the positive and negative axes at points increasingly removed from zero. Compared to the normal distribution, however, these distributions have more "spread", i.e., the "tails" of the distribution approach zero more slowly and the peak value is lower (the integrated value is always unity). For increasing N, the distributions approach more closely the normal distribution, becoming coincident at $N = \infty$.

^h The capability to accurately reposition these slides for the tare measurement was the primary motivation for the construction and use of the aluminum adapter ring rather than using the PWR stainless-steel adapter ring. The fact that the aluminum adapter ring is also about 15 lb. lighter is also advantageous to the accuracy of the measurement. The aluminum adapter ring and the design features described are depicted in the rendering shown in Figure 21. Complete construction details are provided in INL Drawings 751210 and 751214 – 751217.

The t_v distributions are mathematically complicated but are tabulated in standard statistics texts for a given value of v and user-selected probability. For the four data points in Table 3 and with 99% confidence interval, the value that leaves 0.5% of the integrated distribution in each tail (thus, the 1% overall), is $t_{v,0.005} = 5.841$.

The arithmetic average of the measurements, \bar{y} , is the best estimate of the mean value, η , and with a 99% confidence interval, the true value of the mean lies within the interval

$$\eta = \bar{y} \pm t_{v,0.005} \sqrt{\frac{s^2}{N}}$$

Therefore, relative to the coordinate system centered on the mass standard datum and parallel to the coordinates of the MP instrument (i.e., the primed coordinates), the actual measured data in Table 3 show that the mean CG location in Position No. 1, with a 99% confidence interval, lies within the intervals

$$\begin{aligned}\eta_{X'} &= 0.00308 \pm 0.00398 \text{ in.} \\ \eta_{Y'} &= 0.00068 \pm 0.00257 \text{ in.}\end{aligned}$$

Similarly, in Position No. 2 the mean CG location is found to lie within the intervals

$$\begin{aligned}\eta_{X'} &= 0.00553 \pm 0.00188 \text{ in.} \\ \eta_{Z'} &= 11.226 \pm 0.00110 \text{ in.}\end{aligned}$$

Upon discarding the X' measurement in Position No. 2, as discussed in Section 8.4, the CG position for the mass standard, with a 99% confidence interval, is determined to lie within the rectangular prism region defined by

$$\begin{aligned}\eta_{X'} &= 0.00308 \pm 0.00398 \text{ in.} \\ \eta_{Y'} &= 0.00068 \pm 0.00257 \text{ in.} \\ \eta_{Z'} &= 11.226 \pm 0.00110 \text{ in.}\end{aligned}$$

It is emphasized that this interval represents only the statistical variation in the mass standard test data. For example, an adjustment for the tilt of the test article's axes still needs to be manually appended to express the CG offset relative to coordinates aligned to the mass standard (a different coordinate system from the primed coordinates, whose origin is simply offset from that of the MP instrument but whose axes are parallel to those of the MP instrument). Tilt parameters were shown in Table 2 and Figures 30 and 31 to be small from the metrological evaluation using the mass standard, viz., 0.00236 in. and 0.00101 in. for the X'' and Y'' dimensions, respectively. However, there could be some difference between how plumb the MMRTG mounts are as compared to the mass standard. Therefore, in lieu of providing a specific adjustment to the CG measurements for the MMRTG, a conservative tilt contribution of 0.003 in. to its overall CG position uncertainty has been assigned in Section 12. Other uncertainties, e.g., those that arise from temperature effects in the fixtures, are addressed and added to the total uncertainty in subsequent sections of this report.

9.2 Measurement Sensitivity

Measurements described in the previous section with the mass standard established the overall accuracy capabilities of the MP testing system. Another informative check is to confirm the sensitivity of the measurement apparatus, i.e. is a small physical perturbation readily detectable. This was assessed by positioning a small, accurately known weight at an accurately known displacement from the MP instrument's rotational centerline in conjunction with the mass standard. One of the small, $\frac{3}{4}$ in./diameter fixture alignment pins described previously was used to make this assessment. By design, these pins provide a snug slip fit to the precision alignment holes in the base of the cradle permitting very accurate positioning. This feature makes these pins also very useful as special weights for making accurate analytical predictions of the sensitivity of the CG measurements. The exercise is described below.

First, a basic PART measurement was made with the mass standard in Position No. 1 (Run No. 1614).ⁱ Without disturbing either the mass standard or the fixtures, the shortest alignment pin, having an accurately determined weight of 0.3319 lb., was placed in cradle base hole H located 9.9991 in. from the cradle centerline along the +X axis, as shown in Figure 11. Another PART measurement was performed (Run No. 1615). The auxiliary pin was then sequentially moved to the other three cradle holes (all also nominally 10 in. from the cradle centerline and positioned as described below) then additional PART runs, No. 1616, 1617, and 1618 were performed. Those measurements are described subsequent to the discussion below for the initial measurement using cradle base hole H.

The mass standard and auxiliary pin were removed, the mounting slides reset and secured, and the mounting screws and washers with the plastic standoffs were installed. A TARE measurement was made (Run No. 1619). This tare was applicable to the basic test and all four of the perturbed mass tests. The CG calculation (Run No. 1620) for the base case, using the PART Run No. 1614 with the common TARE run, was then performed. As shown in the calculation sheet, the mass standard net CG location along the X and Y axes was 0.0014 in. and 0.0028 in. respectively, as measured from the MP instrument's centerline.

For the slightly modified test article, now comprising the mass standard plus the auxiliary pin, the CG calculation (Run No. 1621) was performed using PART Run No. 1615, the measurement made with the auxiliary pin in hole H. This calculation found the X and Y coordinates of the net CG to now be at +0.0356 in. and +0.0031 in. respectively, relative to the MP instrument's centerline.^j

ⁱ Printouts from the MP software discussed in this section are provided in Appendix C, identified in the upper section by run number. The run number is a sequential number automatically assigned by the Space Electronics software to each operation. These printouts also serve as examples of the output from the software. The originals of these and the numerous other printouts generated during the course of the MP testing program for the MMRTG are kept at the MP testing station.

^j The Y component of this measurement should not have changed. The 0.0003 in. (0.0031 in. - 0.0028 in.) change measured may be a genuine small offset of the hole H centerline from the X axis or just an indication of the variation that occurred when remounting the mass standard. This and the other measurements described in the remainder of this section prompted the further inclusion of a conservative 0.002-in positioning allowance in the overall uncertainty computation developed in Section 12.0.

By analysis, the net CG of the combined mass standard and auxiliary pin should have been located at a position determined by the dividing the total net moment M by the total net weight W . Letting the subscripts MS and pin denote the mass standard and auxiliary pin respectively, the CG location along the X axis, denoted as CG_X , should now be located at

$$\begin{aligned} CG_X &= \frac{\sum M_X}{\sum W} = \frac{W_{MS} * X_{MS} + W_{pin} * X_{pin}}{W_{MS} + W_{pin}} \\ &= \frac{(97.198lb.)*(+0.0014in.) + (0.3319lb.)*(+9.9991in.)}{97.198lb. + 0.3319lb.} \\ &= +0.03542in. \end{aligned}$$

The discrepancy Δ between analytical prediction and measurement, rounded to four decimal places, is therefore

$$\begin{aligned} \Delta &= +0.0354in. - (+0.0356in.) \\ &= -0.0002in. \end{aligned}$$

On a relative basis, the discrepancy is

$$\Delta = \left| \frac{-0.0002in.}{+0.03542in.} \right| = 0.0056 = 0.56\%$$

Placing the auxiliary pin into cradle base hole I on the -X axis similarly shows a predicted CG_X of -0.03263 in. as compared to a measured CG_X of -0.0331 in. (Run No. 1616 & 1622). The discrepancy in this case is +0.0005 in. or 1.44 %.

Similar measurements were made with the auxiliary pin placed along the Y axis. Placing the auxiliary pin on the +Y axis (hole A), the predicted CG_Y was found to be 0.03682 in. while the measurement result (Runs 1617 and 1623) was 0.0368 in. indicating a discrepancy that rounds off to zero, within the four decimal places reported. For the -Y axis with the auxiliary pin in hole G, the predicted CG_Y is -0.03125 in. while the measurement showed -0.0316 in. (Runs 1618 and 1624) for a discrepancy of -0.0003 in. or 1.1 %.

The comparisons between measurements and the corresponding analytical predictions on both axes were all less than 0.0005 in. or 1.5 %. The purpose of these comparisons was only to establish that sufficiently sensitive measurements can be obtained with the new MP mounting equipment.

9.3 Moment Measurements Using the Space Electronics Instrument

The Space Electronics system includes a load cell that senses the offset moments along the instrument's two orthogonal axes in the horizontal plane. The mechanism is pre-loaded such that balanced loads register moments of approximately 2075 in-lb. This is demonstrated in the balancing tests shown in Table 1, where the moments on all axes converge to approximately 2075 in-lb as the balance is improved. The preload could be subject to drift, however. The development below shows how this term can be negated, thereby avoiding drift errors.

Net moments along both the positive and negative sides of a given axis produce forces that are sensed by the load cell. An off-center CG on the positive side of the X axis for example, will increase the moment on that side of the axis over and above the preload value, while the moment on the opposite side of the axis will correspondingly decrease relative to the preload. The preload moment is denoted by a zero subscript, viz., M_0 . The excess moment relative to the preload on either side of the axis is denoted as M_{ex} . Furthermore, the actual measured moment along the positive side of a given axis is denoted by M^+ and that on the negative side of the same axis by M^- . For an imbalance toward the positive axis, as in this example, equations for both measurements can be written using this terminology as

$$\begin{aligned} M^+ &= M_0 + M_{ex}^+ \\ M^- &= M_0 - M_{ex}^- \end{aligned}$$

Solving these equations simultaneously eliminates the preload, giving

$$M_{ex}^+ + M_{ex}^- = M^+ - M^-$$

Although the M_{ex} terms are ostensibly equal, there could be a very small difference that results from any measurement errors. The best estimate, M_{BE} , of the true moment value relative to the preload is the arithmetic average of the relative moments,

$$M_{BE} = \frac{M_{ex}^+ + M_{ex}^-}{2}$$

Upon combining these last two equations, the best estimate is related to the measurements themselves, as

$$M_{BE} = \frac{M^+ - M^-}{2}$$

This moment pertains to whatever equipment is mounted. Two measurements are required to deduce the net moment for the test article alone. The first, the PART measurement, includes the test article, fixtures, and everything else that is mounted on the MP instrument when this measurement is performed. The second measurement, the TARE, is made with all of the same items mounted in exactly the same physical configuration except the actual test article has been removed. Each of these measurements yields a best estimated value per the above development. If a subscript p denotes the PART measurements and a subscript t denotes the TARE measurements, these equations become

$$\begin{aligned} M_{BE-p} &= \frac{M_p^+ - M_p^-}{2} \\ M_{BE-t} &= \frac{M_t^+ - M_t^-}{2} \end{aligned}$$

The difference between these two quantities is the net moment applicable to the test article alone, M_{TA} .

$$M_{TA} = M_{BE-p} - M_{BE-t}$$

Upon combining these,

$$M_{TA} = \frac{M_p^+ - M_p^-}{2} - \frac{M_t^+ - M_t^-}{2} = \frac{1}{2} (M_p^+ - M_p^- - M_t^+ + M_t^-)$$

is derived.

The Space Electronics Instrument software automatically uses the user-specified PART and TARE moment measurements to perform these calculations without any user intervention. The development above is provided to support the consideration of temperature variation and the resulting measurement uncertainties in the results addressed in latter sections of this report where user intervention is needed.

9.4 Test article Weight and CG Uncertainty

After the net test article moment M_{TA} has been measured, it must be divided by the user furnished testarticle weight to obtain the test article's CG offset along a given axis. With the weight denoted by W , the CG offset on the particular axis is therefore

$$CG = \frac{M_{TA}}{W_{TA}}$$

Since the test article weight is a user furnished parameter, an accurate CG offset calculation depends on an accurate determination of the test article weight. This is complicated further by the fact that the weighing of the MMRTG includes, out of handling and operational necessity, several equipment items that are not installed during the MP measurements. The net weight of the as-tested test article is found by subtracting the weight of these ancillary items to arrive at the as-tested weight (see Appendix J). Uncertainties in each of these terms affect the CG calculation uncertainty.

The gross weight of the test article, configured as weighed, is indicated by the subscript g and the group of ancillary items removed thereafter, and absent during the MP measurement, is indicated by the subscript a. The net test article weight is therefore

$$W_{TA} = W_g - W_a$$

Uncertainty in the moment measurement is denoted δM , and the uncertainty for each weight W is denoted δW . These produce an uncertainty in the calculated CG by an amount δCG where, using the rules of differentiation,

$$\delta CG = \delta \left[\frac{M_{TA}}{W_{TA}} \right] = \frac{\delta M_{TA}}{W_{TA}} - M_{TA} \frac{\delta W_{TA}}{W_{TA}^2}$$

The uncertainties in the previously cited definitions of M_{TA} and W_{TA} are given by

$$\delta M_{TA} = \frac{1}{2} (\delta M_p^+ - \delta M_p^- - \delta M_t^+ + \delta M_t^-)$$

and

$$\delta W_{TA} = \delta W_g - \delta W_a$$

Combining these, the uncertainty in the CG calculation itself, that results from the uncertainties in the moments and weight measurements, becomes

$$\delta CG = \frac{1}{2W_{TA}} (\delta M_p^+ - \delta M_p^- - \delta M_t^+ + \delta M_t^-) - \frac{M_{TA}}{W_{TA}^2} (\delta W_g - \delta W_a)$$

This equation comprises six independent terms in δM or δW , each term of which can be either positive or negative. Multiple terms are usually combined in a square-root-of-the-sum-of-squares fashion to account for the low likelihood of all terms either stacking up in a common direction or fortuitously cancelling one another. Applying this approach, the estimated CG uncertainty is found to be

$$\delta CG = \sqrt{\left[\frac{1}{4W_{TA}^2} (\delta M_p^{+2} + \delta M_p^{-2} + \delta M_t^{+2} + \delta M_t^{-2}) \right] + \left[\frac{M_{TA}^2}{W_{TA}^4} (\delta W_g^2 + \delta W_a^2) \right]}$$

For well balanced fixtures and test article relative to the particular axis being measured, the net moment M_{TA} will be quite small and the square of this quantity causes the second term to rapidly become insignificant. This demonstrates the benefit of carefully balancing the fixtures and mounting the test article such that its CG is as close as practical to the center of rotation of the MP instrument. For such configurations, the CG uncertainty is controlled by the uncertainties in the individual moment measurements. This equation has been evaluated for several hypothetical situations parametrically in Table 4, which shows the intermediate results as well. Even for less well balanced configurations, when the uncertainties in the weights are small, the second term remains very small in comparison to the first term, as shown in Table 4. The design requirements specifications (Ref. 2) required that the mass of the MMRTG be known to within 0.5%. For the approximately 100 lb. MMRTG, the allowable margin of error is 0.5 lb. The accuracy of the calibrated platform scale utilized for these tests is considerably better, always within 0.008 lb. and typically within 0.002 lb. The scale accuracy was checked using currently calibrated standards over the range 0 – 200 lb. prior to each official weighing. A record of the platform scale calibration check is provided in Appendix H.

Conservative values for the moment uncertainties in the equation above can be gleaned from the repetitive runs listed in Table 5, showing

$$\delta M \approx 0.1 \text{ in-lb}$$

Assume a comfortably conservative value for the weight uncertainties of

$$\delta W \approx 0.01 \text{ lb. (max.)}$$

For a CG offset at the specified maximum radial limit of 5 mm (0.197 in.), the net moment for the approximately 100 lb. MMRTG would nominally be approximately 19.9 in-lb. Parametric cases No. 1, 3, and 4 in Table 4 show that these would contribute less than a 0.001 in. uncertainty to the calculated CG position. This is probably the magnitude to be expected from moment and weighing measurement errors. This value has been included in the overall uncertainty shown in Section 12.1.

9.5 Measurement Results

Table 6 provides the results as reported by the MP instrument software. The table includes the measurement results for both the MMRTG and the four witnessed tests conducted with the mass standard. Since multiple tests were conducted with the mass standard, including the mounting/dismounting of the item, those results provide a reasonable basis for estimating the confidence intervals associated with all the test results. Since multiple tests were generally conducted, the run numbers of the PART and TARE data reports that were used for the calculations are shown in bold font. Reports for these calculations are provided in Appendix I. The results are shown relative to both the MP instrument and the user's coordinate system. The translation to the user coordinates is based on the user furnished metrological information discussed in Section 8.

The mean X, Y, Z coordinates of the CG position for the MMRTG in its test configuration, as calculated in Table 6, are listed below relative to its datum at the center of the mounting pads plane. Section 9.1 provides a complete explanation of the confidence interval evaluation.

$$X = 0.0968 \pm 0.0040 \text{ in.}$$

$$Y = 0.0276 \pm 0.0026 \text{ in.}$$

$$Z = 10.816 \pm 0.0011 \text{ in.}$$

These offset values are the as-reported measurement results. The X and Y components of the CG coordinates reflect the non-symmetry in the MMRTG due to the presence of non-flight parts, such as the close-coupled Y-cable, bracket, cooling tube caps, etc., that were present during testing. Corrections for these items are to be made by the design agency, PWR.

Results from statistics calculations for the 99% confidence interval specified in Reference 1 are also shown in Table 6 and summarized above. The confidence intervals cited represent a right prismatic region within which the CG is expected to lie with a 99% confidence interval as depicted in Figure 22. These confidence intervals and the implied region were statistically determined from that data. In essence, the confidence intervals are based only on the observed variation inherent in the data. Systemic errors (biases), such as the induced tilt of the test article due to mountings, errors caused by expansion, or contraction from temperature variation that occurred between the PART and TARE measurements, are not reflected in these intervals. Uncertainties for such biases are added to the intervals shown above in Section 12, based on considerations discussed in this report to arrive at a total estimated uncertainty.

10. TEMPERATURE CHANGES IN THE MOUNTING FIXTURES

Test articles, such as radioisotope generators, whose temperatures differ markedly from that of typical room temperature have the potential to create temperature changes in the mounting fixtures. Such temperature changes can induce thermal expansions or contractions that, if sufficient in magnitude, effectively reposition both the fixtures and the test article. Repositioning affects both the calculated position of the CG relative to the MP instrument datum, as well as the translation of the CG position to the test article coordinates. This section quantifies these effects for the MMRTG testing.

10.1 General Thermal Considerations

The temperatures in the fixtures were monitored to provide data to support analytical corrections to the MP measurements, if determined necessary, since very accurate mass properties are typically desired.

Temperature measurements were taken after the test article was mounted and the equipment was allowed at least two hours to reach stable thermal conditions. An accurate MP measurement requires that the TARE measurement be made with all items save the test article, in their exact same positions as during the PART measurement. Should the fixture temperatures during the TARE differ from the temperatures when the PART measurement was made, their resulting expansion or contraction could cause the calculation for the net test article moment to be in error. Because of the time required to dismount the test article and reconfigure the fixtures for the TARE, temperatures may well have changed.

The temperature phenomenon described above directly impacts the MP measurements relative to the MP instrument coordinates. Temperature variation can also affect the positional relationships between the test article datum and that of the MP instrument. The positional relationship, established by metrological investigation of the mounting fixtures at room temperature prior to operations with the test article, will be compromised by any fixture expansion or contraction. Such effects move the plane of the generator's mounting pads relative to the MP instrument's datum. This impacts the accurate translation of the CG and/or MOI measurements results from the MP instrument coordinate system to that of the test article.

In Position No. 1 the symmetry of the mounting fixtures and that of the MMRTG tend to negate the impact of any growth/contraction. By allowing the fixture temperatures to stabilize for a period of time after mounting the MMRTG in Position No. 1, the relative position of the MMRTG to the MP instrument rotational axis should not have changed in the horizontal plane. This is depicted in Figure 23. As indicated in the legend, all thermal growth is expected to be positive and symmetric, so that the only net movement of the test article's CG is upward from the MP instrument datum. Since the MP instrument only senses the mass properties in the horizontal plane, this thermal growth is of little concern for the CG measurement in this position. However, since MOI properties depend on the entire mass distribution, such measurements, if applicable, could very well be impacted.

In Position No. 2, longitudinal growth or contraction of the test article and its mounting fixtures is along the Y axis of the MP instrument, one of the coordinates that is sensed. In addition, non-symmetrical thermal effects occur. These are depicted in Figure 24. Fixture members physically above the generator will tend to be further heated by rising convective air currents while those members below the generator may begin to cool. The mounting fixtures are all fabricated from Type 6061-T651 (ASTM B209 and B211) aluminum, a material that has a relatively high coefficient of thermal expansion, at approximately $13.1 \times 10^{-6} \text{ F}^{-1}$. The length of time required to reposition the generator and to perform new measurements limits the ability to quickly perform the measurement so as to minimize the time over which any thermal changes can occur.

The issues described above are in addition to whatever further considerations need to be made for the possibility that the temperature distribution in the test article during MP testing may differ from that during the mission application. This needs to be considered by the design agency based on the applicable conditions during the mission. Interestingly, the MMRTG itself can also be distorted by the non-symmetrical temperatures induced in its shell while in a non-vertical position, such as Position No. 2. Vigorous convective cooling on the lower side, coupled with immersion in significantly heated air on the upper side, will cause the shell to bow slightly about a horizontal axis with the convex side upward. Deformation of the MMRTG may or may not be a concern to the mission application, since thermal induced buoyancy only occurs when immersed in a gaseous environment and in the presence of a gravitational field. Regardless, this phenomenon does not seriously impact the MP measurements. MP measurements in Position No. 2 are only used to obtain the longitudinal axis component of the CG and a slight axial bowing of the generator will not materially affect this value.

Specific marks were made on the cradle, rotation fixture, and adapter ring to use as consistent targets for a direct reading contact-type temperature probe. Temperature readings at these locations were taken prior to and following the PART and TARE measurements. The intent was to either demonstrate negligible temperature changes or, if found not to be the case, to use these measurements to estimate the temperatures that prevailed as a basis to analytically correct the data. In the interest of minimizing operator radiation dose, not all stations were recorded when symmetry suggested only minor variation, e.g., side-to-side. In retrospect, additional measurements, e.g., on the upper members of the rotation fixture, would have been beneficial to the ultimate detailed analysis of the data.

10.2 Evaluation of Fixture Temperature Variation

As was developed in Section 9.4, the CG is located at a position measured from whatever datum the moment M_{TA} is measured from, as

$$CG = \frac{M_{TA}}{W_{TA}}$$

It was further shown that to compute M_{TA} the moments of the PART and TARE were required, where the positions of all items during the TARE were presumed identical to those during the PART measurement but without the test article present. Therefore, per the previous discussion, the question arises: suppose the fixture positions have, indeed, changed during the TARE for whatever reason, e.g. in the present investigation as a result of temperature changes in the fixtures. Then the TARE moment would no longer be M_t , but rather some different value denoted as M_t' . Can the measurement be salvaged? The discussion in this section shows that it can be, and how this needs to be handled.

The test article moment is computed as was shown in Section 9.3 from the PART and TARE measurements as

$$M_{TA} = \frac{M_p^+ - M_p^-}{2} - \frac{M_t^+ - M_t^-}{2}$$

For brevity in the present discussion, this is written simply as

$$M_{TA} = M_p - M_t$$

M_p and M_t are understood to be contractions for their full definitions, as written before. Without changing the equation, the TARE moment term can be rewritten as

$$M_t = M_t' + M_t - M_t'$$

Upon inserting this into the previous equation,

$$M_{TA} = (M_p - M_t') - (M_t - M_t')$$

This can be recast into a CG form by dividing by the test article weight and rearranging the last term, giving

$$CG_{TA} = \frac{M_{TA}}{W_{TA}} = \frac{(M_p - M'_t)}{W_{TA}} - \frac{(M_t - M'_t)}{W_{TA}} = CG'_{TA} + \frac{(M'_t - M_t)}{W_{TA}}$$

The first term CG'_{TA} replaces its counterpart for the case where no displacement (here resulting from thermal expansion or contraction, but could be from any phenomenon) has occurred. The measurement software, being unaware that temperature effects may have occurred, only uses the actual PART and TARE measurement calculations, oblivious to any physical repositioning that has occurred to the hardware. The second term is the correction required to negate the error introduced by the CG displacement and thereby reestablish the validity of the test article CG calculation. This correction term must be manually appended to the CG'_{TA} value that is reported by the software.

The correction term can be computed once the displacements of all the components as occurred during the TARE have been evaluated. The total TARE moments are the summations of the individual moments among those components comprising the TARE. For example, the individual moment correction for the j^{th} component can be written as

$$(M'_t - M_t)_j = W_j * (Y' - Y)_j$$

Defining $(Y' - Y)_j$ as ΔY_j , this equation can be written as

$$(M'_t - M_t)_j = W_j * \Delta Y_j$$

By invoking the thermal expansion coefficient, $\alpha_j(T)$, normally temperature dependent, for this j^{th} component, each of the ΔY_j terms can be evaluated as

$$\Delta Y_j = \alpha_j(T) Y_j \Delta T_j$$

The quantity ΔY_j is the displacement (algebraic) that occurred to the individual CG of the j^{th} component (or j^{th} segment, if a large component had been divided into discrete segments) relative to its position during the PART measurement when the temperature of the component changed from its PART value T to the TARE value T' . Calculation of the correction term becomes a matter of determining the CG displacements of each affected component or element, multiplying these displacements by their weights, summing these and dividing by the test article weight, yielding a final result for the overall CG of

$$CG_{TA} = CG'_{TA} + \frac{1}{W_{TA}} \sum_j W_j * \Delta Y_j$$

This equation is evaluated and discussed in detail in Appendix E, taking into account the following observations from an inspection of the fixture temperature maps from the MMRTG test procedure (Ref. 3). These maps are provided in Appendix D. Temperature maps designated K-1 and K-2 respectively, show the temperatures measured on the cradle and on the rotation fixture with adapter ring as recorded just prior to the CG measurements. The cradle map K-1 shows there was only a very modest, approximately 2.5° F temperature increase in the cradle members from base upward toward the rotation fixture pivot point. The temperature increase in the higher elevation parts of the structure were the result of buoyancy induced convective heat transport. However, since these components were on the fringes of the convective flow patterns that developed around the generator, only these minimal temperature increases occurred. Furthermore, any symmetrical vertical growth or contractions in the cradle fixture will not affect the CG measurement.

The pre-test temperatures in the rotation fixture are all somewhat warmer than the local ambient temperature, which was not measured but, judging by the temperatures near the base of the cradle, was estimated to have been approximately 70° F. The temperatures are a few degrees hotter near the bottom of the fixture and hotter still near the adapter ring. Since these measurements were made in Position No. 1, the temperature gradient indicates there was substantial heat conduction from the base of the generator into the adapter ring and rotation fixture base and then up into the upright members. This was in addition to any convective heat transport to the upright members.

Temperature map K-4 shows temperatures in the rotation fixture upon completion of the PART measurements and made as soon as the generator was returned to Position No. 1. Evidently, the continued conduction into the base of the fixture during the 75 min between pre- and post-test PART measurements and/or the distortion caused by being in Position No. 2 raised the temperatures in the rotation fixture about 2° F further and the temperature in the adapter ring by approximately 5° F, although the temperature distribution is similar to that before the measurements.^{k,l} The local ambient temperature increase inside the testing cell may have also contributed. For ease of comparison, both the pre-test and post-test temperature distributions in the rotation fixture are plotted in Figure 25. As indicated in the figure, the temperatures included at the base and at the pivot point of the uprights (viz., the 0. in. and 18.1 in. positions, respectively) are extrapolations from the limited measurements.

Following the CG testing, the generator was left in Position No. 1 overnight. This presumably allowed recovery of the temperature distributions that existed prior to the PART measurements. Immediately after dismounting the generator the next morning in preparation for TARE measurements, the temperatures in the fixtures were once more measured and recorded, as shown in temperature map K-6. The TARE in each position was performed, the rotation fixture returned to Position No. 1, and again the fixture temperatures were taken, as seen in temperature map K-8. The pre- and post-TARE temperature distributions are also plotted in Figure 25 for ease of comparison to the PART measurements. It is evident that some cooling occurred during the approximately one hour required to perform the TARE measurements in both positions.

^k The rotation fixture temperatures were only measured on the -X side. These members had been above the generator while in Position No. 2. This may have been at least partially responsible for the temperature increase.

^l This phenomenon had been anticipated. To hasten the return to Position No. 1 and in view of the typical consistency of the MP measurements, only a single PART measurement was performed on the MMRTG in Position No. 2. In Position No. 1 three measurements were made and the data from the most intermediate PART and TARE measurements were used in the calculations.

Temperatures in the rotation fixture members just prior to the tares compared favorably to those prior to the testing performed the previous day, being generally just a fraction of a degree Fahrenheit warmer for corresponding measurement positions. Surprisingly, however, the temperatures recorded in the adapter ring are about 16° F cooler than those found previously (compare temperature maps K-4 and K-6). Note that the post-tare record, temperature map K-8, shows the adapter ring is now actually cooler than the adjacent members of the rotation fixture. Although this is not an impossible situation, it certainly indicates that the adapter ring cooled much faster than the adjacent members. This does not seem likely given the thick structure of the adapter ring. These observations cast some suspicion on the adapter ring temperature measurements and/or their record just prior to and following the tares. However, since no other data was available, the recorded data was used to conservatively estimate the fixture positions attributed to expansion/contraction, but an allowance was included in the reported overall uncertainty to reflect this and other similar secondary concerns.

The observed temperature changes that occurred between the PART and TARE measurements for Position No. 2 detailed calculations in Appendix E indicated that the required correction to the CG axial position was -0.0006 in. i.e. an adjustment of the composite CG toward the base of the MMRTG of 0.0006 in. This would normally be algebraically added to the axial CG position reported by the Space Electronics system. Given the small magnitude, an alternative treatment would be to assign an uncertainty contribution of 0.001 in. to the axial CG location to cover this modest temperature effect. This allowance is specifically identified in Section 12.

11. COORDINATES TRANSLATION

The measurement correction described in Section 10 refers to correcting the CG calculation that is reported by the Space Electronics software relative to the MP instrument datum should the TARE positions of the mounting equipment differ from their positions when the PART measurement was made. The CG position is also reported relative to the test article datum, since this is the datum ultimately of interest. The Space Electronics software computes this position by an algebraic translation of the CG position coordinates based on the user-furnished X and Y offsets between the MP instrument datum and the test article datum, as were determined by the metrology investigation described in Section 8. This section discusses the translation of the measurement results and the consequences to the overall uncertainty.

The vertical offset of the test article's origin from the origin of the MP instrument was determined from design drawings of the mounting fixtures that controlled the actual dimensions when the fixtures were fabricated at room temperature. Figure 26 shows an adaptation of a view from INL Drawing 751208. The dimensions shown reflect the post-fabrication inspection. The as-built surfaces of the mounting slides on the Mk-II adapter ring are seen to be 11.096 in. from the rotation fixture pivot axis. When in Position No. 2, this is the Y (or Z, to the test article) offset between the MP instrument rotational centerline and the mounting surfaces for the test article on the Mk-II adapter ring. However, this as-fabricated offset value needs to be corrected to the value that pertains to the temperatures that exist in both the rotation fixture and Mk-II adapter ring during the PART measurement.

Upon mounting the MMRTG onto the fixtures and allowing the temperature transient to stabilize, the heat released caused all of the mounting fixtures to expand. Fortuitously, the elongation in the vertical members of the rotation fixture moved the base away from the pivots very nearly the same distance as the growth of the shorter, but hotter, adapter ring, moving the MMRTG mounting pads away from the rotation fixture base and nearer to the pivot. The net result was that during the PART measurement the position of the generator's mounting pads (the plane of the MMRTG datum) hardly moved at all. This can be seen in Spreadsheet E-1 (Table 7) from Appendix E by summing for both the adapter ring and the rotation fixture the applicable position entries (including only those that stack, which are shown in bold font) in the column labeled *Thermal Growth or Shrinkage*.^m The upper surfaces of the adapter ring moved toward the pivot by 0.002246 in. while the upper surface of the rotation fixture base moved away from the pivot axis by 0.002446 in. Therefore, the net axial displacement of the tops of the mounting slides is seen to be away from the rotation fixture pivot by only 0.0002 in. This miniscule displacement of the tops of the adapter ring mounting slides showed that the room temperature offset of 11.096 in., when rounded, would still apply in this case. This is the value that is shown on the Space Electronics calculation reports for the Position No. 2 measurements.

During the TARE measurements, the growth of the fixtures was not balanced. Spreadsheet E-2 (Table 8) shows that (at least on the basis of the data recorded) the elongation of the rotation fixture arms was over twice the growth in the adapter ring height, causing a net displacement of 0.00127 in. at the tops of the adapter ring mounting slides away from the pivot. This is the same situation described in the previous section, i.e. where temperature changes occurred in the equipment causing their TARE positions to differ from their positions during the PART measurement. Section 10 provides the mathematical basis that allowed this phenomenon to be handled properly and the result reported there continues to apply.

12. SUMMARY AND CONCLUSIONS

The actual, as-tested CG position relative to the MMRTG datum at the center of a plane formed by the lower surface of the mounting pads was measured and found to be

$$X = 0.0968 \text{ in.}$$

$$Y = 0.0276 \text{ in.}$$

$$Z = 10.816 \text{ in.}$$

These data must be adjusted for MMRTG applications having a different physical configuration and to correct for known errors in the physical position of the mounting equipment during the TARE measurement as compared to the equipment positions during the PART measurements. Potential random measurement errors manifest in uncertainties in the test article's CG position in all coordinates. This section summarizes the applicable adjustments required to these data and the individual uncertainty contributions from various testing considerations described in this report to arrive at the best estimate of the CG position and its overall confidence interval. Adjustments to the measured CG position for specific applications of the MMRTG to account for hardware configurations that may differ from the configuration when tested are the responsibility of the design agency.

^m Spreadsheets from Appendix E have been assigned a sequential table number and are collected with other tables in this report.

The non-random physical position errors were evaluated in this report using the methodology developed in Sections 10 and 11. However, because these were so small (a 0.0006 in. correction to the Z component of the MMRTG CG position was calculated), it was decided instead to just include an allowance for this error in the uncertainties associated with the reported CG position.

12.1 Uncertainties Summary

Basis	Contribution (in.)	Reference
MP instrument moment statistical repeatability	0.005*	Table 6
Fixture re-positioning error	0.002	Footnote 9
Coordinates translation	0.001	Table 2
Tilt	0.003	Sections 8.4 and 9.1
Corrections for fixture temperature changes	0.001	Appendix E
Moments/weight uncertainty effect in CG	0.001	Section 9.1 & Table 4
Miscellaneous allowance	0.005	non-specific
Total estimated absolute uncertainty	0.018 in.	

* This value represents the maximum radial uncertainty within the rectangular prismatic confidence interval found in the statistical determination cited in Section 9.5. This conservative value was selected to use for estimating the overall spherical confidence interval as well, since the other uncertainties listed are generally not related to a particular coordinate direction.

12.2 Conclusions

The best estimated, corrected CG position for the MMRTG, configured as tested, was determined to lie at

$$X = 0.0968 \text{ in.}$$

$$Y = 0.0276 \text{ in.}$$

$$Z = 10.816 \text{ in.}$$

This point lies in the center of a spherical region having, with 99% certainty, a radius of 0.018 in. Thus, the estimated total uncertainty is comfortably enveloped within the PWR specified spherical uncertainty criterion of 10 mm (0.394 in.).

13. REFERENCES

1. PWR document No. EID-09038, Mars Science Laboratory Radioisotope Thermoelectric Generator Test Plan / Requirements
2. PWR Specification No. RJ00554, Design Requirements [for the Mars Science Laboratory Multi-Mission Radioisotope Thermoelectric Generator]
3. INL test procedure, RPS/HS-OI-28220, MMRTG Mass Properties Test
4. INL test procedure, SSPSF-OI-28200, Mass Properties Testing Station Operation
5. American Society for Metals, Metals Handbook 9th Ed., Vol. 2, *Properties and Selection: Non-ferrous Alloys and Pure Metals*, pp. 115-116.
6. J. S. Hunter, Design of Experiments, Westinghouse Learning Corporation (1966).

Table 1. Balancing the Mounting Fixtures

Test No.	Run No.	Max. Moment		Min. Moment		Maximum Variation (in-lb)
		Axis	Value (in-lb)	Axis	Value (in-lb)	
1	001566	90	2077.037	270	2076.110	0.927
2	001567	90	2076.749	270	2076.283	0.466
3	001568	90	2076.592	270	2076.418	0.174
4	001569	270	2076.489	0	2076.386	0.103
5	001570	90	2075.804	270	2075.666	0.138
6	001571	90	2075.838	180	2075.735	0.103

Table 2. Metrology Summary for the Mass Standard

Parameter	Definition (see Figures 27-31)	Value*	Units
Φ	Angle of the projection onto the X-Z plane, measured from the Z' axis	0.0046	degrees
θ	Actual angle, measured from the Z' axis	0.0052	degrees
ξ	Angle of the projection on the X-Y plane, measured from the X' axis	27.92	degrees
β	Angle of the projection onto the Y-Z plane, measured from the Z' axis	0.0024	degrees
X_0	Offset of the test article origin from that of the MP instrument along the X axis	-0.00273	inch
Y_0	Offset of the test article origin from that of the MP instrument along the Y axis	0.00276	inch
Z_0	Offset of the test article origin from that of the MP instrument along the instrument's Z axis	14.904	inch
X_{CG}	Measured position of the CG as measured on the MP instrument X axis	0.00053	inch
Y_{CG}	Measured position of the CG as measured on the MP instrument Y axis	0.00333	inch
Z_{CG}	Computed position of the CG as measured on the MP instrument's Z axis	26.134	inch
X'_{CG}	Computed position of the CG as measured on the X' axis of the mounting fixtures, $X'_{CG} = X_{CG} - X_0$	0.00326	inch
Y'_{CG}	Computed position of the CG as measured on the Y' axis of the mounting fixtures, $Y'_{CG} = Y_{CG} - Y_0$	0.00195	inch
Z'_{CG}	Computed position of the CG as measured on the Z' axis of the rotation fixture	11.226	inch
X''_{CG}	Computed position of the CG as measured on the X'' axis of the test article	0.00236	inch
Y''_{CG}	Computed position of the CG as measured on the Y'' axis of the test article	0.00101	inch
Z''_{CG}	Computed position of the CG as measured on the Z'' axis of the test article	11.226	inch

* Values are best-estimated results of multiple measurements.

Table 4. Parametric Evaluation of CG Uncertainty Contributors

Term	Units	Example Case No.						
		1	2	3	4	5	6	7
M_p^+	in-lb	2075	2075	2080	2090	2090	2090	2205
M_p^-	in-lb	2075	2075	2070	2060	2060	2060	1945
M_t^+	in-lb	2075	2075	2075	2075	2075	2075	2075
M_t^-	in-lb	2075	2075	2075	2075	2075	2075	2075
M_{net}	in-lb	0	0	5	15	15	15	130
Each δM	in-lb	0.1	0.2	0.1	0.1	0.2	0.3	0.3
W_{net}	lb	100	100	100	100	100	100	100
δW_g	lb	0.010	0.010	0.010	0.010	0.010	0.010	0.010
δW_a	lb	0.010	0.010	0.010	0.010	0.010	0.010	0.010
$[(\delta M_p^-)^2 + (\delta M_p^+)^2 + (\delta M_t^-)^2 + (\delta M_t^+)^2] / 4W_{net}^2$	in	1.00E-06	4.00E-06	1.00E-06	1.00E-06	4.00E-06	9.00E-06	9.00E-06
$M_{net}^{-2} / W_{net}^{-4} * (\delta W_g^{-2} + \delta W_a^{-2})$	in	0.00E+00	0.00E+00	5.00E-11	4.50E-10	4.50E-10	4.50E-10	3.38E-08
δCG	in	0.0010	0.0020	0.0010	0.0010	0.0020	0.0030	0.0030

Table 5. Confidence Intervals for PART and TARE Measurements

[illegible]

Table 6. Mass Properties Data and Calculations

Case No.	Test Description	Test Position & Run Numbers *				Metrology User Datum X [in] Y (or Z) [in]	CG Calculation Results		User CG Position Statistics								
		Position	PART	TARE	CG Calc.		Mach. CG X [in] Y (or Z) [in]	User CG X [in] Y (or Z) [in]	$Y_i - Y_{bar}$ X [in] Y (or Z) [in]	$(Y_i - Y_{bar})^2$ X [in ²] Y (or Z) [in ²]							
FL-1	MMRTG-MSL Witnessed test of flight generator, 05/01-05/02/2009	1	1552	1559	1562	-0.0030	0.0030	0.0938	0.0306	0.0968	0.0276						
		1	1553	1560													
		1	1554	1561													
		2	1555	1556	1626	-0.0140	-11.0960	0.0871	-0.2803	0.1008	10.8157						
		2	1557														
MS-1	Mass Standard Witnessed test No.1 in preparation for flight-generator tests, 04/29-04/30/2009	1	1538	1544	1550	-0.0030	0.0030	0.0002	0.0031	0.0032	0.0001	0.00013	-0.00058	1.563E-08	3.306E-07		
		1	1539	1545													
		1	1540	1546													
		2	1541	1547	1627	-0.0140	-11.0960	-0.0073	0.1298	0.0063	11.2258	0.00078	-0.00038	6.008E-07	1.406E-07		
		2	1542	1548													
MS-2	Mass Standard Supplementary test No.1 in preparation for flight-generator tests, 06/02 - 06/08/2009	2	1543	1549													
		1	1572	1578	1584	-0.0030	0.0030	-0.0005	0.0041	0.0025	0.0011	-0.00058	0.00043	3.306E-07	1.806E-07		
		1	1573	1579													
		1	1574	1580													
		2	1575	1581	1628	-0.0140	-11.0960	-0.0082	0.1305	0.0058	11.2265	0.00027	0.00032	7.562E-08	1.056E-07		
MS-3	Mass Standard Supplementary test No. 2, 06/08 - 06/09/2009	2	1576	1582													
		2	1577	1583													
		1	1597	1599	1601	-0.0030	0.0030	0.0019	0.0028	0.0049	-0.0002	0.00183	-0.00088	3.331E-06	7.656E-07		
		2	1598	1600	1629	-0.0140	-11.0960	-0.0089	0.1299	0.0051	11.2259	-0.00043	-0.00028	1.806E-07	7.563E-08		
		1	1606	1608	1610	-0.0030	0.0030	-0.0013	0.0047	0.0017	0.0017	-0.00138	0.00103	1.891E-06	1.051E-06		
MS-4	Mass Standard Supplementary test No. 4, 06/28 - 06/30/2009	2	1607	1609	1630	-0.0140	-11.0960	-0.0091	0.1305	0.0049	11.2265	-0.00063	0.00032	3.906E-07	1.056E-07		
												Sum, Position 1:		5.568E-06	2.328E-06		
												Sum, Position 2:		1.248E-06	4.275E-07		
Mass-Standard Statistics		Position	n	v	$t_{v,0.005}$	$Y_{bar} (average)$ X [in] Y (or Z) [in]		$Y_{bar} (average)$ X [in] Y (or Z) [in]		$Y_{bar} (average)$ X [in] Y (or Z) [in]		$s^2 = ((n-1) * \sum (Y_i - Y_{bar})^2) / (n-1)$ X [in ²] Y (or Z) [in ²]		$\sqrt{(s^2/n)}$ X [in] Y (or Z) [in]		$\pm t_{v,0.005} \sqrt{(s^2/n)}$ X [in] Y (or Z) [in]	
		1	4	3	5.841		0.00008 0.00368		0.00308 0.00068				1.856E-06 7.759E-07		6.811E-04 4.404E-04		3.979E-03 2.572E-03
		2	4	3	5.841		-0.00838 0.13018		0.00553 11.22618				4.158E-07 1.425E-07		3.224E-04 1.887E-04		1.883E-03 1.102E-03
		* Note: Run numbers in bold font indicate those selected for the associated calculations.															
		CG mean value: $\eta = Y_{bar} \pm t_{v,0.005} \sqrt{(s^2/n)}$															

Table 7. Adjustments for Temperature Changes, (Spreadsheet E-1), Room Temp > Pre-test (Map K-2)

As Adjusted to Alternate Temperature														
As Designed, Nominal Values From Pro-E Output						As Adjusted to Alternate Temperature								
Adapter Ring Datum: Centerline, plane of feet														
Item No.	Description	Material	Item Mass [lb]	Y-position of CG [in]	Item Moment [in-lbf]	Nominal (RT) Item Height from Datum [in]	Temp. Change [F]	Material Expansion Coefficient [F ⁻¹]	Thermal Growth (+) or Shrinkage (-) [in]	Temp-Adjusted Item Height [in]	CG Shift from Datum [in]	Adjusted Y-CG position [in]	Adjusted Moment from Datum [in-lbf]	Check Calc. W _g ΔY [in-lbf]
1	Base	Al	10.2627	4.31521	44.28571	6.0000	23.8	1.3100E-05	1.8707E-03	6.0019	1.3454E-03	4.3166	44.2995	0.0138
2	Mounting Slide	Ti	0.541263	5.84668	3.16459	1.7500	23.8	9.0000E-06	3.7485E-04	1.7504	1.2521E-03	5.8479	3.1653	0.0007
3	Mounting Slide	Ti	0.541261	5.84667	3.16457	1.7500	23.8	9.0000E-06	3.7485E-04	1.7504	1.2521E-03	5.8479	3.1653	0.0007
4	Mounting Slide	Ti	0.541228	5.84662	3.16435	1.7500	23.8	9.0000E-06	3.7485E-04	1.7504	1.2521E-03	5.8479	3.1650	0.0007
5	Mounting Slide	Ti	0.54124	5.84664	3.16444	1.7500	23.8	9.0000E-06	3.7485E-04	1.7504	1.2521E-03	5.8479	3.1651	0.0007
6	Flat Washer, 1/4-in	Al	1.42E-03	6.02250	0.00857						8.0172E-04	6.0233	0.0086	0.0000
7	Flat Washer, 1/4-in	Al	1.42E-03	6.02250	0.00857						8.0172E-04	6.0233	0.0086	0.0000
8	Flat Washer, 1/4-in	Al	1.42E-03	6.02250	0.00857						8.0172E-04	6.0233	0.0086	0.0000
9	Flat Washer, 1/4-in	Al	1.42E-03	6.02250	0.00857						8.0172E-04	6.0233	0.0086	0.0000
10	Socket-Hd Screw, 1/4x1-1/4-in long	Ti	1.37E-02	5.62602	0.07706						8.0172E-04	5.6268	0.0771	0.0000
11	Socket-Hd Screw, 1/4x1-1/4-in long	Ti	1.37E-02	5.62602	0.07706						8.0172E-04	5.6268	0.0771	0.0000
12	Socket-Hd Screw, 1/4x1-1/4-in long	Ti	1.37E-02	5.62602	0.07706						8.0172E-04	5.6268	0.0771	0.0000
13	Socket-Hd Screw, 1/4x1-1/4-in long	Ti	1.37E-02	5.62602	0.07706						8.0172E-04	5.6268	0.0771	0.0000
14	Bracket	Al	3.09E-02	5.62611	0.17382						1.7927E-03	5.6279	0.1739	0.0001
15	Bracket	Al	3.09E-02	5.62611	0.17382						1.7927E-03	5.6279	0.1739	0.0001
16	Bracket	Al	3.09E-02	5.62611	0.17382						1.7927E-03	5.6279	0.1739	0.0001
17	Bracket	Al	3.09E-02	5.62611	0.17382						1.7927E-03	5.6279	0.1739	0.0001
18	Socket-Hd Screw, No. 10x1/2-in long		4.25E-03	5.62500	0.02389						1.7538E-03	5.6268	0.0239	0.0000
19	Socket-Hd Screw, No. 10x1/2-in long		4.25E-03	5.62500	0.02389						1.7538E-03	5.6268	0.0239	0.0000
20	Socket-Hd Screw, No. 10x1/2-in long		4.25E-03	5.62500	0.02389						1.7538E-03	5.6268	0.0239	0.0000
21	Socket-Hd Screw, No. 10x1/2-in long		4.25E-03	5.62500	0.02389						1.7538E-03	5.6268	0.0239	0.0000
22	Socket-Hd Screw, No. 10x1/2-in long		4.25E-03	5.62500	0.02389						1.7538E-03	5.6268	0.0239	0.0000
23	Socket-Hd Screw, No. 10x1/2-in long		4.25E-03	5.62500	0.02389						1.7538E-03	5.6268	0.0239	0.0000
24	Socket-Hd Screw, No. 10x1/2-in long		4.25E-03	5.62500	0.02389						1.7538E-03	5.6268	0.0239	0.0000
25	Socket-Hd Screw, No. 10x1/2-in long		4.25E-03	5.62500	0.02389						1.7538E-03	5.6268	0.0239	0.0000
26	Locator Screw, special		1.08E-02	5.62578	0.06102						1.7540E-03	5.6275	0.0610	0.0000
27	Locator Screw, special		1.08E-02	5.62578	0.06102						1.7540E-03	5.6275	0.0610	0.0000
28	Locator Screw, special		1.08E-02	5.62578	0.06102						1.7540E-03	5.6275	0.0610	0.0000
29	Locator Screw, special		1.08E-02	5.62578	0.06102						1.7540E-03	5.6275	0.0610	0.0000
30	Flat Washer, 3/8-in		2.93E-03	7.46900	0.02185	0.0625	23.8	1.3100E-05	1.9486E-05	0.0625	2.1207E-03	7.4711	0.0219	0.0000
31	Flat Washer, 3/8-in		2.93E-03	7.46900	0.02185	0.0625	23.8	1.3100E-05	1.9486E-05	0.0625	2.1207E-03	7.4711	0.0219	0.0000
32	Flat Washer, 3/8-in		2.93E-03	7.46900	0.02185	0.0625	23.8	1.3100E-05	1.9486E-05	0.0625	2.1207E-03	7.4711	0.0219	0.0000
33	Flat Washer, 3/8-in		2.93E-03	7.46900	0.02185	0.0625	23.8	1.3100E-05	1.9486E-05	0.0625	2.1207E-03	7.4711	0.0219	0.0000
34	Shoulder Screw		2.90E-02	7.25630	0.21007	0.4635	23.8	9.0000E-06	9.9282E-05	0.4636	2.0613E-03	7.2584	0.2101	0.0001
35	Shoulder Screw		2.90E-02	7.25630	0.21007	0.4635	23.8	9.0000E-06	9.9282E-05	0.4636	2.0613E-03	7.2584	0.2101	0.0001
36	Shoulder Screw		2.90E-02	7.25633	0.21072	0.4635	23.8	9.0000E-06	9.9282E-05	0.4636	2.0613E-03	7.2584	0.2108	0.0001
37	Shoulder Screw		2.90E-02	7.25633	0.21072	0.4635	23.8	9.0000E-06	9.9282E-05	0.4636	2.0613E-03	7.2584	0.2108	0.0001
			-----	-----	-----								-----	
	Sums		12.81680		59.34567								59.3629	0.0172
	CG, above bottom of mounting feet: Pro-E output show s:			4.630302 in 4.630305									4.6316 in 0.0013 in 0.0013 in	
									CG, above bottom of mounting feet: Magnitude of CG movement (new - nominal):					
									Check: Change in CG _A					

Table 7. (cont.)

[illegible]

Note: Items in RED font are directly changed; others just move along with these. BLUE font numbers are parameters subject to user variation

4.631007	in
0.00070	in
0.00070	in

Table 8. (cont.)

Rotation Fixture - Simple														As Designed, Nominal Values										As Adjusted to Alternate Temperature									
Datum: Centerline, bottom of base plate, 19.1 in from pivot at R.T.																																	
Alternate Datum: Centerline, at pivot																																	
Item No.	Description	Material	Item Mass [lbf]	Y-position of CG [in]	Item Moment [in-lbf]	RT Item Length Perpendicular to datum [in]	Temp. Change [F]	Material Expansion Coefficient [F ⁻¹]	Thermal Growth (+) or Shrinkage (-) [in]	Temp-Adjusted Item Height ppd [in]	CG Shift from Datum [in]	Adjusted Y-CG position [in]	Adjusted Moment from Datum [in-lbf]	Check Calc. W _j *ΔY _j [in-lbf]																			
1	Pumb Stantions (above Oblique junction)	Al	7.1773	4.5250	32.4773	9.050	10	1.31E-05	1.19E-03	9.0512	5.93E-04	4.5256	32.4815	0.00425																			
2	Pumb Stantions (below Oblique junction)	Al	7.1773	13.5750	97.4318	9.050	10	1.31E-05	1.19E-03	9.0512	1.78E-03	13.5768	97.4446	0.01276																			
3	Oblique Braces (approximate)	Al	7.9307	12.0667	95.6973	10.000	10	1.31E-05	1.31E-03	10.0013	1.84E-03	12.0685	95.7119	0.01460																			
4	Footpads (8x)	Al	5.4400	17.8500	97.1040	0.5	10	1.31E-05	6.55E-05	0.5001	2.40E-03	17.8524	97.1171	0.01308																			
5	Base Plate	Al	75.1503	18.6000	1397.7962	1.000	10	1.31E-05	1.31E-04	1.0001	2.50E-03	18.6025	1397.9843	0.18803																			
Sums			102.87565		1720.5066								1720.7394	0.2327																			
CG, below pivot: Pro-E output show s:				16.724139	in					CG, below pivot: Magnitude of CG _{Tn} movement (new - nominal): Check: Change in CG _{Tn}		16.726401 0.00226 0.00226	in in in																				
Upper Stantions (above pivot)			7.7265			22.5																											
Total fixture sums			110.6021		(Pro-E model show s actual of 108.88)																												

Table 9. Spreadsheet B-1 - Y Offset Constructions Characteristics

View (cf., Fig. 14)	Cradle-Pin Position	ΔP Direction (cf., App. B)	
		Y-axis Ambiguous	Y-axis <i>Not</i> Ambiguous
2 (+), 4 (-)	Near	Red	Black
2 (+), 4 (-)	Away	Black	Red
1 (-), 3 (+)	Near	Black	Red
1 (-), 3 (+)	Away	Red	Black



Figure 1. Leveling the MP instrument



Figure 2. Equipment setup for calibrating the MP instrument



Model : KSR1320-1500	RunNumber : 001603
Version : 4.2.3	Date : June 26, 2009
Serial : 2938/72818	Time : 11:24
	Operator : Chris Browning

CG Calibration Results

Readings

	Step 1 Readings (counts)	Step 1 Angles (deg)	Step 2 Readings (counts)	Step 2 Angles (deg)
Reading Position 1 :	84259.0	0.000	36810.2	0.000
Reading Position 2 :	60468.0	90.000	60616.1	90.000
Reading Position 3 :	36843.1	180.000	84285.9	180.000
Reading Position 4 :	60656.9	270.000	60488.3	270.000

Excessive Variation : FALSE

Calculated Calibration Values

Calibration Constant :	0.03427590 lb-in/counts	PASSED
Calibration Angle :	359.809 deg	PASSED
	PASSED	

Shawn R. Miller
6/26/09

Figure 3. MP instrument calibration report

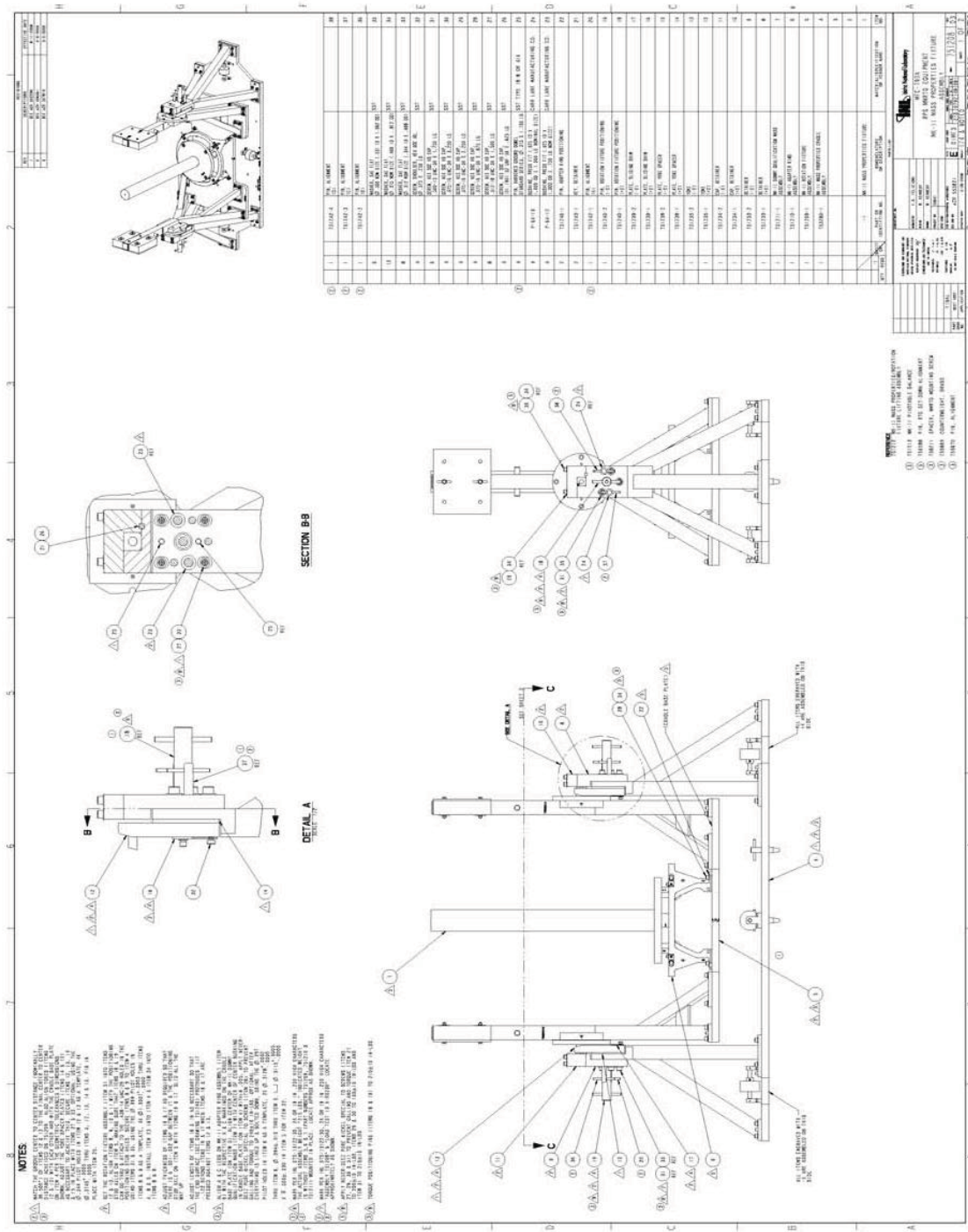


Figure 4. MP Mark-II mounting fixtures (mass standard shown installed)

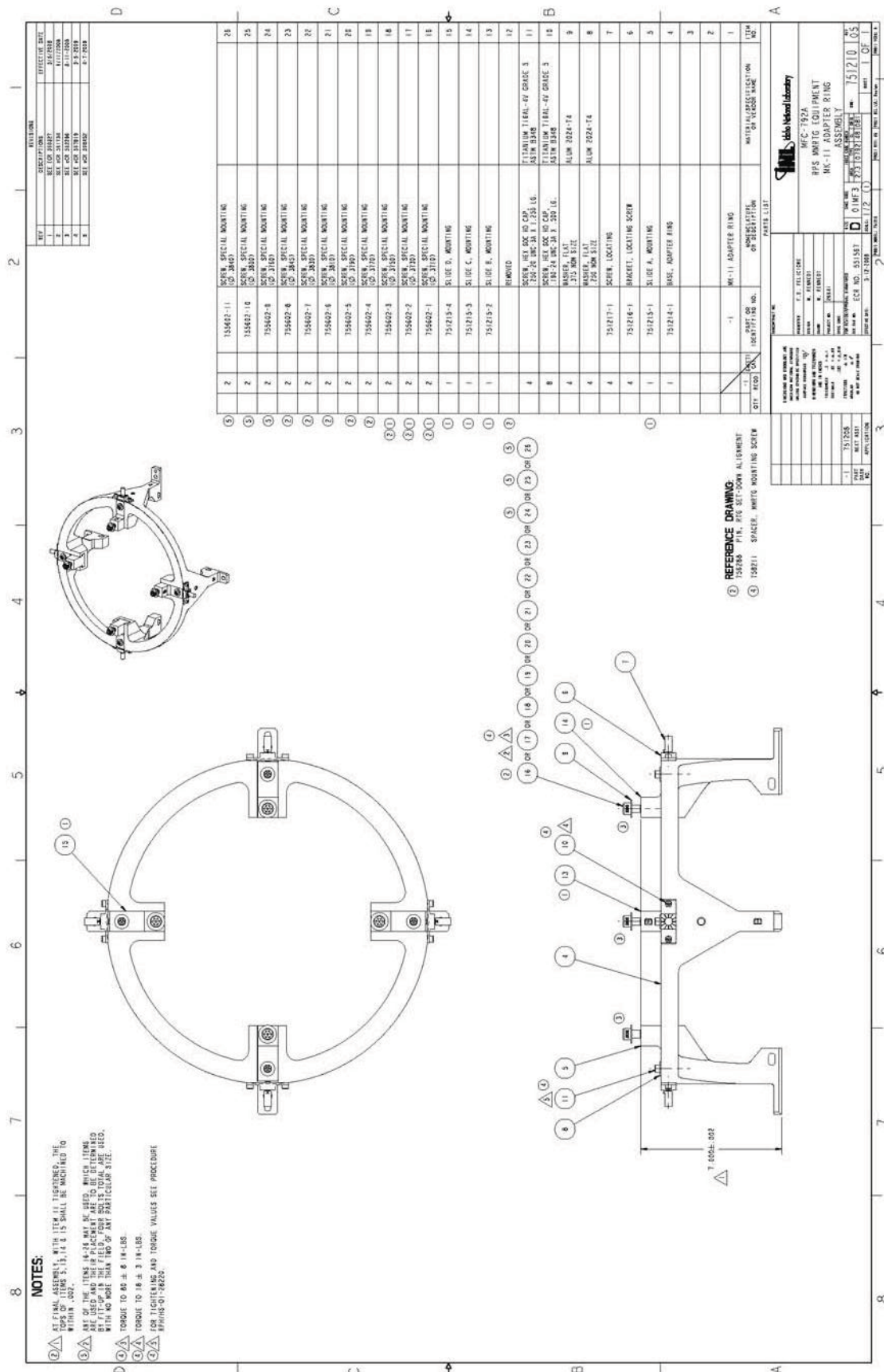


Figure 5. Mark-II (aluminum) adapter ring

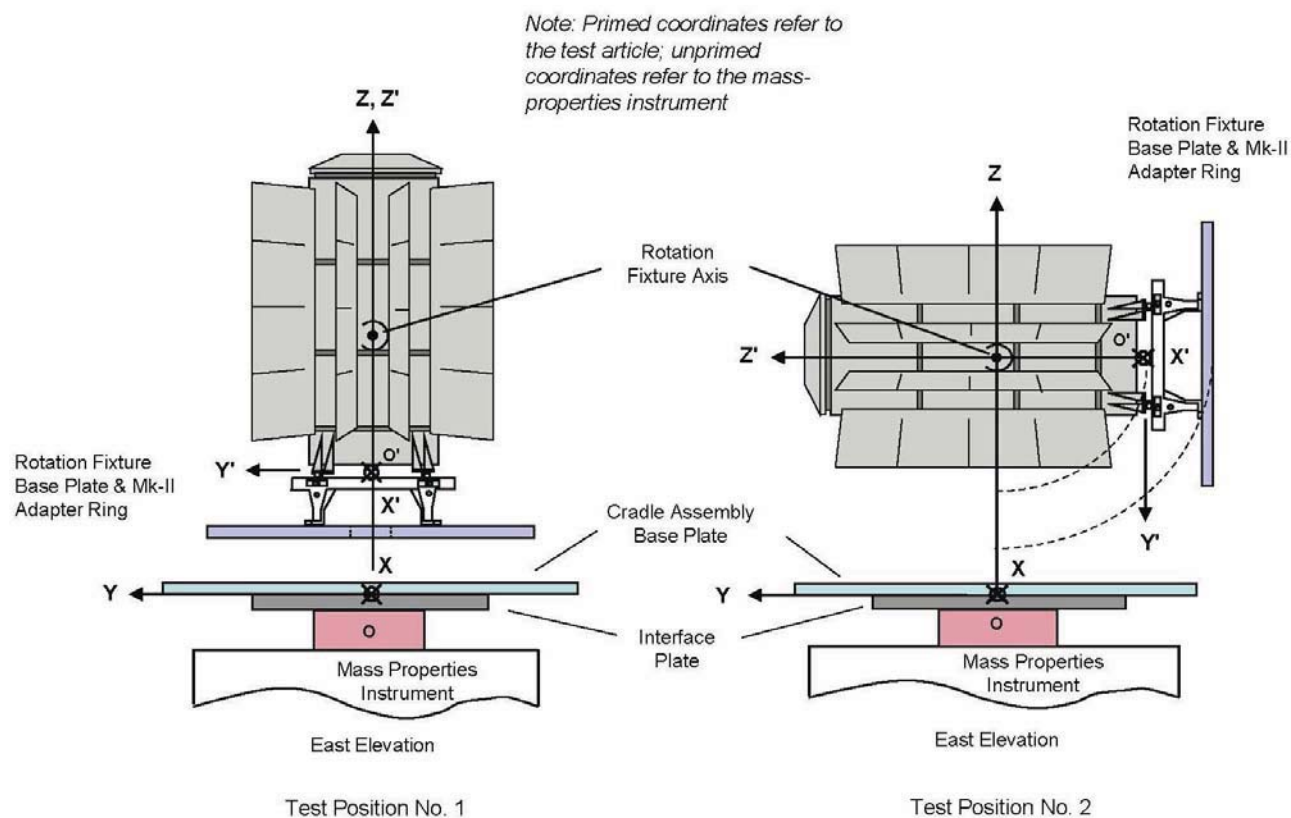
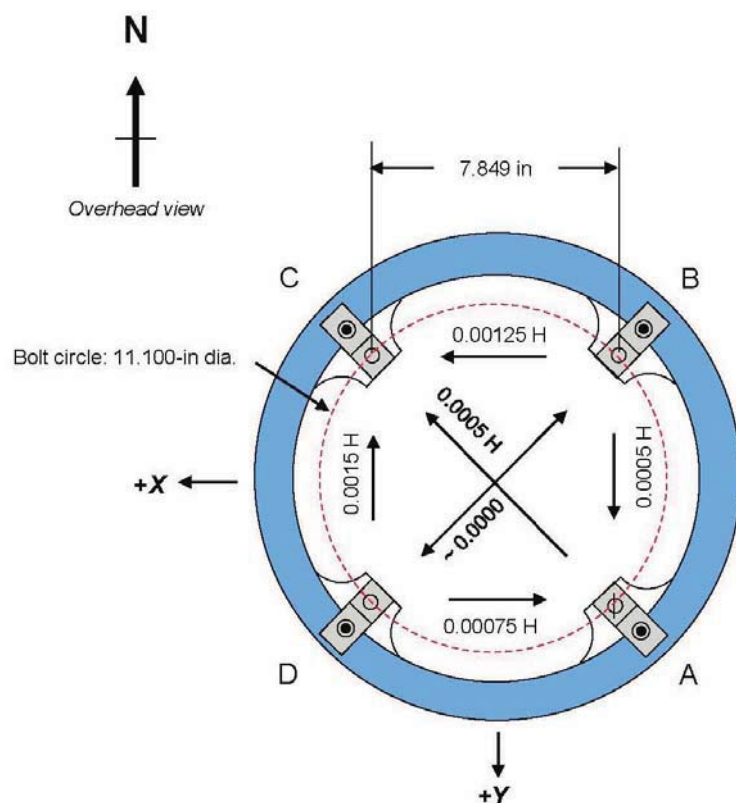


Figure 6. Coordinate systems and test positions



Measurement Equipment:

Type: Starrett Precision Level, 0.0005 in/ft/div

ID Number: S/N A0661

Calibration Due Date: 08 June 2010

Measurement Date: 02 July 2009

Remarks: Level placed on top of adjacent & diagonal mounting slides; arrowheads denote the high side (H) of the level. Measurements indicated are in *in/ft*, as read on instrument.

Measurements

<i>path</i>	<i>as read</i> [in/ft]	<i>actual</i> [in]
DABC	0.00150	0.000981
DC	0.00150	0.000981
ABC	0.00075	0.0004906
AC	0.00050	0.0004625

Therefore, an apparent discrepancy of
ABC-AC 0.000250 0.0000281

Figure 7. Final level checking of the MP mounting fixtures



Figure 8. Precision transit setup for alignment determination

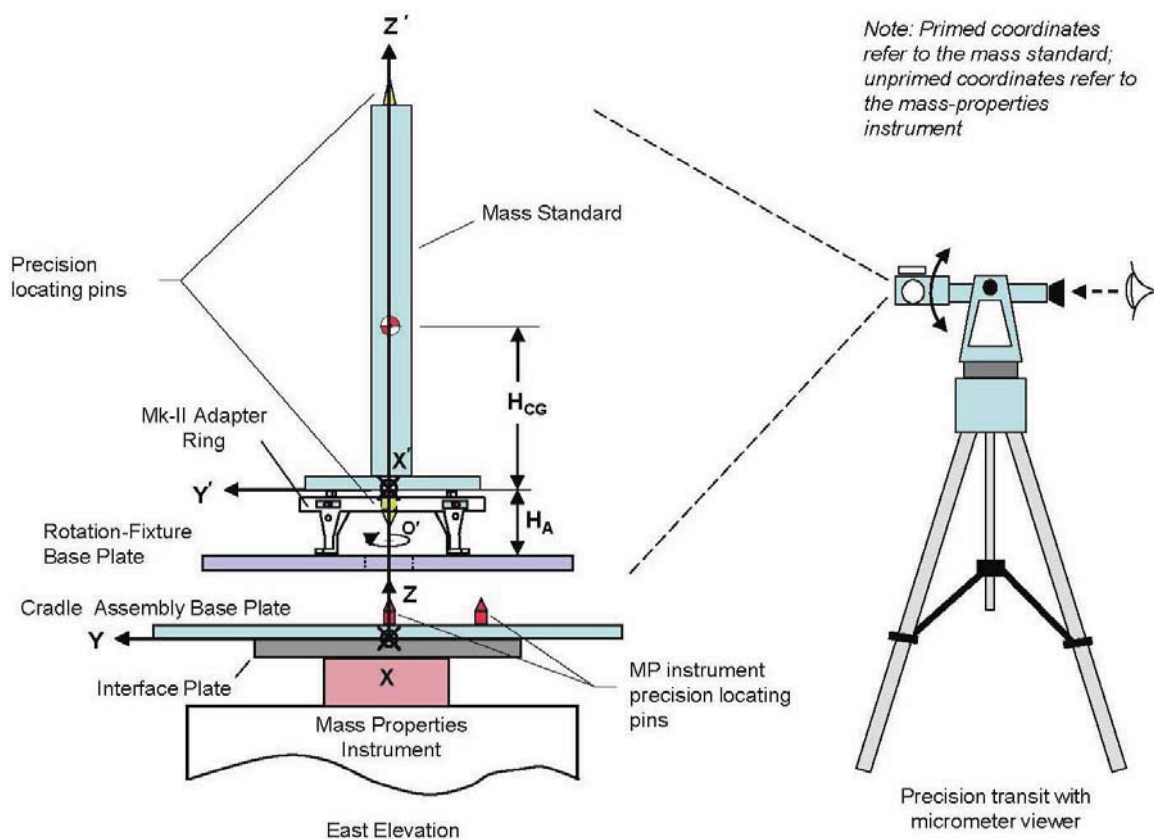


Figure 9. Determining offsets of coordinate systems

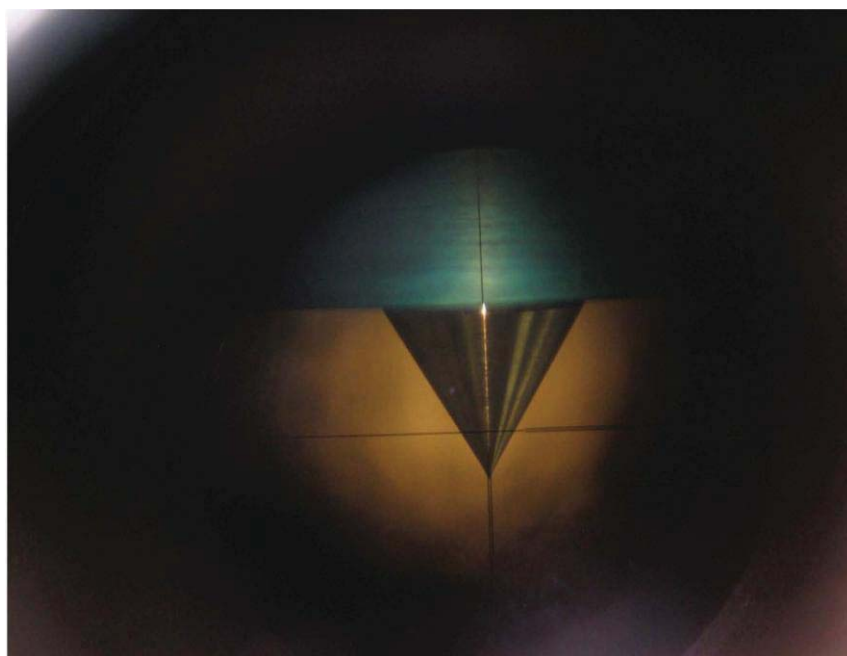


Figure 10. Typical view of lower alignment pin through precision transit

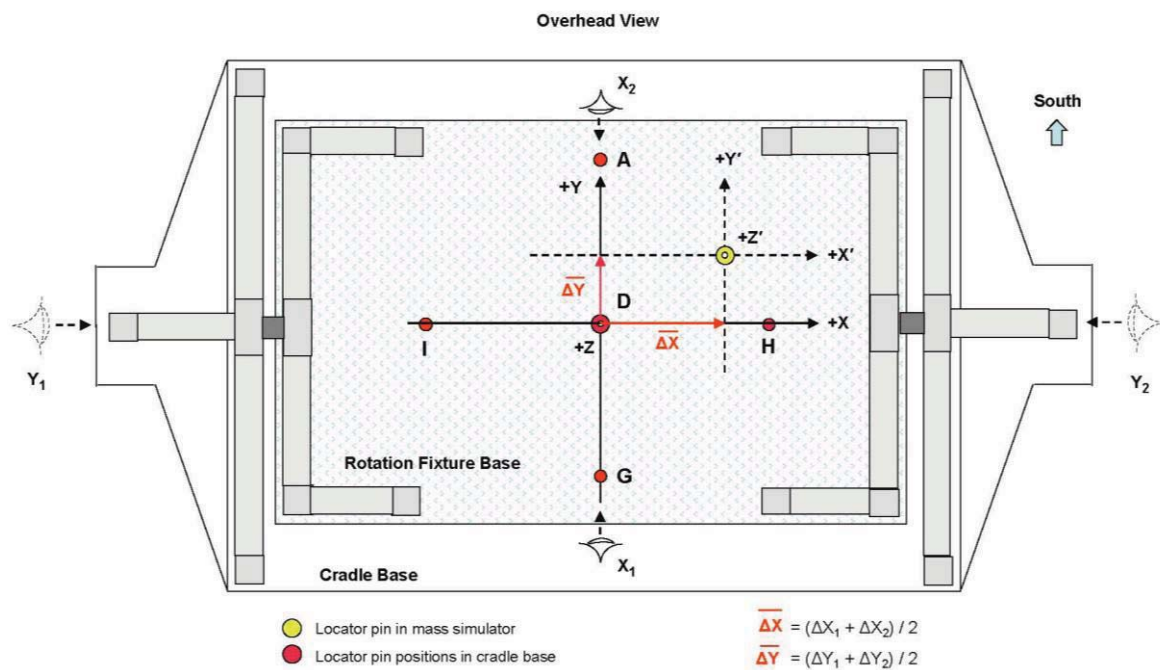


Figure 11. Determining offsets of test article relative to MP instrument

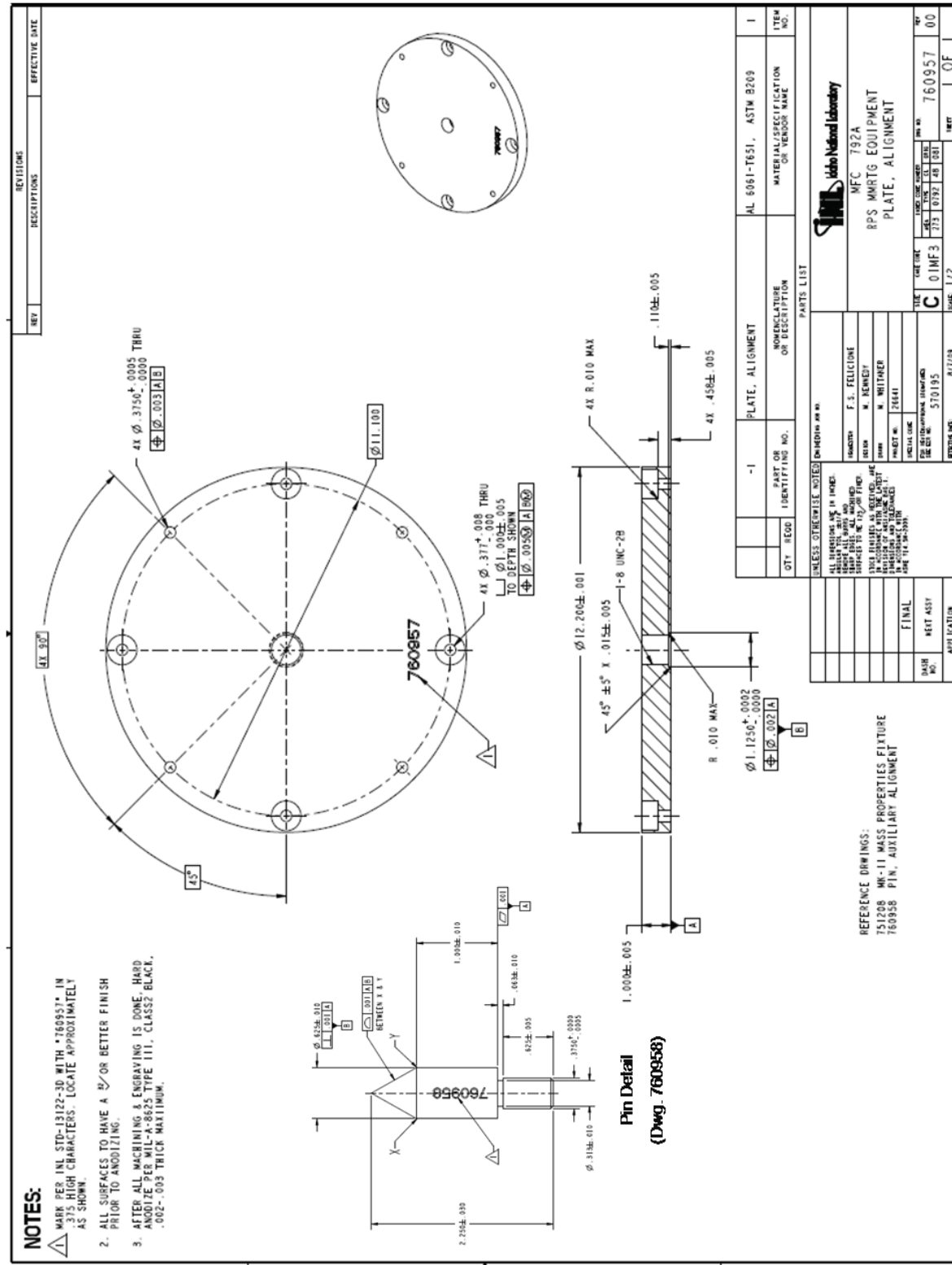


Figure 12. Auxiliary alignment flange (pin detail superimposed)

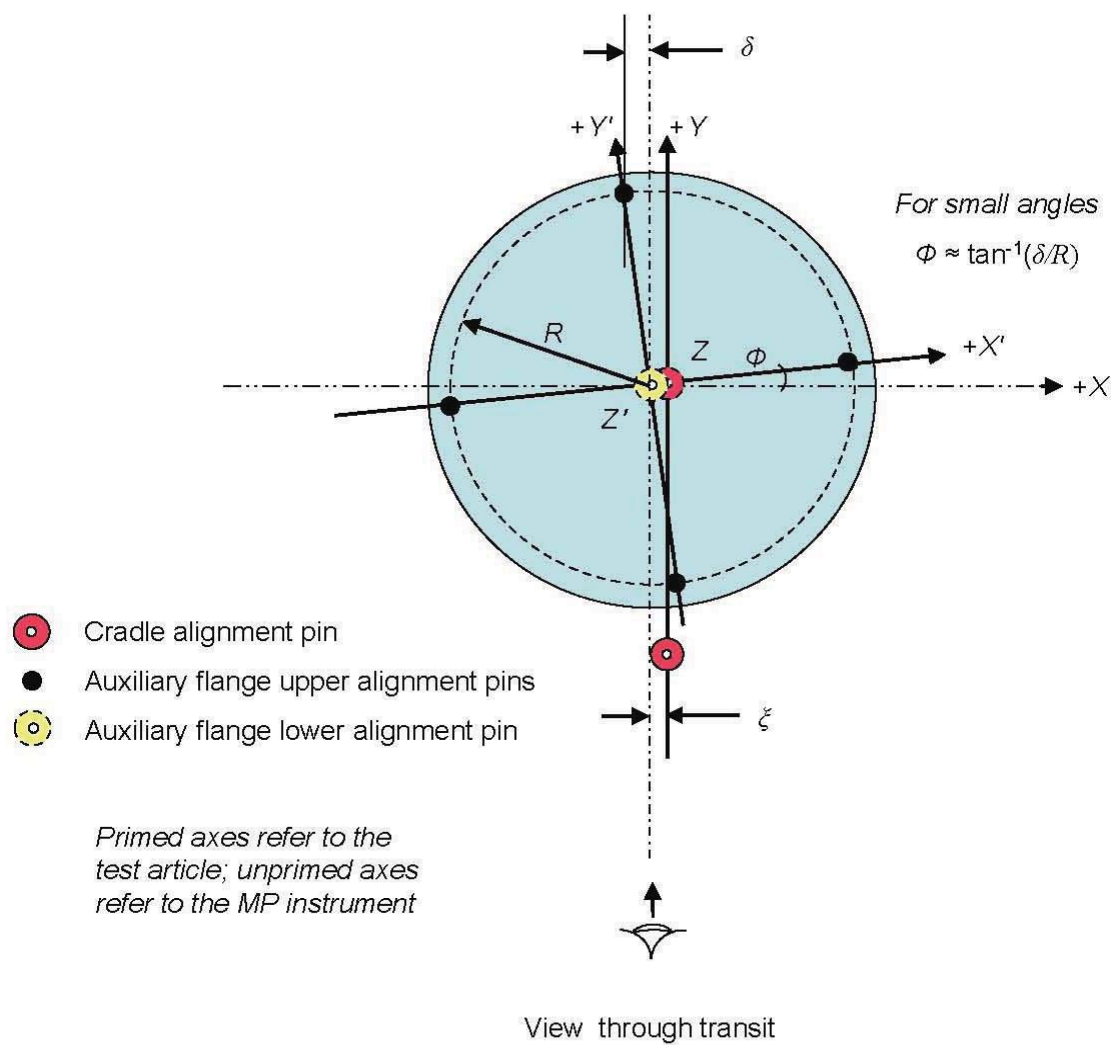


Figure 13. Rotational alignment of the test article and MP instrument

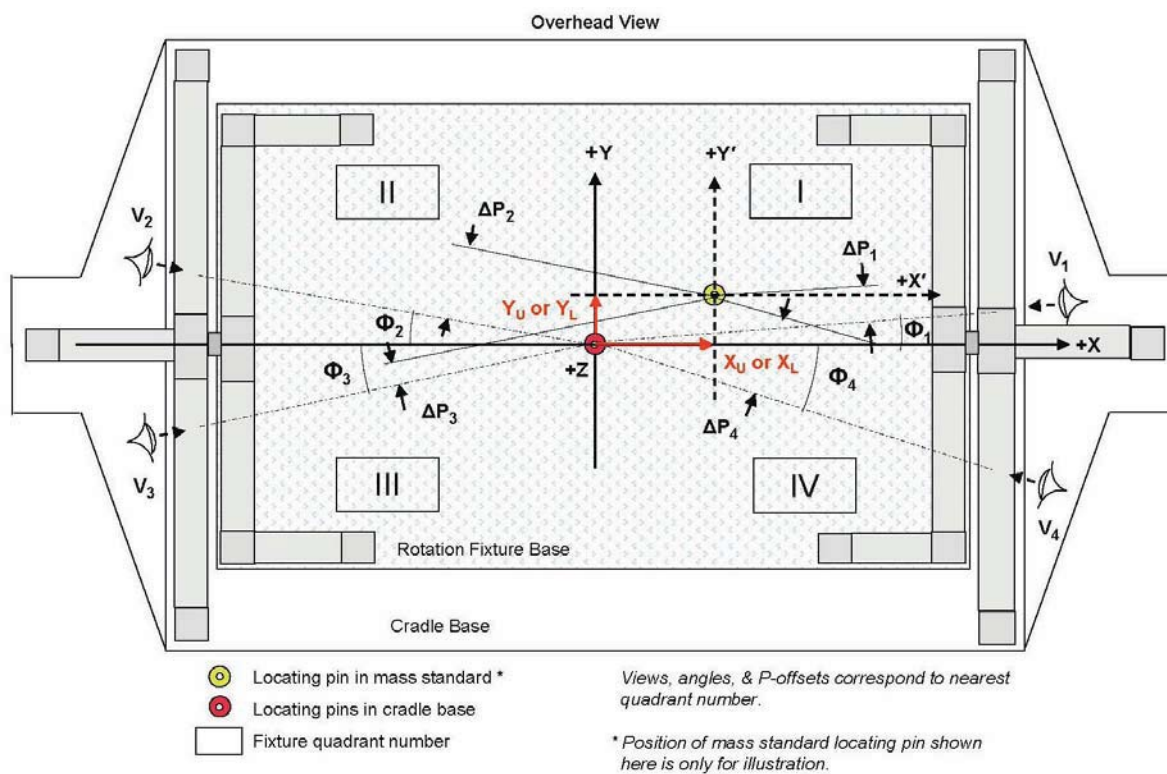


Figure 14. Oblique viewing angles to determine the Y offset of the test article coordinates



Figure 15. Oblique perspective to determine Y offset

Note: +/- signs in the view labels and figure caption indicate the applicable signs for the axes. For this construction A & ΔP are always positive.

Locating Pins, Position No. 1

- Locating pin in cradle base center
- Locating pin in mass standard
- Alternate position satisfying criteria

Measured: Φ , ΔP

Known: ΔX

View No. 2 (+) or No. 4 (-)

$$A = \Delta P / \sin(\Phi)$$

$$B = A - |\Delta X|$$

$$\Delta P_0 = |\Delta X| \sin(\Phi)$$

If $\Delta P > \Delta P_0$

for V2 (+) $i = +1$ ($\Delta Y > 0$)

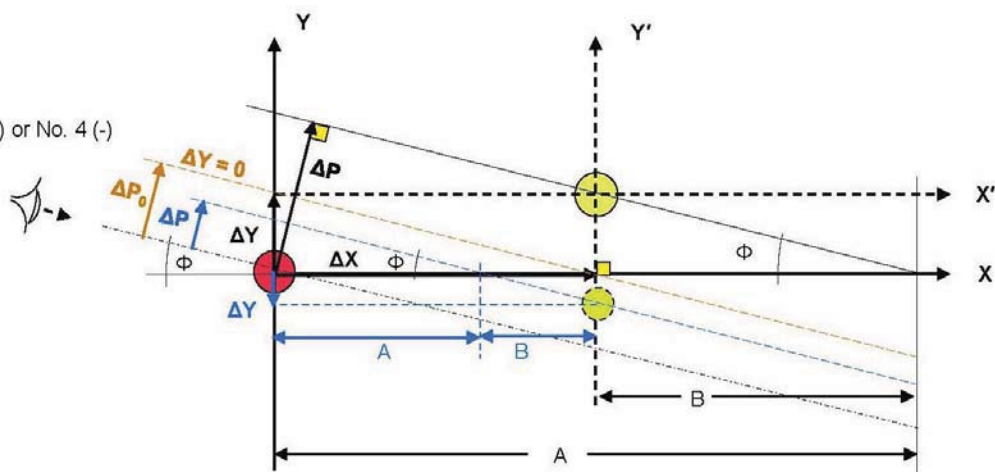
for V4 (-) $i = -1$ ($\Delta Y < 0$)

If $\Delta P < \Delta P_0$

for V2 (+) $i = -1$ ($\Delta Y < 0$)

for V4 (-) $i = +1$ ($\Delta Y > 0$)

$$\Delta Y = i|B| \tan(\Phi)$$



Selected construction depends on view, position of the cradle pin, and direction (left or right) of ΔP .

Figure 16. Typical construction to determine ΔY

Unprimed symbols refer to the MP instrument coordinates. Primed symbols refer to a parallel coordinate system displaced to the test-article origin. Double-primed symbols refer to a displaced and rotated coordinate system centered on the test article origin and aligned to the principal axes.

Basic Dimensions

$$H = 31.980 \text{ in}$$

$$P_U = 1.8844$$

$$P_L = 3.405$$

$$Z_0 = 14.900 \text{ (per Fig. 26)}$$

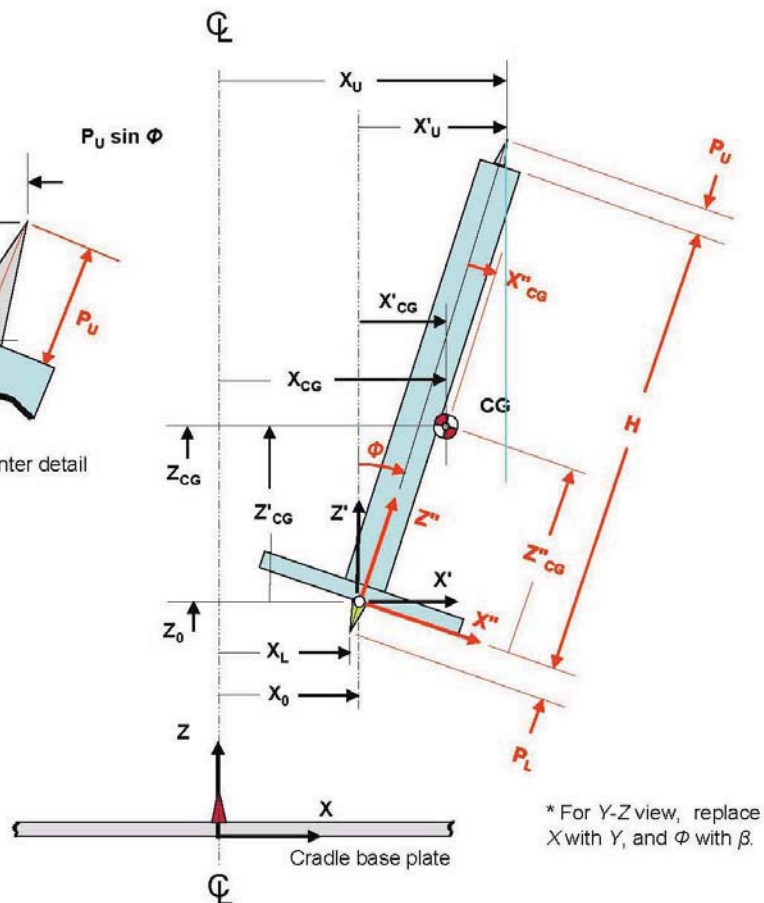
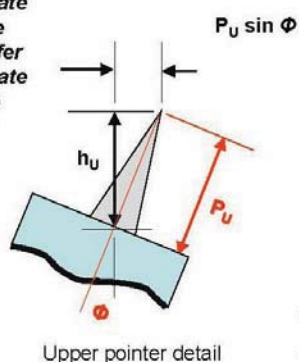
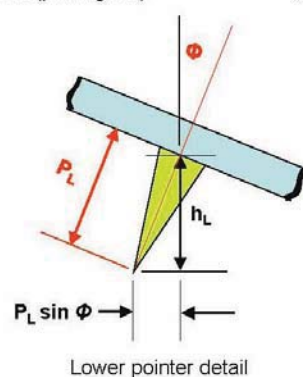


Figure 17. Tilt geometry model in X-Z view (exaggerated)

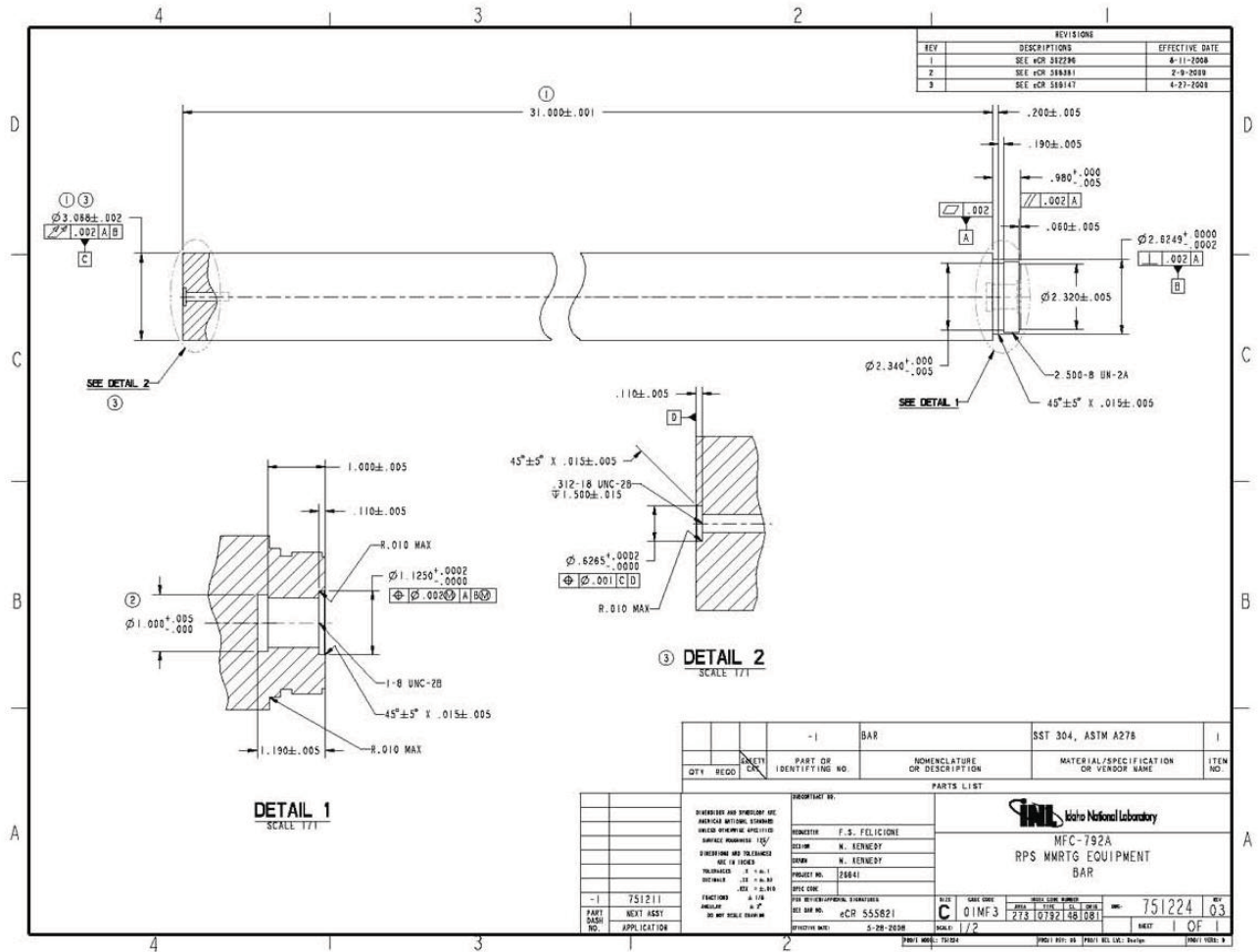


Figure 18. Mass standard column

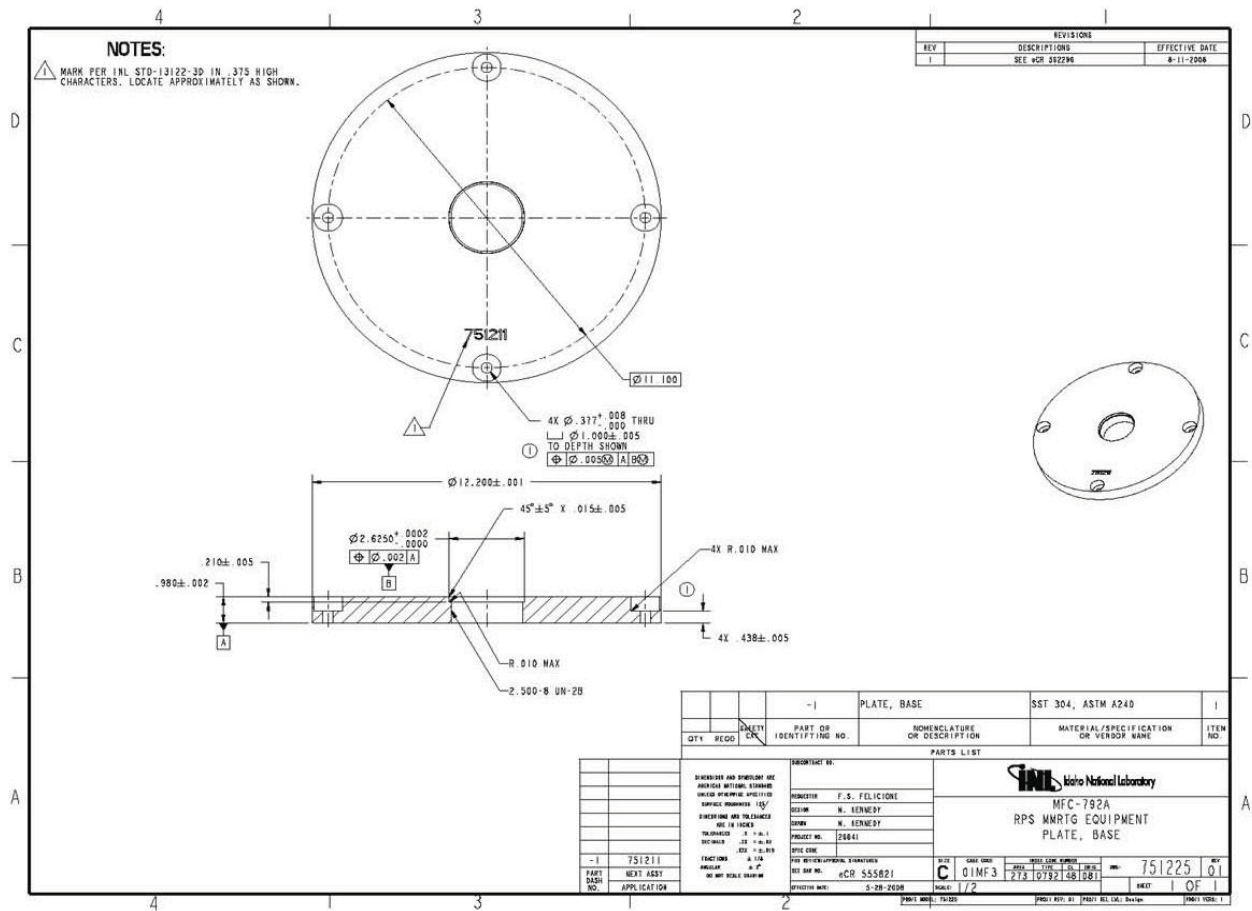


Figure 19. Mass standard base flange

```

VOLUME = 3.4072535e+02 INCH^3
SURFACE AREA = 6.0522181e+02 INCH^2
AVERAGE DENSITY = 2.9000000e-01 POUND / INCH^3
MASS = 9.8810350e+01 POUND

CENTER OF GRAVITY with respect to _751211 coordinate frame:
X Y Z 0.0000000e+00 1.1230146e+01 0.0000000e+00 INCH

INERTIA with respect to _751211 coordinate frame: (POUND * INCH^2)

INERTIA TENSOR:
Ixx Ixy Ixz 2.3679464e+04 0.0000000e+00 0.0000000e+00
Iyx Iyy Iyz 0.0000000e+00 6.7918022e+02 1.9867289e-02
Izx Izy Izz 0.0000000e+00 1.9867289e-02 2.3679470e+04

INERTIA at CENTER OF GRAVITY with respect to _751211 coordinate frame:
(POUND * INCH^2)

INERTIA TENSOR:
Ixx Ixy Ixz 1.1217879e+04 0.0000000e+00 0.0000000e+00
Iyx Iyy Iyz 0.0000000e+00 6.7918022e+02 0.0000000e+00
Izx Izy Izz 0.0000000e+00 0.0000000e+00 1.1217885e+04

PRINCIPAL MOMENTS OF INERTIA: (POUND * INCH^2)
I1 I2 I3 6.7918022e+02 1.1217879e+04 1.1217885e+04

ROTATION MATRIX from _751211 orientation to PRINCIPAL AXES:
0.00000 0.00000 1.00000
1.00000 0.00000 0.00000
0.00000 1.00000 0.00000

ROTATION ANGLES from _751211 orientation to PRINCIPAL AXES (degrees):
angles about x y z 0.000 90.000 90.000

RADI OF GYRATION with respect to PRINCIPAL AXES:
R1 R2 R3 2.6217501e+00 1.0655017e+01 1.0655020e+01 INCH
    
```

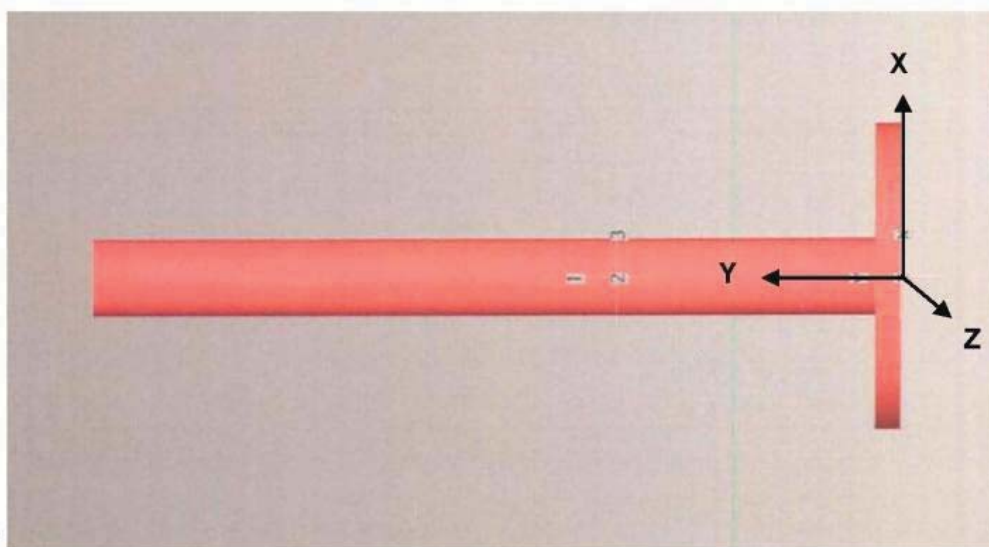


Figure 20. Pro-E software determination of CG in the mass standard

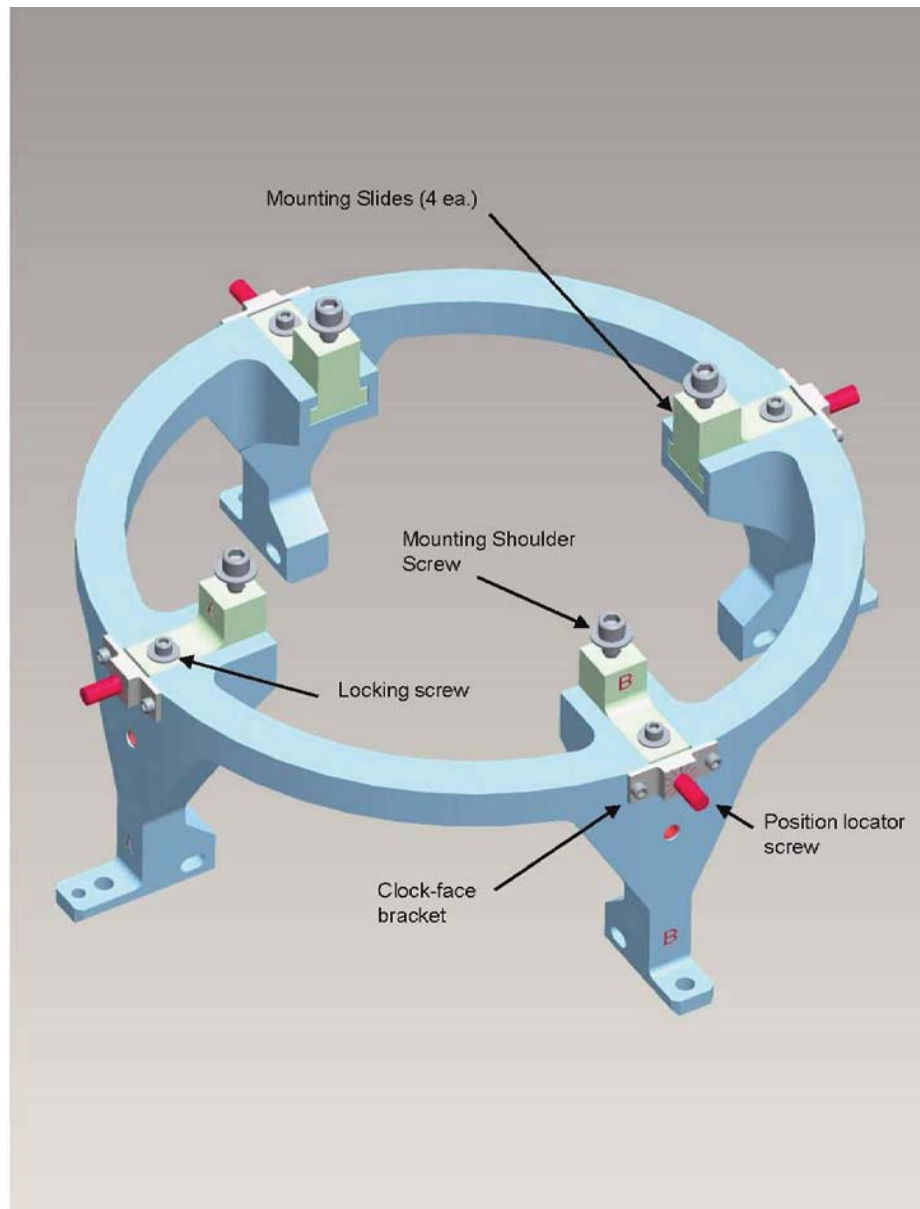


Figure 21. Mk-II (aluminum) adapter ring alignment features

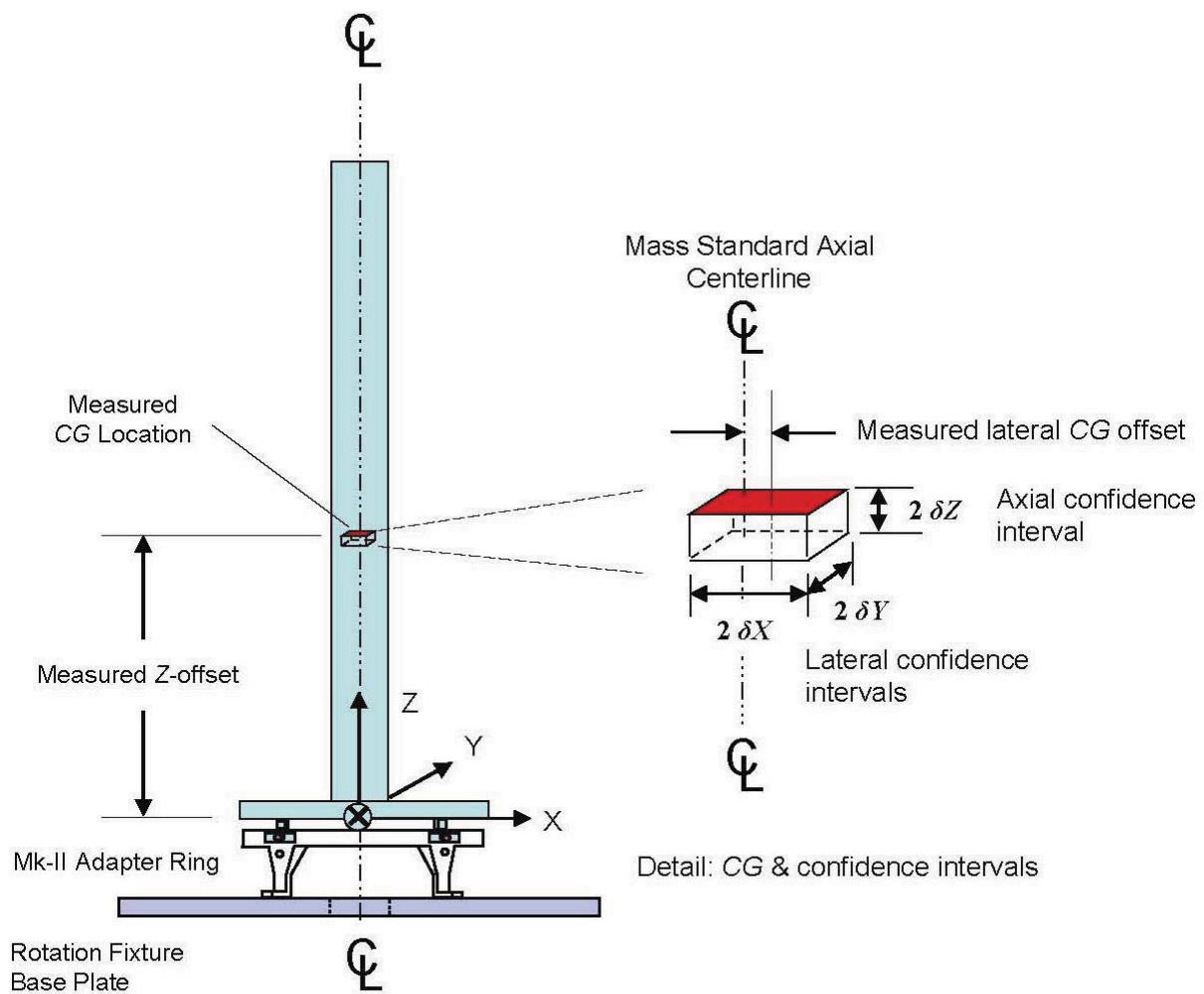


Figure 22. Measured CG location and confidence intervals for the mass standard

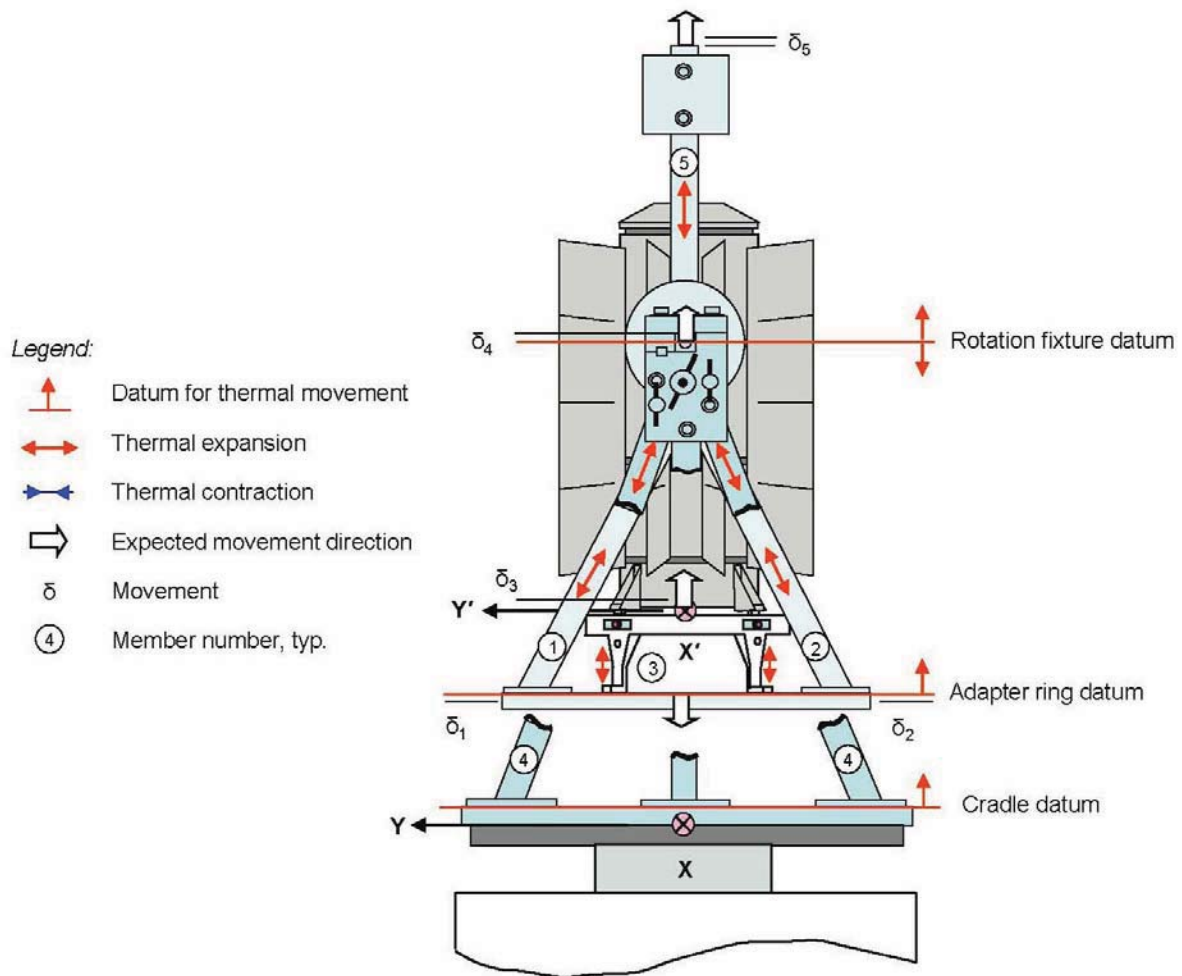
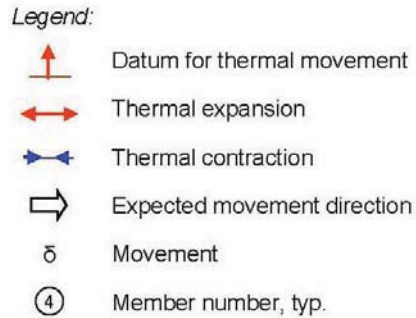


Figure 23. Thermal effects after mounting the MMRTG



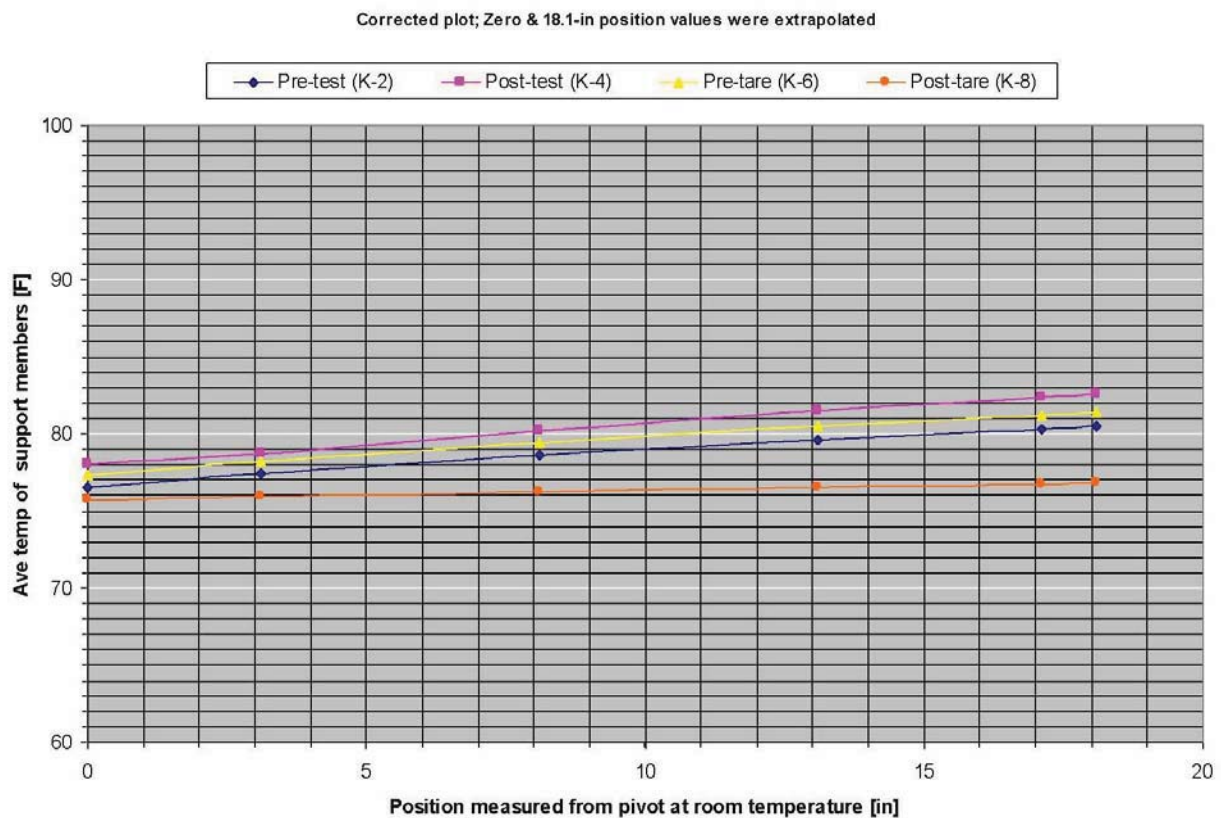


Figure 25. Temperature distributions in the rotation fixture (see temperature maps, Appendix D)

Basic Geometric Dimensions: $L_C = 26.000$ in $L_R = 18.100$ in $L_{AR} = 7.004$ in $P_L = 3.405$ in
 Y_O (Test article datum offset from pivot axis) $= L_R - L_{AR} = 18.100 - 7.004 = 11.096$ in
Measured Data: Y_2 (Space Electronics Y-component measurement, Position No. 2)
 $Z'_{CG} = Y_2 - Y_O$ (algebraic)

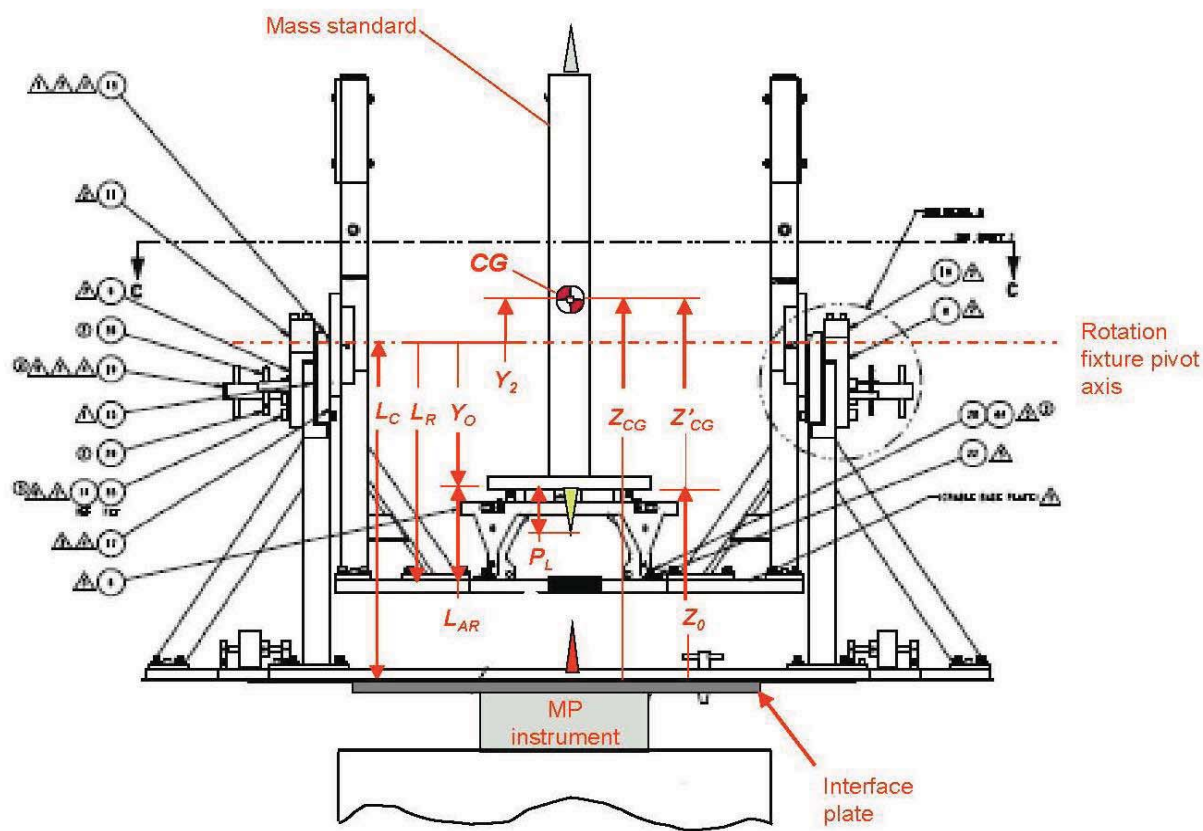


Figure 26. Key dimensions for the mounting fixtures and the test article CG position

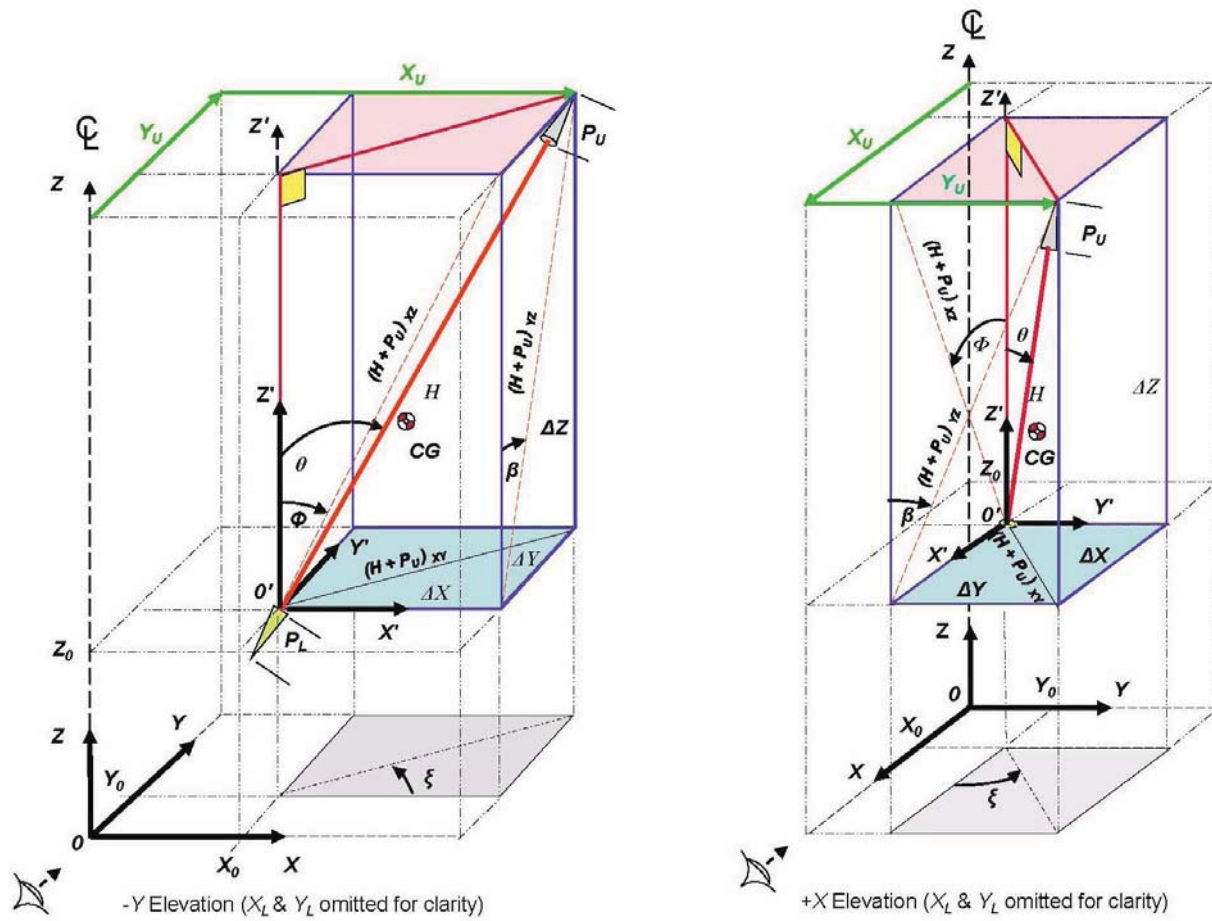


Figure 27. Alignment geometry, isometric views (see Figures 28 & 29)

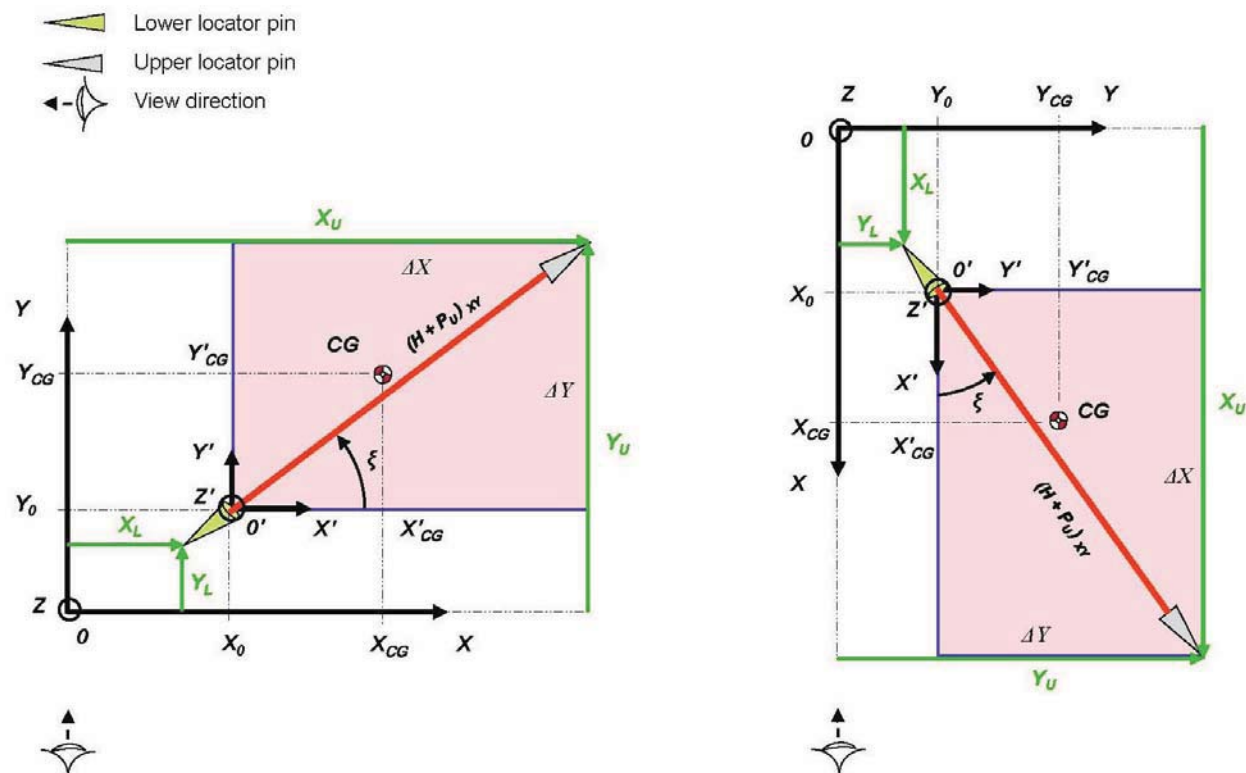


Figure 28. Alignment geometry, overhead views, X-Y, Position No. 1

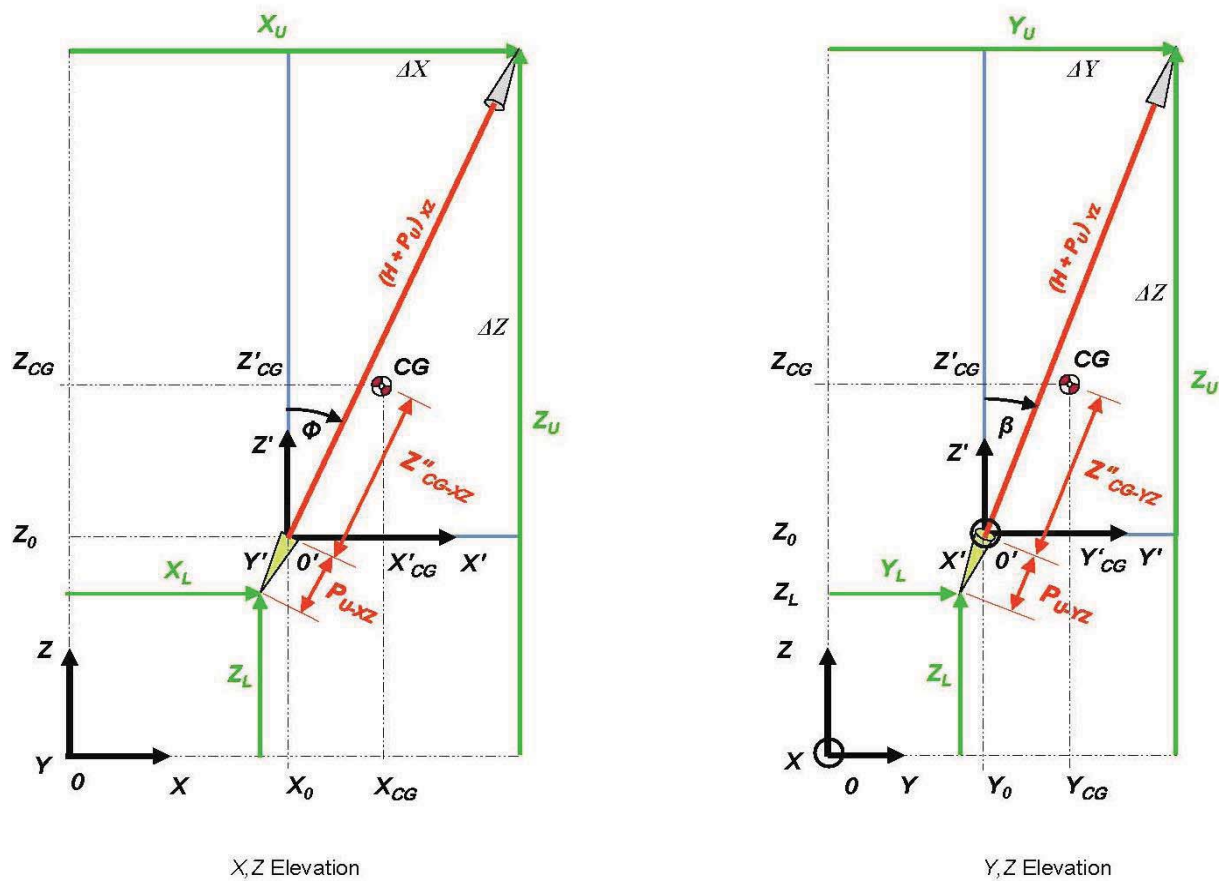


Figure 29. Alignment geometry, elevation views

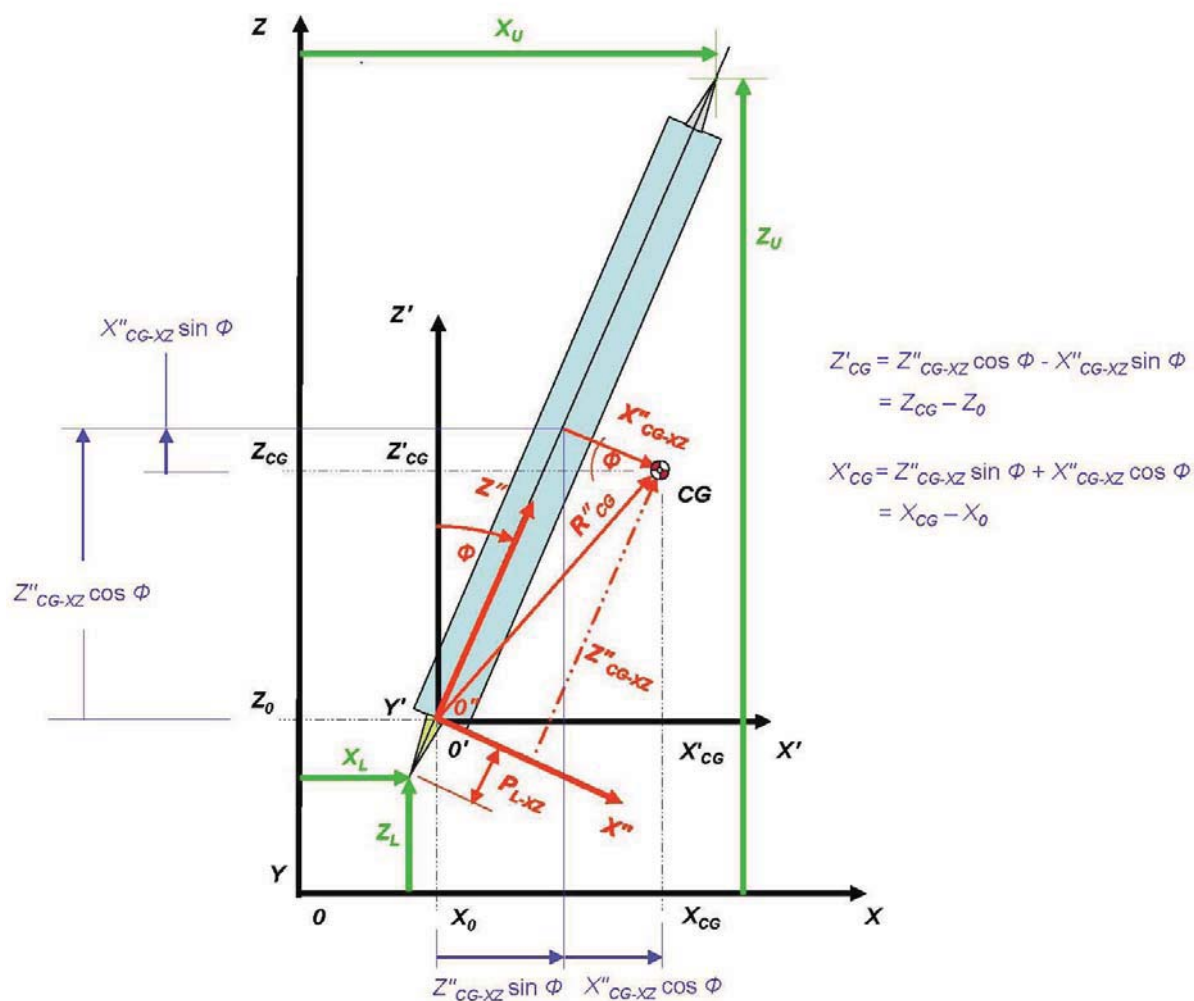
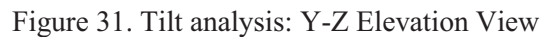


Figure 30. Tilt Analysis: X-Z Elevation View



INTENTIONALLY BLANK

Appendix A

INL Mass Properties Testing System Drawings List

Appendix A

INL Mass Properties testing System Drawings Listing

Drawing Number	Titleⁿ
751208	Mk-II Mass Properties Fixture Assembly
751209	Mk-II Rotation Fixture Assembly
751210	Mk-II Adapter Ring Assembly
751211	Mk-II Dummy Qualification Mass Assembly
751212	Mk-II Mass Properties/Rotation Fixture Lifting Assembly
751213	Mk-II Pivotal Balance Assembly
751214	Base, Adapter Ring
751215	Slide A, Mounting
751216	Bracket, Locating Screw
751217	Screw, Locating
751218	Rotation Fixture Cradle Assembly
751219	Axle,, Positioning Stub
751220	Counterbalance
751221	Plate, Counterbalance Mounting
751222	Rod, Pivot
751223	Weight, Balance
751224	Bar
751225	Plate, Base
751226	Pin, Cross Hair Locating
751227	Pin, Locating
751228	Brace, Lifting
751229	T-Bar, Mass Properties Fixture
751230	T-Bar, Rotation Fixture
751231	Plate, Cradle Base
751232	Brace, Cradle Support
751233	Retainer
751234	Cap, Retainer
751235	Yoke
751236	Bracket, Mounting Counterbalance, Inside
751237	Bracket, Mounting Counterbalance, Outside
751238	Plate, Yoke Spacer
751239	Plate, Sliding Shim

ⁿ All drawings include the building number, *MFC-792A*, and the topic designation, *RPS MMRTG [Equipment]* in their titles. These are omitted in the list in this appendix.

751240	Pin, Rotation Fixture Positioning
751241	Pin, Cradle Locating
751242	Pin, Alignment
751243	Key, Retainer
751244	Counterbalance
751245	Rod, Counterbalance Mounting
751246	Pin, Adapter Ring Positioning
753280	Mk-II Mass Properties Cradle Assembly
755602	Screw, Special Mounting
755820	Plate, Cradle Base
755821	Brace, Cradle Support
756288	Pin, RTG Set-down Alignment
758211	Spacer, MMRTG Mounting Screw
759601	Close Coupled Y-Cable Socket
759869	Counterweight, Brass
759870	Pin, Alignment (Adaptor Ring to MP Fixture)
760033	Pin, Auxiliary Mass-Simulator Alignment
760120	Push Tool, Sliding Shim
760957	Plate, Alignment
760958	Pin, Auxiliary Alignment

INTENTIONALLY BLANK

Appendix B

Geometric Constructions for Determining Offsets of the Coordinate Systems

Appendix B

Geometric Constructions for Determining Offsets of the Coordinate Systems

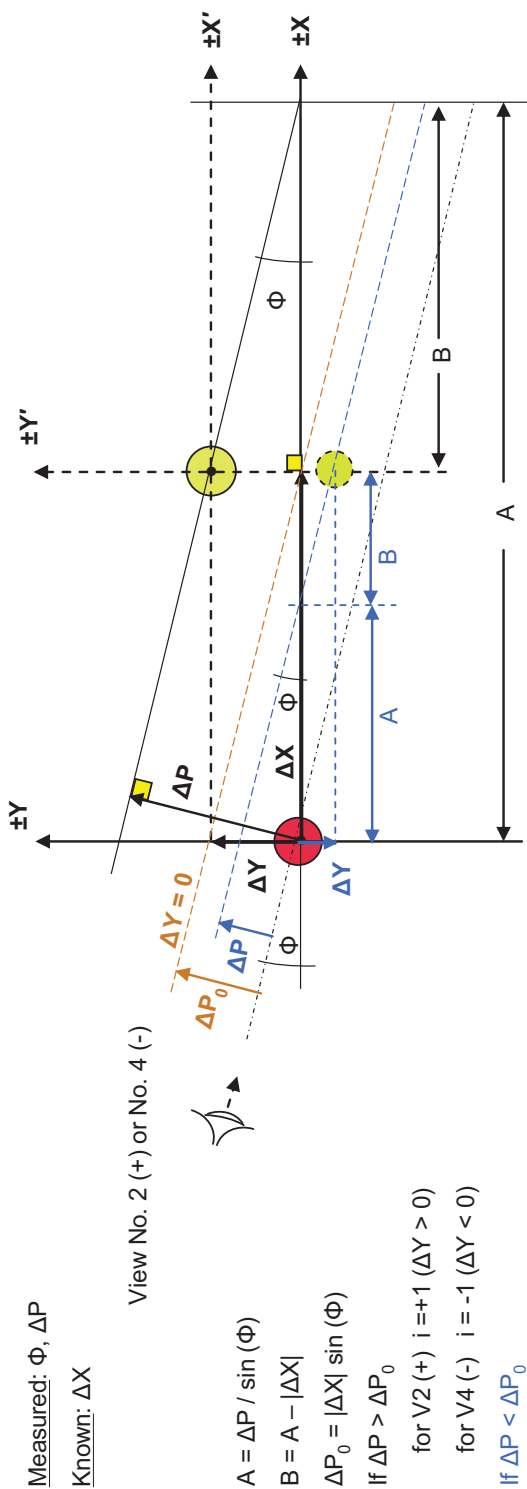
Note: target items that are not lined up with the reference point will lie either to the left or the right of the reference point when viewed in the transit. The micrometer on the transit has a **red** scale to measure the offset of targets lying to the left of the reference and a **black** scale to measure targets lying to the right. To ensure that the field metrology data were recorded with the minimum of operator interpretation, the target positions were recorded using the red or black indications accordingly. Constructions in this appendix continued this use of the terminology, **Red** or **Black**.

Half of the constructions shown in this appendix, viz., Constructions A, C, E, and G involve viewing angles that would allow the Y offset of the target pin to be either on the positive or negative side of the Y axis even though remaining on the same side of the reference pin when viewed in the transit. An “alternate position” target pin symbol is included on these constructions to handle this possibility. The critical displacement for reversal of the axis side is denoted as ΔP_0 on these constructions (at $\Delta P = \Delta P_0$ the Y offset is zero). The algorithms listed on the constructions properly account for this apparent ambiguity. The circumstances when this can or cannot occur are summarized in Spreadsheet (B-1) (Table 9).^o This occurs when larger or smaller offsets ΔP have the geometric possibility to cause the mass standard target pin to cross the X axis as the magnitude of ΔP varies but without reversing its position relative to the reference pin.

^o Spreadsheet(s) from Appendix B have been assigned a sequential table number and are collected with other tables in this report.

Note: +/- signs in the view labels and figure caption indicate the applicable signs for the axes. For this construction A & ΔP are always positive.

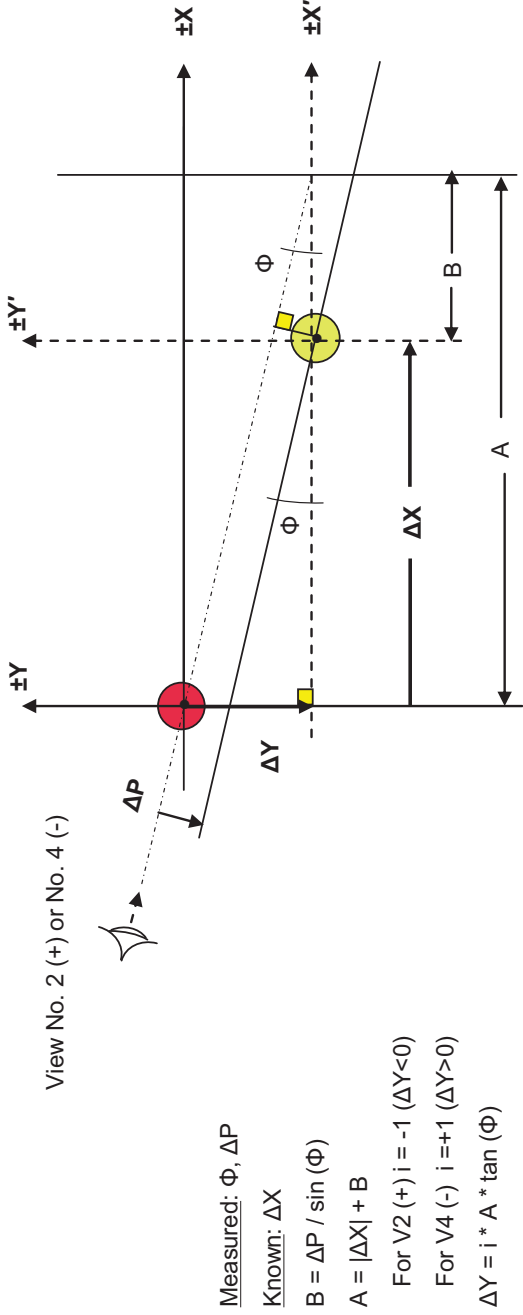
- Locating Pins, Position No. 1
- Locating pin in cradle base center
 - Locating pin in mass standard
 - Alternate position satisfying criteria



Construction A. Determination of ΔY , View No. 2 (+) or No. 4 (-) when cradle pin is **near**, ΔP is **red**

Note: +/- signs in the view labels and figure caption indicate the applicable signs for the axes. For this construction A & ΔP are always positive.

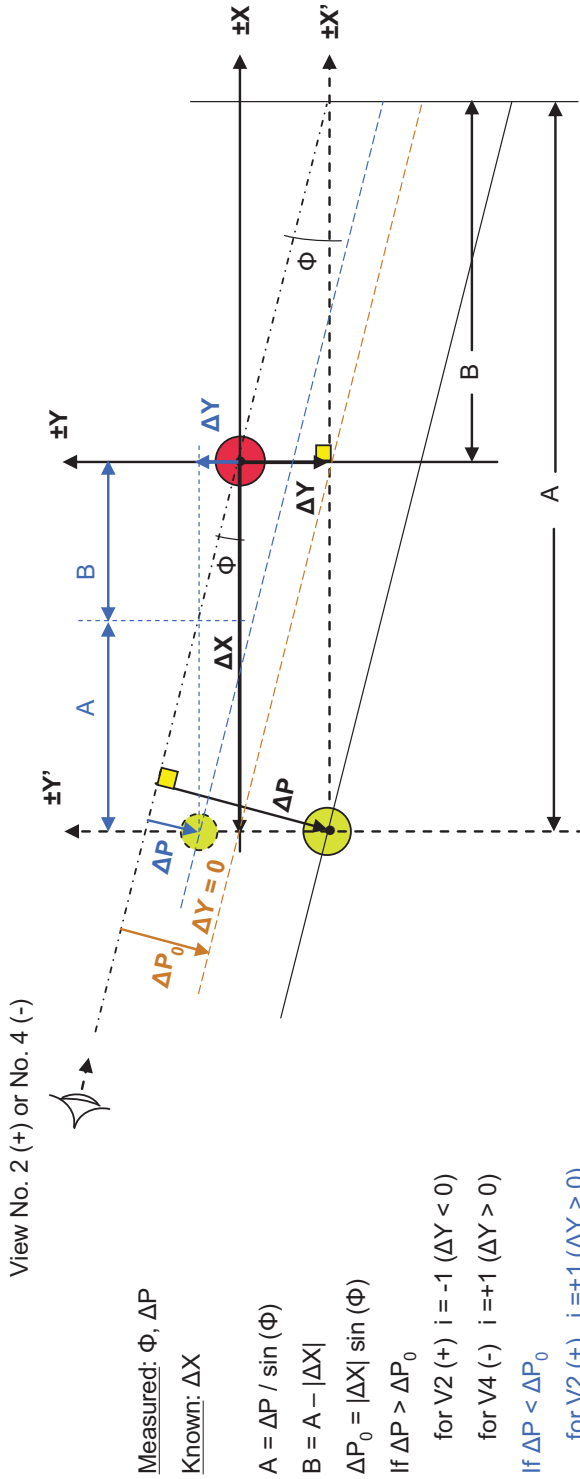
- Locating Pins, Position No. 1
- Locating pin in cradle base center
 - Locating pin in mass standard
- (No alternate position satisfying criteria)



Construction B. Determination of ΔY , View No. 2 (+) or No. 4 (-) when cradle pin is **near**, ΔP is **black**

Note: +/- signs in the view labels and figure caption indicate the applicable signs for the axes. For this construction A & ΔP are always positive.

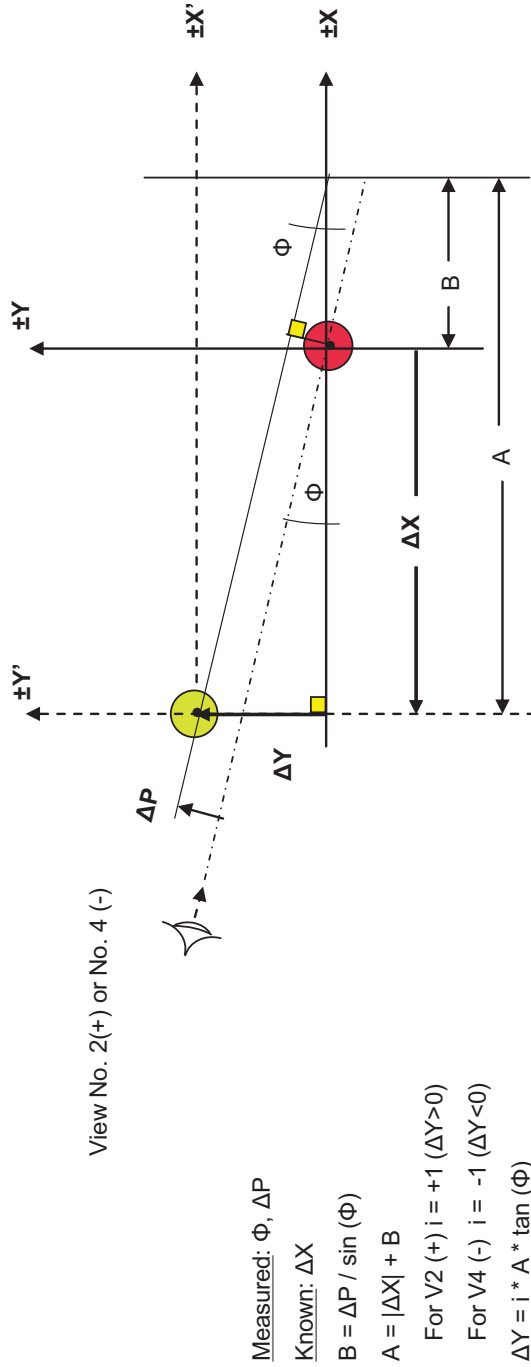
- Locating Pins, Position No. 1
- Locating pin in cradle base center
 - Locating pin in mass standard
 - Alternate position satisfying criteria



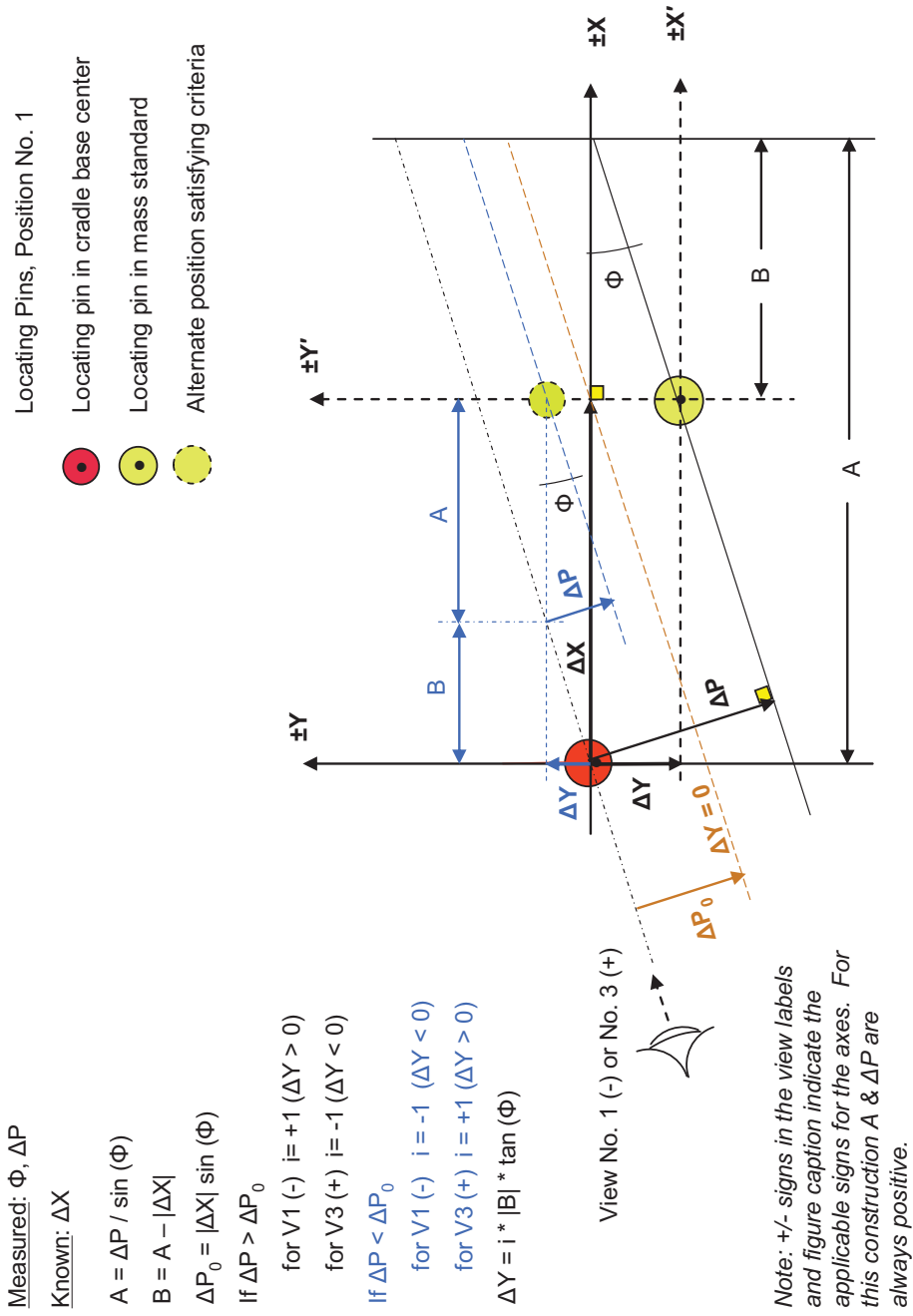
Construction C. Determination of ΔY , View No. 2 (+) or No. 4 (-) when cradle pin is **away**, ΔP is **black**

Note: +/- signs in the view labels and figure caption indicate the applicable signs for the axes. For this construction A & ΔP are always positive.

- Locating Pins, Position No. 1
- Locating pin in cradle base center
 - Locating pin in mass standard
- (No alternate position satisfying criteria)



Construction D. Determination of ΔY , View No. 2 (+) or No. 4 (-) when cradle pin is **away**, ΔP is **red**



Construction E. Determination of ΔY , View No. 1 (-) or No. 3 (+) when cradle pin is **near**, ΔP is **black**

Note: +/- signs in the view labels and figure caption indicate the applicable signs for the axes. For this construction A & ΔP are always positive.

Locating Pins, Position No. 1



Locating pin in cradle base center



Locating pin in mass standard

(No alternate position satisfying criteria)

Measured: $\phi, \Delta P$

Known: ΔX

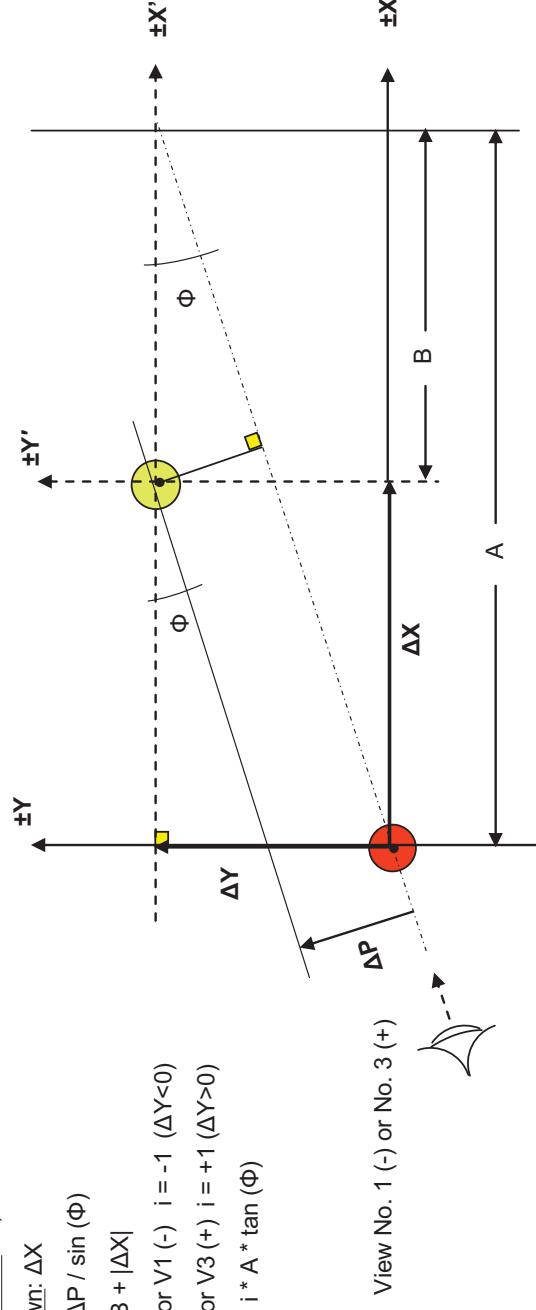
$$B = \Delta P / \sin(\phi)$$

$$A = B + |\Delta X|$$

For V1 (-) i = -1 ($\Delta Y < 0$)

For V3 (+) i = +1 ($\Delta Y > 0$)

$$\Delta Y = i^* A^* \tan(\Phi)$$



Construction F. Determination of ΔY , View No. 1 (-) or No. 3 (+) when cradle pin is **near**, ΔP is **red**

Note: +/- signs in the view labels and figure caption indicate the applicable signs for the axes. For this construction A & ΔP are always positive.

Measured: Φ , ΔP [no sign]

Known: ΔX

$$A = \Delta P / \sin(\Phi)$$

$$B = A - |\Delta X|$$

$$\Delta P_0 = |\Delta X| \sin(\Phi)$$

If $\Delta P > \Delta P_0$

for V1 (-) $i = -1$ ($\Delta Y < 0$)

for V3 (+) $i = +1$ ($\Delta Y > 0$)

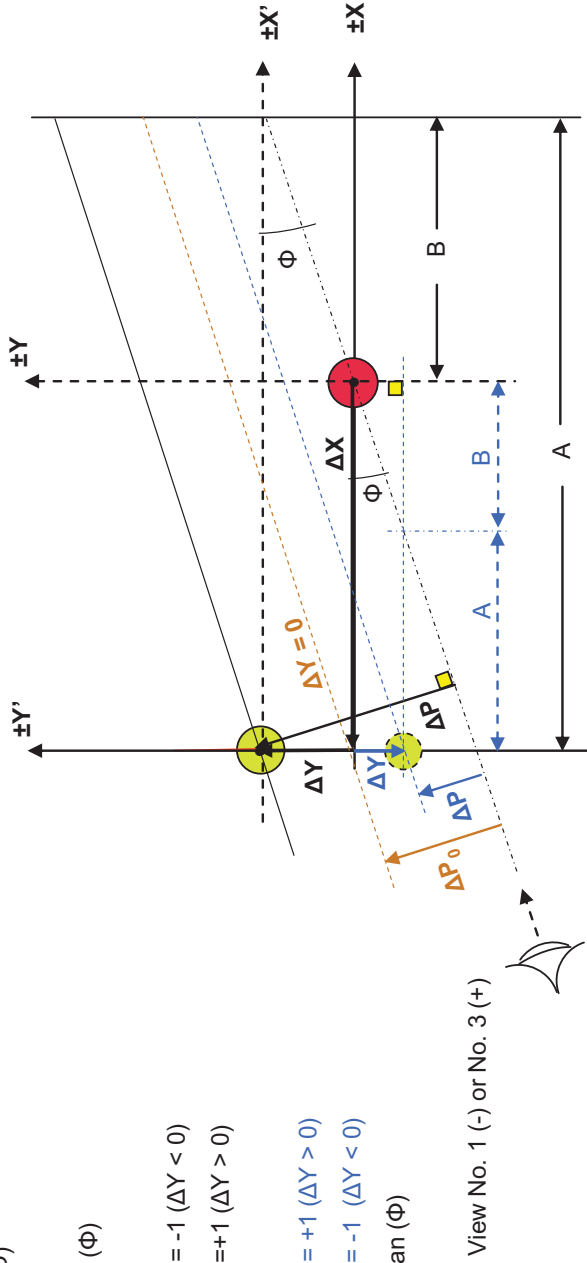
If $\Delta P < \Delta P_0$

for V1 (-) $i = +1$ ($\Delta Y > 0$)

for V3 (+) $i = -1$ ($\Delta Y < 0$)

$$\Delta Y = i * |B| * \tan(\Phi)$$

- Locating Pins, Position No. 1
- Locating pin in cradle base center
 - Locating pin in mass standard
 - Alternate position satisfying criteria



Construction G. Determination of ΔY , View No. 1 (-) or No. 3 (+) when cradle pin is **away**, ΔP is **red**

Note: +/- signs in the view labels and figure caption indicate the applicable signs for the axes. For this construction A & ΔP are always positive.

Locating Pins, Position No. 1



(No alternate position satisfying criteria)

Measured: Φ , ΔP

Known: ΔX

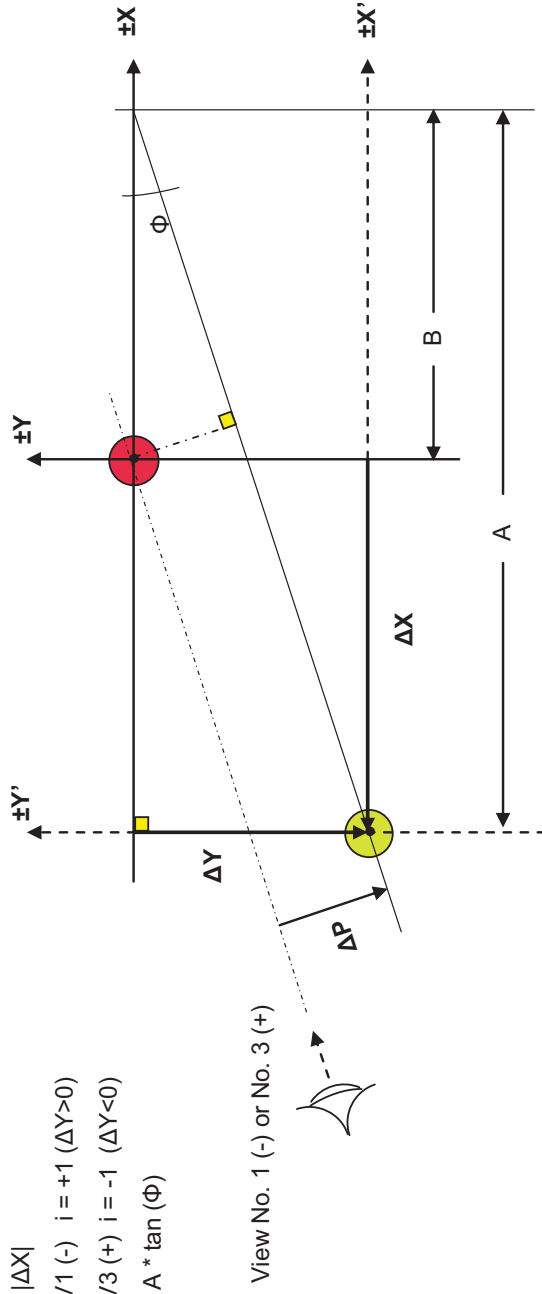
$$B = \Delta P / \sin(\Phi)$$

$$A = B + |\Delta X|$$

$$\text{For V1 (-) } i = +1 (\Delta Y > 0)$$

$$\text{For V3 (+) } i = -1 (\Delta Y < 0)$$

$$\Delta Y = i * A * \tan(\Phi)$$




Construction H. Determination of ΔY , View No. 1 (-) or No. 3 (+) when cradle pin is **away**, ΔP is **black**

Appendix C

Specific Measurement System Output – Mass Standard

Appendix C

Specific Measurement System Output – Mass Standard



Model : KSR1320-1500

Version : 4.2.3

Serial : 2938/72818

RunNumber : 001614

Date : July 2, 2009

Time : 10:25

Operator : Browning

Part ID : Mass simulator

Part Serial : Position 1 run 2

Comments : Comparison measurement for the following
- Sensitivity measurement.

CG Part Measurement Results

Moment Readings

Excessive Variation : False

	Transducer Reading (counts)	Transducer Moment (lb-in)	Reading Angle (deg)
Reading Position 1 :	60592.8689	2076.875	0
Reading Position 2 :	60610	2077.462	90
Reading Position 3 :	60589	2076.743	180
Reading Position 4 :	60576.9836	2076.331	270

This is a 4 position measurement.

Guann Keller
 7/2/09



Model : KSR1320-1500 RunNumber : 001615
 Version : 4.2.3 Date : July 2, 2009
 Serial : 2938/72818 Time : 10:39
 Operator : Browning
 Part ID : Mass simulator
 Part Serial : Position 1
 Comments : sensitivity measurement with pin in hole H (+Xaxis)

CG Part Measurement Results

Moment Readings

Excessive Variation : False

	Transducer Reading (counts)	Transducer Moment (lb-in)	Reading Angle (deg)
Reading Position 1 :	60690.7869	2080.231	0
Reading Position 2 :	60608	2077.394	90
Reading Position 3 :	60492.0656	2073.420	180
Reading Position 4 :	60573.9836	2076.228	270

This is a 4 position measurement.

Sueann Keller
7/2/09



Model : KSR1320-1500	RunNumber : 001616
Version : 4.2.3	Date : July 2, 2009
Serial : 2938/72818	Time : 10:48
Operator : Browning	
Part ID : Mass simulator	
Part Serial : Position 1	
Comments : sensitivity measurement with pin in hole I (-X-axis)	
:	

CG Part Measurement Results

Moment Readings

Excessive Variation : **False**

	Transducer Reading (counts)	Transducer Moment (lb-in)	Reading Angle (deg)
Reading Position 1 :	60494.5902	2073.507	0
Reading Position 2 :	60605	2077.291	90
Reading Position 3 :	60687	2080.102	180
Reading Position 4 :	60571.9836	2076.159	270

This is a 4 position measurement.

Sueann Keller
7/2/09



Model : KSR1320-1500	RunNumber : 001617
Version : 4.2.3	Date : July 2, 2009
Serial : 2938/72818	Time : 10:58
	Operator : Browning
Part ID : Mass simulator	
Part Serial : Position 1	
Comments : sensitivity measurement with pin in hole A (+Y axis)	

CG Part Measurement Results

Moment Readings

Excessive Variation : False

	Transducer Reading (counts)	Transducer Moment (lb-in)	Reading Angle (deg)
Reading Position 1 :	60589.8689	2076.772	0
Reading Position 2 :	60703.082	2080.653	90
Reading Position 3 :	60586	2076.640	180
Reading Position 4 :	60476.1803	2072.876	270

This is a 4 position measurement.

Juan Keller
7/2/09



Model : KSR1320-1500 RunNumber : 001618
 Version : 4.2.3 Date : July 2, 2009
 Serial : 2938/72818 Time : 11:07
 Operator : Browning
 Part ID : Mass simulator
 Part Serial : Position 1
 Comments : sensitivity measurement with pin in hole G (-Y axis)

CG Part Measurement Results

Moment Readings

Excessive Variation : False

	Transducer Reading (counts)	Transducer Moment (lb-in)	Reading Angle (deg)
Reading Position 1 :	60589.9836	2076.776	0
Reading Position 2 :	60506	2073.898	90
Reading Position 3 :	60588	2076.708	180
Reading Position 4 :	60669	2079.485	270

This is a 4 position measurement.

Sue Ann Keller
7/2/09



Model : KSR1320-1500	RunNumber : 001619
Version : 4.2.3	Date : July 2, 2009
Serial : 2938/72818	Time : 13:02
Operator : Browning	
Tare ID 1 : Fixture Tare after simulator removed	
Tare ID 2 : Position 1	
Comments : applys to runs 1614-1618	

CG Tare Measurement Results

Moment Readings

Excessive Variation : False

	Transducer Reading (counts)	Transducer Moment (lb-in)	Reading Angle (deg)
Reading Position 1 :	60573	2076.194	0
Reading Position 2 :	60586	2076.640	90
Reading Position 3 :	60577.0492	2076.333	180
Reading Position 4 :	60569	2076.057	270

This is a 4 position measurement.



Model : KSR1320-1500 **RunNumber :** 001620
Version : 4.2.3 **Date :** July 2, 2009
Serial : 2938/72818 **Time :** 13:11
Operator : Browning
Part ID : MS CG Calculation
Part Serial : Position 1
Comments : Base calculation

Calculation Data

CG Tare : 001619 July 2, 2009 13:02 **Fixture Tare after simulator removed**
CG Part : 001614 July 2, 2009 10:25 **Mass simulator**
Part Weight : 97.1980 lb **Part Estimated CG Height :** 26.1000 in
Machine Angle at Part 0 Degrees : 0.000 deg
User Angle System Polarity : Positive (CCW INCREASING ANGLE)
User Datums Offset below are in Machine Angle System
User Datum Offset X : -0.0030 in **User Datum Offset Y :** 0.0030 in

Calculation Results

Calculated Static CG (see Note 1)

Machine Referenced	CG Offset (in)	CG Moment (lb-in)
Static CG X :	0.0014	0.135
Static CG Y :	0.0028	0.275
Static CG Mag :	0.0031	0.306
Static CG Angle :	63.885	63.885

Sue Ann Keller
 7/2/09

User Referenced	CG Offset (in)	CG Moment (lb-in)
Static CG X :	0.0044	0.426
Static CG Y :	-0.0002	-0.017
Static CG Mag :	0.0044	0.427
Static CG Angle :	357.717	357.717

Notes

1. CG Uncertainty

CG Moment Uncertainty 0.169 lb-in
 CG Offset Uncertainty 0.0017 in



Model : **KSR1320-1500** RunNumber : **001621**
 Version : **4.2.3** Date : **July 2, 2009**
 Serial : **2938/72818** Time : **15:00**
 Operator : **Browning**
 Part ID : **MS CG Calculation**
 Part Serial : **Position 1**
 Comments : **Calculation with pointer weight offset in hole H (+X axis)**

Calculation Data

CG Tare : **001619** July 2, 2009 13:02 Fixture Tare after simulator removed
 CG Part : **001615** July 2, 2009 10:39 Mass simulator
 Part Weight : **97.5299** lb Part Estimated CG Height : **26.1000** in
 Machine Angle at Part 0 Degrees : **0.000** deg
 User Angle System Polarity : **Positive (CCW INCREASING ANGLE)**
 User Datums Offset below are in **Machine Angle System**
 User Datum Offset X : **-0.0030** in User Datum Offset Y : **0.0030** in

Calculation Results

Calculated Static CG (see Note 1)

Machine Referenced	CG Offset (in)	CG Moment (lb-in)
Static CG X :	0.0356	3.470
Static CG Y :	0.0031	0.303
Static CG Mag :	0.0357	3.483
Static CG Angle :	4.988	4.988

User Referenced	CG Offset (in)	CG Moment (lb-in)
Static CG X :	0.0386	3.762
Static CG Y :	0.0001	0.010
Static CG Mag :	0.0386	3.762
Static CG Angle :	0.156	0.156

Guann Keller
 7/2/09

Notes

1. CG Uncertainty

CG Moment Uncertainty **0.173 lb-in**
 CG Offset Uncertainty **0.0018 in**



Model : KSR1320-1500 RunNumber : 001622
 Version : 4.2.3 Date : July 2, 2009
 Serial : 2938/72818 Time : 15:01
 Operator : Browning
 Part ID : MS CG Calculation
 Part Serial : Position 1
 Comments : Calculation with pointer weight offset in hole I (-X axis)

Calculation Data

CG Tare : 001619 July 2, 2009 13:02 Fixture Tare after simulator removed
 CG Part : 001616 July 2, 2009 10:48 Mass simulator
 Part Weight : 97.5299 lb Part Estimated CG Height : 26.1000 in
 Machine Angle at Part 0 Degrees : 0.000 deg
 User Angle System Polarity : Positive (CCW INCREASING ANGLE)
 User Datums Offset below are in Machine Angle System
 User Datum Offset X : -0.0030 in User Datum Offset Y : 0.0030 in

Calculation Results

Calculated Static CG (see Note 1)

Machine Referenced	CG Offset (in)	CG Moment (lb-in)
Static CG X :	-0.0331	-3.225
Static CG Y :	0.0027	0.263
Static CG Mag :	0.0332	3.236
Static CG Angle :	175.331	175.331

User Referenced	CG Offset (in)	CG Moment (lb-in)
Static CG X :	-0.0301	-2.932
Static CG Y :	-0.0003	-0.029
Static CG Mag :	0.0301	2.933
Static CG Angle :	180.571	180.571

Guann Keller
 7/2/09

Notes

1. CG Uncertainty

CG Moment Uncertainty 0.172 lb-in
 CG Offset Uncertainty 0.0018 in



Model : KSR1320-1500 **RunNumber : 001623**
Version : 4.2.3 **Date : July 2, 2009**
Serial : 2938/72818 **Time : 15:02**
Operator : Browning
Part ID : MS CG Calculation
Part Serial : Position 1
Comments : Calculation with pointer weight offset in hole A (+Y axis)

Calculation Data

CG Tare : 001619 **July 2, 2009** **13:02** **Fixture Tare after simulator removed**
CG Part : 001617 **July 2, 2009** **10:58** **Mass simulator**
Part Weight : 97.5299 lb **Part Estimated CG Height : 26.1000 in**

Machine Angle at Part 0 Degrees : 0.000 deg

User Angle System Polarity : Positive (CCW INCREASING ANGLE)

User Datums Offset below are in Machine Angle System

User Datum Offset X : -0.0030 in **User Datum Offset Y : 0.0030 in**

Calculation Results

Calculated Static CG (see Note 1)

Machine Referenced	CG Offset (in)	CG Moment (lb-in)
Static CG X :	0.0013	0.124
Static CG Y :	0.0368	3.593
Static CG Mag :	0.0369	3.595
Static CG Angle :	88.031	88.031

Sue Ann Keller
7/2/09

User Referenced	CG Offset (in)	CG Moment (lb-in)
Static CG X :	0.0043	0.416
Static CG Y :	0.0338	3.301
Static CG Mag :	0.0341	3.327
Static CG Angle :	82.814	82.814

Notes

1. CG Uncertainty

CG Moment Uncertainty 0.173 lb-in
CG Offset Uncertainty 0.0018 in



Model : KSR1320-1500 **RunNumber : 001624**
Version : 4.2.3 **Date : July 2, 2009**
Serial : 2938/72818 **Time : 15:02**

Part Serial : Position 1

Comments : Calculation with pointer weight offset in hole G (-Y axis)

Calculation Data

CG Tare : 001619 July 2, 2009 13:02 Fixture Tare after simulator removed
CG Part : 001618 July 2, 2009 11:07 Mass simulator

Part Weight : 97.5299 lb Part Estimated CG Height : 26.1000 in

Machine Angle at Part 0 Degrees : 0.000 deg

User Angle System Polarity : Positive (CCW INCREASING ANGLE)

User Datums Offset below are in Machine Angle System

User Datum Offset X : -0.0030 in User Datum Offset Y : 0.0030 in

Calculation Results

Calculated Static CG (see Note 1)

Machine Referenced	CG Offset (in)	CG Moment (lb-in)	User Referenced	CG Offset (in)	CG Moment (lb-in)
Static CG X :	0.0012	0.114	Static CG X :	0.0042	0.406
Static CG Y :	-0.0316	-3.081	Static CG Y :	-0.0346	-3.373
Static CG Mag :	0.0316	3.083	Static CG Mag :	0.0348	3.398
Static CG Angle :	272.111	272.111	Static CG Angle :	276.865	276.865

Sue Ann Keller
7/2/09

Notes

1. CG Uncertainty

CG Moment Uncertainty **0.172 lb-in**
 CG Offset Uncertainty **0.0018 in**

Appendix D

Fixture Temperature Maps

Appendix D

Fixture Temperature Maps

Note: Temperature maps in this appendix were copied from the actual MMRTG test procedure, RPS-OI-28220. The header information and Appendix designator (K) shown on these maps pertain to the test procedure document, not to the present document.

Idaho National Laboratory

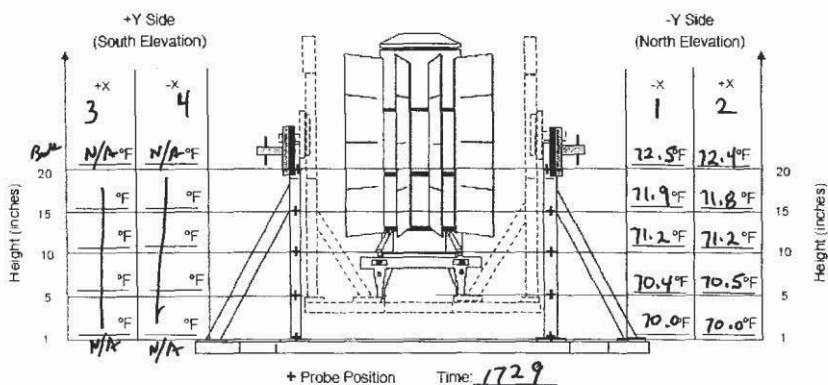
Form 417 09 (Rev 10)

MMRTG MASS PROPERTIES TEST

Identifier: RPS/HS-OI-28220
 Revision: 0
 Effective Date: 04/28/09 Page: 153 of 167

Appendix K**Fixture Temperature Maps****1st Attempt**

NOTE: Enter N/A for any map position not measured



Temperature Probe S/N:	723220	QAR	FA
Readout Panel S/N:	A 52394	Date	5/01/09

Cradle Assembly Temperature Map K-1
 (Pre-test Measurements)

N/A pg

Appendix K

Idaho National Laboratory

MMRTG MASS PROPERTIES TEST

Identifier: RPS/HS-OI-28220

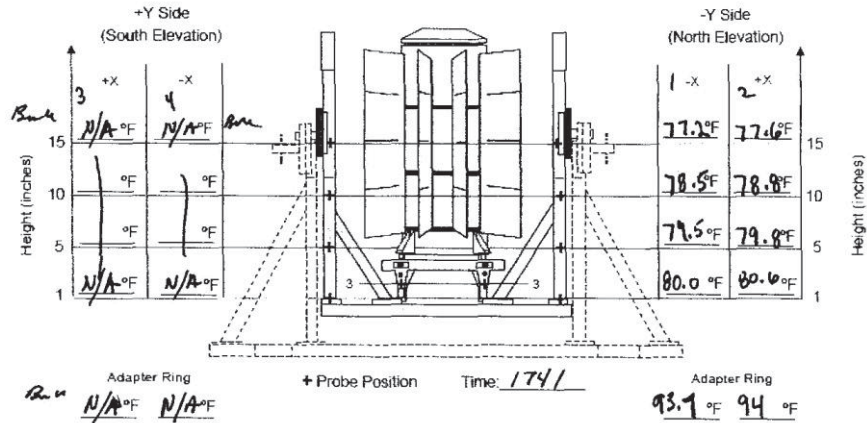
Revision: 0

Effective Date: 04/28/09

Page: 156 of 167

1st Attempt

NOTE: Enter N/A for any map position not measured



Rotation Fixture Assembly Temperature Map K-2
(Pre-test Measurements)

Temperature Probe 723220
 Readout A 52394
 FR 5/1/09

N/A pg

Idaho National Laboratory

Form 412.09 (Rev. 10)

MMRTG MASS PROPERTIES TEST

Identifier: RPS/HS-OI-28220

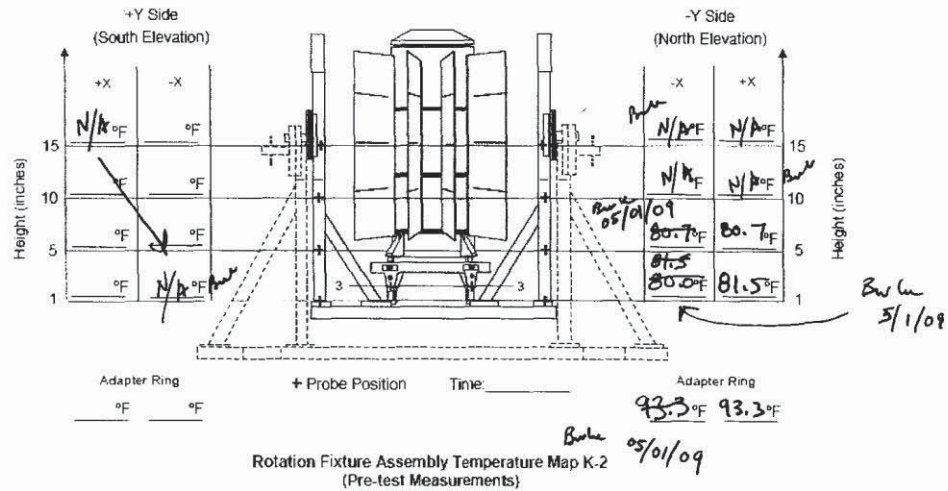
Revision: 0

Effective Date: 04/28/09

Page: 157 of 167

2nd Attempt

NOTE: Enter N/A for any map position not measured



This is a spot check to ensure the temperature of the fixture has not changed.

Bw 05/01/09

N/A pg

Appendix K

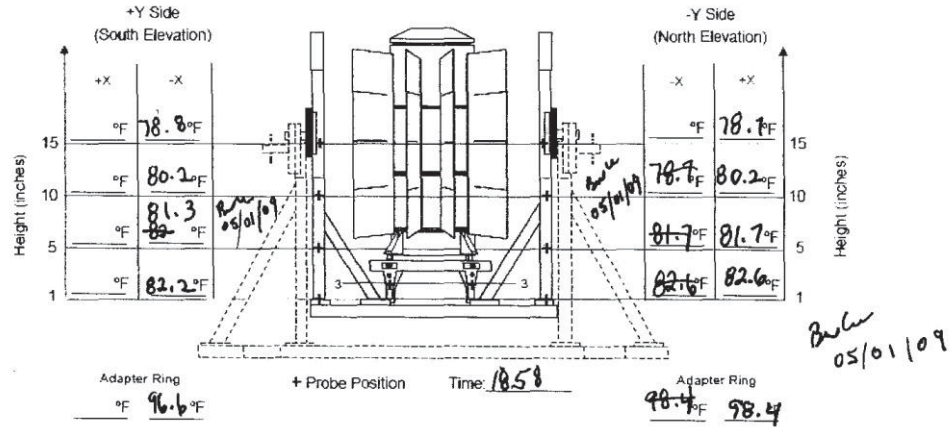
Idaho National Laboratory

MMRTG MASS PROPERTIES TEST	Identifier:	RPS/HS-OI-28220
	Revision:	0
	Effective Date:	04/28/09

Page: 160 of 167

1st Attempt

NOTE: Enter N/A for any map position not measured



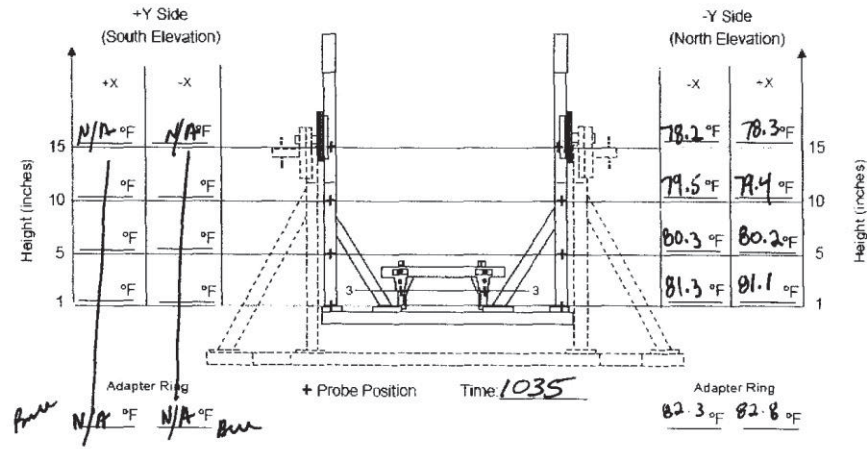
Rotation Fixture Assembly Temperature Map K-4
(Post-test Measurements)

N/A pg

Idaho National Laboratory	Identifier: RPS/HS-OI-28220
MMRTG MASS PROPERTIES TEST	Revision: 0
	Effective Date: 04/28/09 Page: 162 of 167

1st Attempt

NOTE: Enter N/A for any map position not measured



Rotation Fixture Assembly Temperature Map K-6
(Pre-Tare Temperatures)

STEP 5.12.1.3

N/A pg

Idaho National Laboratory

MMRTG MASS PROPERTIES TEST

Identifier: RPS/HS-OI-28220

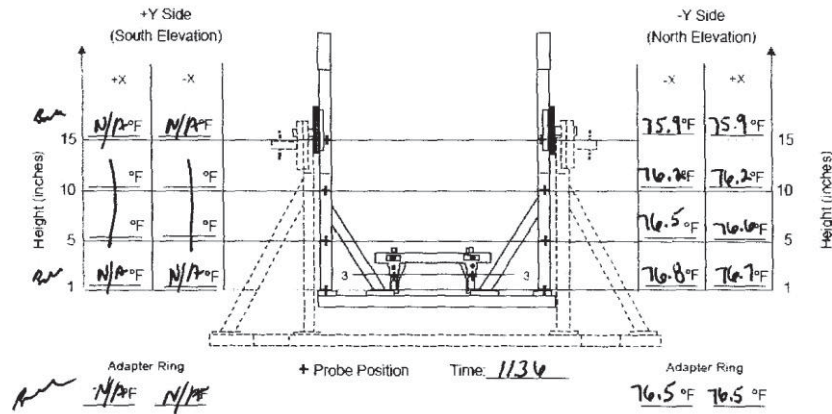
Revision: 0

Effective Date: 04/28/09

Page: 164 of 167

1st Attempt

NOTE: Enter N/A for any map position not measured



Rotation Fixture Assembly Temperature Map K-8
(Post-Tare Temperatures)

STEP 5.12.4.2

N/A pg

INTENTIONALLY BLANK

Appendix E

Temperature Induced CG Corrections

Appendix E

Temperature Induced CG Corrections

The data from the Pro-E model of the adapter ring and rotation fixture were used to determine the temperature induced corrections to the MMRTG CG position. An Excel spreadsheet was constructed and used to track the positions of components that comprise these fixtures. Two different approaches may be used that will yield the same result: (1) the direct temperature changes between the PART and TARE conditions for corresponding components can be used; or (2) calculations may be made separately for the PART and TARE conditions with the temperature changes referenced to the nominal room temperature conditions and the PART offset subtracted from the TARE offset. Although equivalent, the latter approach takes advantage of the nominal room temperature dimensions and is the approach that is used in this appendix. The validity of this approach is demonstrated by considering the defining relation for the corrected test article CG as was developed in Section 10.2:

$$CG_{TA} = CG'_{TA} + \frac{1}{W_{TA}} \sum_j W_j * \Delta Y_j$$

Each of the ΔY_j terms represents the difference in the positions of the j^{th} component's CG during the TARE (primes) and the during the PART measurements, $(Y' - Y)_j$. However, each of these positions can also be referenced to the normal room temperature positions denoted by a 0 subscript as follows:

$$\Delta Y = Y' - Y = Y' - Y_0 + Y_0 - Y = Y' - Y_0 - (Y - Y_0) = \Delta Y'_0 - \Delta Y_0$$

Therefore, the test article CG position finally becomes

$$CG_{TA} = CG'_{TA} + \frac{1}{W_{TA}} \sum_j W_j * (\Delta Y'_0 - \Delta Y_0)_j$$

1. Adapter Ring

The adapter ring calculations are shown in the first section of spreadsheet E-1 (Table 7). The Pro-E model has the datum for the adapter ring at the center of the plane of its mounting feet. All of the adapter ring components were accurately included as detailed in the spreadsheet.

The left side of the spreadsheet lists all of the adapter ring components together with their weights and their individual CG positions for the centerline coordinate as determined from the Pro-E design. Nominal design dimensions are assumed to be those that pertain to the components at the prevailing ambient temperature during testing. The component moment relative to the adapter ring datum are calculated from the weight and design CG position. Summing the moments and dividing by the total weight of the adapter ring yields the composite CG position relative to the datum. The value of 4.630302 in. above the datum compares very favorably to the Pro-E reported composite CG position of 4.630305 in. (additional decimal places are included only to illustrate the correctness of the approach).

The right side of the spreadsheet identifies the component height (or length, as applicable), the applicable thermal parameters, and the effects on the component's mass properties that result from the imposed temperature change. There are many miscellaneous components, such as screws, flat

washers, and brackets that comprise the adapter ring. Given their small masses, the primary contribution they make to the changes in the mass properties of the entire adapter ring lies not in their individual dimensional changes rather, the translation they experience by virtue of the expansion or contraction of whatever they are attached to. This greatly simplifies the calculation with insignificant loss of accuracy. As indicated at the top of the spreadsheet expansion/contraction was only applied to components No. 1 – 5. The remainder of the components moved with these, however they still contributed to a change in the overall CG position since their own CG positions relative to the adapter ring datum will have changed. Again, summing the moments and dividing by the total weight of the adapter ring yields the composite CG position relative to the datum. For the case shown, there was an average temperature of about 93.8 F° in the adapter ring during the PART measurement, as shown in temperature map K-2, Appendix D. During the TARE measurement, this had dropped to an average of about 82.5 F°, as shown in temperature map K-6, Appendix D.

The PART conditions create a 23.8 F° (93.8° – 70.0° F) temperature increase over the assumed ambient temperature as shown in the adapter ring section of spreadsheet E-1. This change shifts the adapter ring CG to 4.631643 in. from its datum (the bottom of the feet of the adapter ring). This is a change of only 0.00134 in. from the room temperature CG position.

For the TARE conditions, the adapter ring temperatures were approximately 12.5° F (82.5° – 70.0° F) above room temperature. As shown in the adapter ring section of spreadsheet E-2, this shifts the adapter ring CG to 4.631007 in. from its datum, a change of only 0.00070 in. from the room temperature position. Therefore, the net effect in changing the fixture temperatures from those during the PART measurement to those applicable to the TARE measurement is to change the adapter ring CG distance from its datum by

$$\Delta Y_0' - \Delta Y_0 = 4.631007 \text{ in.} - 4.631643 \text{ in.} = -0.00064 \text{ in.}$$

The negative sign indicates a reduction in the distance from the datum during the TARE as compared to that during the PART measurement, as a result of the cooling that occurred.

2. Rotation Fixture

In principle, the rotation fixture was handled similarly to the adapter ring. However, the Pro-E model of this item was not as conducive to the type of detailed treatment made for the adapter ring. Furthermore, the only temperatures recorded in the temperature maps in Appendix D were below the pivot. So a few liberties were taken that yield conservative results, i.e., greater changes to the mass properties than likely occurred.

First, the upper structure of the rotation fixture above the pivot was presumed to be unaffected by thermal changes. Since the intent of these calculations is to evaluate the corrections to the MMRTG CG on its long axis, only the changes that occurred while in Position No. 2 are of interest. The temperature maps in Appendix D indicate that temperature changes in the rotation fixture diminished from the base plate toward the pivot and this trend no doubt continues above the pivot. Secondly, the temperature induced expansion or contraction that does occur in the upper members mimics what occurs in the lower structure, i.e., these structures all either expand or contract together, albeit not necessarily by the same amount nor at the same rate. There is a tendency for these to negate any overall translation of the rotation fixture's CG. By ignoring the changes that occur in the upper members, the calculated correction to the CG will be somewhat greater than the actual case. The overall uncertainty in the MMRTG CG includes a contribution from the temperature effects as quantitatively estimated by the results from this appendix. Overestimating this contribution will, therefore, be conservative i.e., introduce a slightly larger uncertainty band on the CG location.

The rotation fixture was arbitrarily divided into five discrete sections for this analysis. These are listed in the rotation fixture section of spreadsheet E-2 (Table 8). The “plumb stanchions” are the four outboard members that appear to be plumb when viewed along the Y axis of the rotation fixture. The four “oblique braces” are the short inboard braces of the stanchions. The plumb stanchions were divided into two discrete sections: (1) that portion between the pivot and the attachment point of the oblique member and (2) that portion between the attachment point of the oblique member and the foot pad. The foot pads and the base plate were the other components considered. The masses of multiple items, such as the eight foot pads or the four upper stanchion sections, whose moment arms were identical, were lumped together. The apparatus around the pivot point was ignored, justified by their short moment arms from the pivot. Given the actual geometries of the stanchions and braces, the values assigned for the mass and CG location of each was necessarily crude. The total mass for these components summed to 110.6021 lb. This compared reasonably well to the Pro-E computed mass of 108.88 lb. In the interest of time, no attempt was made to refine the components’ dimensions to obtain an improved match.

Computation of the new CG position was performed as described for the adapter ring. As an example, during the PART measurement the temperatures were approximately 10 ° F above the room temperatures (see temperature map K-2) and about the same during the TARE (temperature map K-6). Thus for the conditions during the MMRTG testing, no noticeable CG position change occurred in the rotation fixture between the PART and TARE measurements.

3. Adjustment to the MMRTG CG Position

From the development at the beginning of this appendix, the final correction to the MMRTG CG position can be found by combining the moment change from the adapter ring (AR) and that from the rotation fixture (RF):

$$\frac{1}{W_{TA}} \sum_j W_j * (\Delta Y'_0 - \Delta Y_0)_j = \frac{1}{W_{TA}} \left[\sum_{AR} W_j * (\Delta Y'_0 - \Delta Y_0)_j + \sum_{RF} W_j * (\Delta Y'_0 - \Delta Y_0)_j \right]$$

As shown before, the rotation fixture summation is zero, therefore the correction is from the adapter ring, - 0.00064 in., negative because the movement of the adapter ring CG is toward its mounting feet. Since the rotation fixture itself did not move, the adapter ring movement is away from the pivot. The conditions that occurred in the present case produced this very small displacement with obviously negligible significance. However, the development may be useful in future testing where much larger temperature changes occur in the fixtures.

Appendix F

Geometry Calculations

Appendix F

Geometry Calculations

Note: the number of decimal places shown is for control use only. These are not indicative of the accuracy.

<i>Parameter & Its Origin</i>	<i>Description</i>	<i>Value</i>	<i>Units/Notes</i>
Per Design Drawings			
H		31.980	in
P _L		3.405	in
P _U		1.884	in
L _C	Rotation-axis distance from MP datum, per Figure 26	26.000	in
L _R	Rotation fixture pivot to upper base distance	18.100	in
L _{AR}	Height of adapter ring to top of mounting slides	7.004	in
Derived Quantities			
Z ₀	L _C -L _R +L _{AR} (Test-article datum distance from MP instr datum)	14.904	Test-article datum position constant
P _L + H + P _U		37.2690	in
H + P _U		33.8640	in
Theoretical CG Position - Per Pro-E Analysis Relative to Test Article Coordinates (adjusted to X-Y in plane of base plate)			
X'' _{CG - (theoretical)}	Confirms symmetry	0.000	in
Y'' _{CG - (theoretical)}	Confirms symmetry	0.000	in
Z'' _{CG - (theoretical)}	Pro-E combined with fixture drawings (Figure 26)	11.230	in
Best Estimates Averaged From Witnessed Metrology Determination [Relative to MP Instrument Coordinate System]			
X _L		-0.003000	in
X _U		0.000000	in
Y _L		0.002610	in
Y _U		0.004200	in
Geometric Calculations based on Metrological Measurements			
X ₀	$X_L + (X_U - X_L) * P_L / (P_L + H + P_U)$	-2.7259E-03	in, rounds to -0.003 in SE software
Y ₀	$Y_L + (Y_U - Y_L) * P_L / (P_L + H + P_U)$	2.7553E-03	in, rounds to +0.003 in SE software
X _U - X _L		3.0000E-03	in
X _U - X ₀		2.7259E-03	in
X ₀ - X _L		2.7409E-04	in
Y _U - Y _L		1.5900E-03	in
Y _U - Y ₀		1.4447E-03	in
Y ₀ - Y _L		1.4527E-04	in

Parameter & Its Origin		Description	Value	Units/Notes
ΔX	$X_U - X_0$		2.7259E-03	in
ΔY	$Y_U - Y_0$		1.4447E-03	in
$(H + P_U)_{XY}$	$\text{SQRT}(\Delta X^2 + \Delta Y^2)$		3.0851E-03	in
ΔZ	$\text{SQRT}((H + P_U)^2 - (H + P_U)_{XY}^2)$		3.3864E+01	in
$P_{L-XY} + (H + P_U)_{XY}$	$\text{SQRT}((X_U - X_L)^2 + (Y_U - Y_L)^2)$		3.3953E-03	in
P_{L-XY}	$\text{SQRT}((X_0 - X_L)^2 + (Y_0 - Y_L)^2)$		3.1020E-04	in
P_{U-XY}	$(H + P_U)_{XY} * P_U / (H + P_U)$		1.7164E-04	in, by proportions
H_{XY}	$(H + P_U)_{XY} * H / (H + P_U)$		2.9135E-03	in, by proportions
$(H + P_U)_{XZ}$	$\text{SQRT}(\Delta X^2 + \Delta Z^2)$		3.3864E+01	
$P_{L-XZ} + (H + P_U)_{XZ}$	$\text{SQRT}((P_L + H + P_U)^2 - (Y_U - Y_L)^2)$		3.7269E+01	
P_{L-XZ}	$(P_L + H + P_U)_{XZ} * P_L / (P_L + H + P_U)$		3.4050E+00	in, by proportions
H_{XZ}	$(P_L + H + P_U)_{XZ} * H / (P_L + H + P_U)$		3.1980E+01	in, by proportions
P_{U-XZ}	$(P_L + H + P_U)_{XZ} * P_U / (P_L + H + P_U)$		1.8840E+00	in, by proportions
$(H + P_U)_{YZ}$	$\text{SQRT}(\Delta Y^2 + \Delta Z^2)$		3.3864E+01	in
$P_{L-YZ} + (H + P_U)_{YZ}$	$\text{SQRT}((P_L + H + P_U)^2 - \Delta X^2)$		3.7269E+01	in
P_{L-YZ}	$(P_L + H + P_U)_{YZ} * P_L / (P_L + H + P_U)$		3.4050E+00	in, by proportions
H_{YZ}	$(P_L + H + P_U)_{YZ} * H / (P_L + H + P_U)$		3.1980E+01	in, by proportions
P_{U-YZ}	$(P_L + H + P_U)_{YZ} * P_U / (P_L + H + P_U)$		1.8840E+00	in, by proportions
Φ (X-Z projection)	$\text{ARCSIN}(\Delta X / (P_L + H + P_U)_{XZ})$		8.0496E-05	Radians
			0.0046	Degrees
β (Y-Z projection)	$\text{ARCSIN}(\Delta Y / (P_L + H + P_U)_{YZ})$		4.2663E-05	Radians
			0.0024	Degrees
ξ (X-Y projection)	$\text{ARCTAN}(\Delta Y / \Delta X)$		4.8736E-01	Radians
			27.9236	Degrees
θ (angle from vertical)	$\text{ARCTAN}((H + P_U)_{XY} / \Delta Z)$ (degrees)		9.1103E-05	Radians
			0.0052	Degrees
CG Test Results (these also use metrology data)				
X_{CG} - (measured)	Ref: Run No. 1550		0.00020	in
	Ref: Run No. 1584		-0.00050	in
	Ref: Run No. 1601		0.00190	in
	Best Estimate (arithmetic average)		0.00053	in
Y_{CG} - (measured)	Ref: Run No. 1550		0.00310	in
	Ref: Run No. 1584		0.00410	in
	Ref: Run No. 1601		0.00280	in
	Best Estimate (arithmetic average)		0.00333	in

Parameter & Its Origin	Description	Value	Units/Notes
$Z_{CG} - (\text{measured})$	Ref: Run No. 1551	0.12980	in
	Ref: Run No. 1586	0.13050	in
	Ref: Run No. 1602	0.12990	in
	Best Estimate (arithmetic average)	0.13007	in
	Top of Adapter Ring + Arithmetic Average of Runs	26.13007	in
$X'_{CG} = X_{CG} - X_0$	Adjusted for non-rounded X_0 value	3.2592E-03	in
$Y'_{CG} = Y_{CG} - Y_0$	Adjusted for non-rounded Y_0 value	5.7807E-04	in
$Z'_{CG} = Z_{CG} - Z_0$	Adjusted for non-rounded Z_0 value	11.22607	in
<i>Calculations Based on Test Results & Geometric Data (see Table 2)</i>			
X''_{CG-XZ}	$Z'_{CG}\sin(\Phi)$	9.0365E-04	in
	$X'_{CG}\cos(\Phi)$	3.2592E-03	in
	$\sin(\Phi)^2 - \cos(\Phi)^2$	-1.0000E+00	in
	$(Z'_{CG}\sin(\Phi) - X'_{CG}\cos(\Phi))/(\sin(\Phi)^2 - \cos(\Phi)^2)$	2.3556E-03	in
	$Z'_{CG}\cos(\Phi)$	11.22607	in
Z''_{CG-XZ}	$X'_{CG}\sin(\Phi)$	2.6236E-07	in
	$(X'_{CG}\sin(\Phi) - Z'_{CG}\cos(\Phi))/(\sin(\Phi)^2 - \cos(\Phi)^2)$	11.22607	in
	$Z'_{CG}\sin(\beta)$	4.7894E-04	in
	$Y'_{CG}\cos(\beta)$	5.7807E-04	in
	$\sin(\beta)^2 - \cos(\beta)^2$	-1.0000E+00	in
Y''_{CG-YZ}	$(Z'_{CG}\sin(\beta) - Y'_{CG}\cos(\beta))/(\sin(\beta)^2 - \cos(\beta)^2)$	9.9131E-05	in
	$Z'_{CG}\cos(\beta)$	1.1226E+01	in
	$Y'_{CG}\sin(\beta)$	2.4662E-08	in
	$(Y'_{CG}\sin(\beta) - Z'_{CG}\cos(\beta))/(\sin(\beta)^2 - \cos(\beta)^2)$	11.22607	in
	$R'_{CG} = \text{SQRT}(X'^2_{CG} + Y'^2_{CG} + Z'^2_{CG})$	11.22607	in
R''_{CG}	$\text{SQRT}(X''^2_{CG-XZ} + Y''^2_{CG-YZ} + Z''^2_{CG-XZ})$	11.22607	in

Appendix G

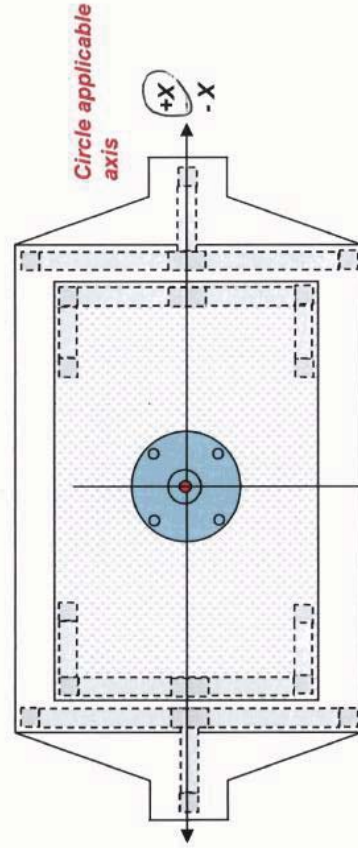
Metrology Data Sheets and Data Reduction

Appendix G

Metrology Data sheets and Data Reduction

Data Sheet - Fixtures Alignment Checks

Mass simulator X offsets from cradle pin



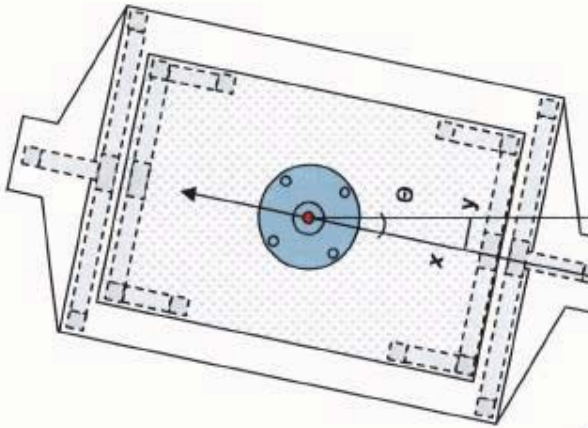
Overhead view

Ave.

Page ____ of ____

Data Sheet - Fixtures Alignment Checks

Mass simulator oblique offsets from cradle pin



X: _____ in
Y: _____ in
 $\Phi = \arctan (y/x) *$
 $\Phi = 19^\circ$
L: _____ in

* Φ may be measured directly

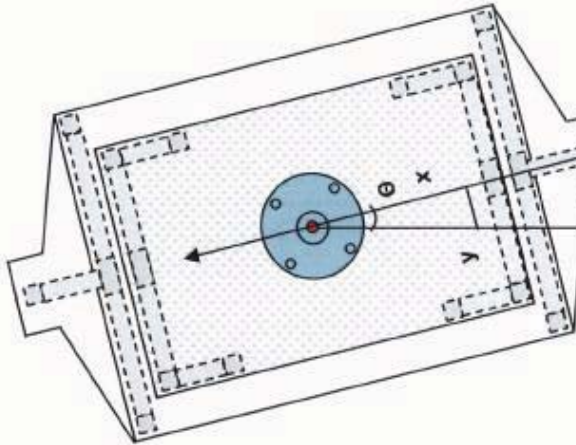
Measurement Equipment:
Type Brunson Instruments Model 76 RH
Model 160 Optical Microometer
ID Number 845060
Calibration Due Date: calibrate prior to use

Measurements:
Date: 4/23/09
Measured by: Michael Dwyer
QAR witness: Ann Keller

Overhead view		North elevation		Ave.	
5/23/09 4/23/09	0.0055 Red	0.0055 Red	0.0055 Red	0.0055 Red	
5/23/09 4/23/09	0.0055 Red	0.0025 Red	0.0025 Red	0.0025 Red	
0.000	0.000	0.000	0.000	0.000	

Data Sheet - Fixtures Alignment Checks

Mass simulator oblique offsets from cradle pin



X: _____ in
Y: _____ in
 $\Phi = \arctan (y/x)^*$
= 17.0
L: _____ in

* Φ may be measured directly

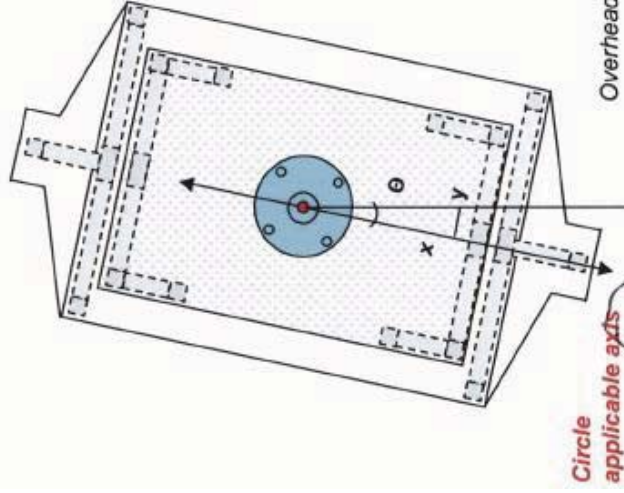
Measurement Equipment:
Type Brunson Instruments Model 70 R4
w/ Model 100 Optical Micrometer
ID Number B15060
Calibration Due Date: calibrate prior to use

Measurements:
Date: 4/23/09
Measured by: Michael D. Long
QAR witness: Jason Keller

Overhead view		Circle X - X applicable axis		North elevation		Ave.	
L	0.0025 Black	0.0025 Black	0.0025 Black	0.0025 Black	0.0025 Black	0.0025 Black	0.0025 Black
L	0.003 Black	0.003 Black	0.003 Black	0.003 Black	0.003 Black	0.003 Black	0.003 Black
L	0.000	0.000	0.000	0.000	0.000	0.000	0.000

Data Sheet - Fixtures Alignment Checks

Mass simulator oblique offsets from cradle pin



X:
.in

Y: _____ in _____

$$\Phi = \arctan (y/x)^{\circ}$$

7: in

* Φ may be measured directly

Measurement Equipment:

Type Brunson Instruments Model 76RH

w/ Model 160 Optical Micrometer

ID Number 815060

Calibration Due Date: Calibrate prior to use

Measurements:

Date: 4/23/00

Date: 1-27-01 Measured by: W. J. J. J.

Measured by: 4 November 2007

Overhead view

Point	Value
0.004	Black
0.0025	Black
0.004	Black

North elevation

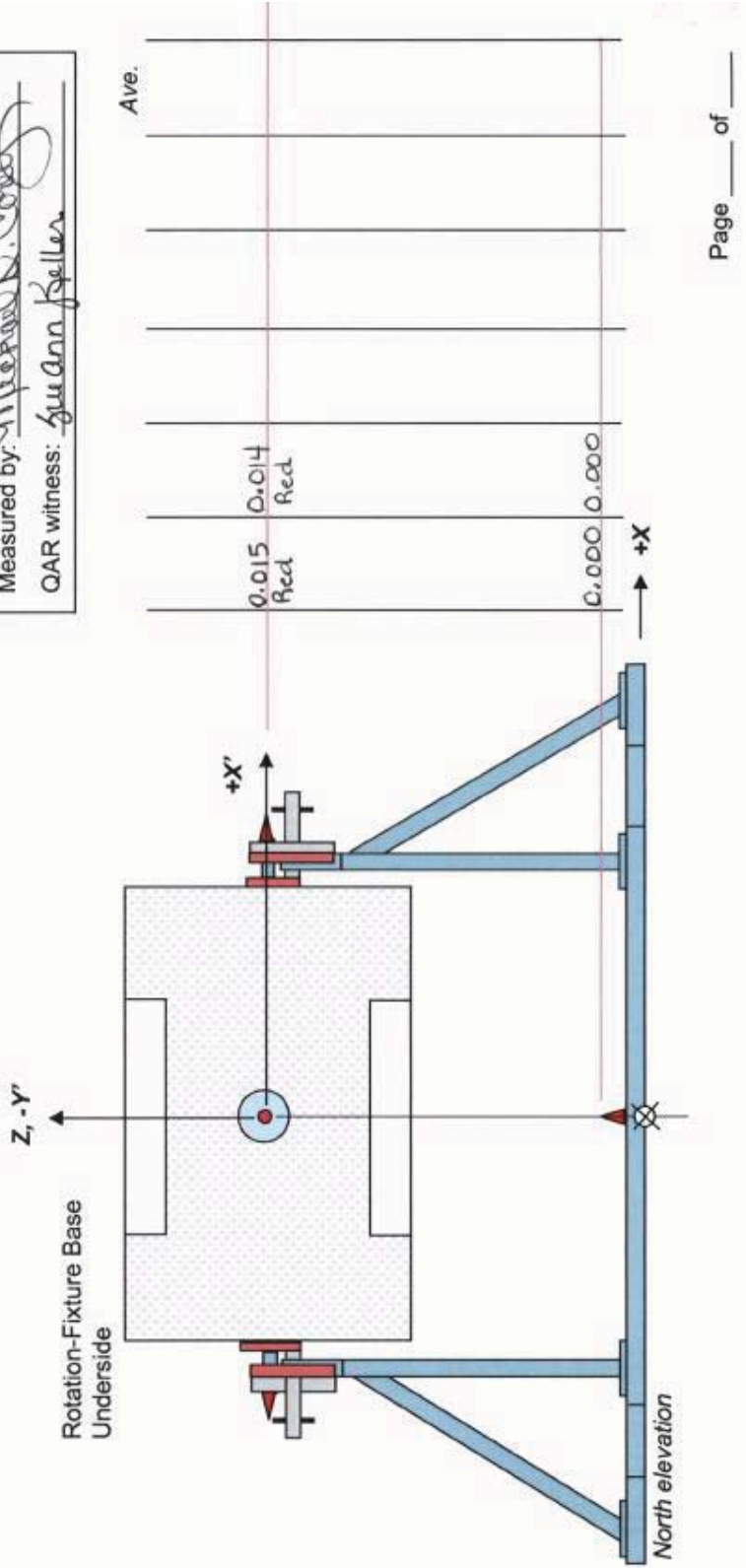
Page ____ of ____

Data Sheet - Fixtures Alignment Checks

Lower Mass-Standard Pin, X-Offset, Position No. 2

Measurement Equipment:
Type Brunson Instruments Model 76R#
Model 160 Optical Micrometer
ID Number 215260
Calibration Due Date: calibrate prior to use

Measurements:
Date: 4/23/09
Measured by: Michael D. Cord
QAR witness: Guanan Keller



Data Sheet - Fixtures Alignment Checks

Top Mass-Standard Pin, X-Offset, Position No. 2

Measurement Equipment:

Type Brunson Instruments Model 76RH

Model 160 Optical Micrometer

ID Number 815060

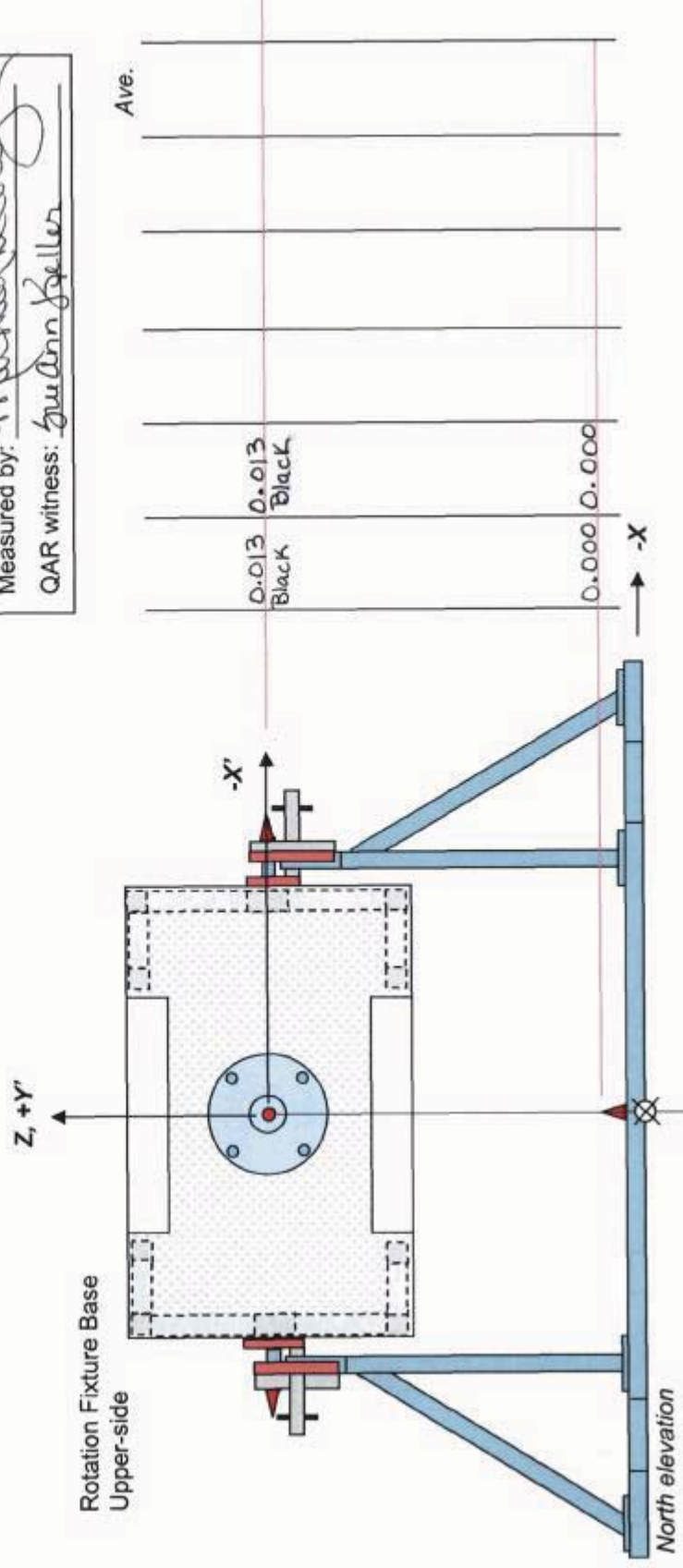
Calibration Due Date: calibrate prior to use

Measurements:

Date: 4/23/09

Measured by: Michael D. Crow

QAR witness: Ann Keller



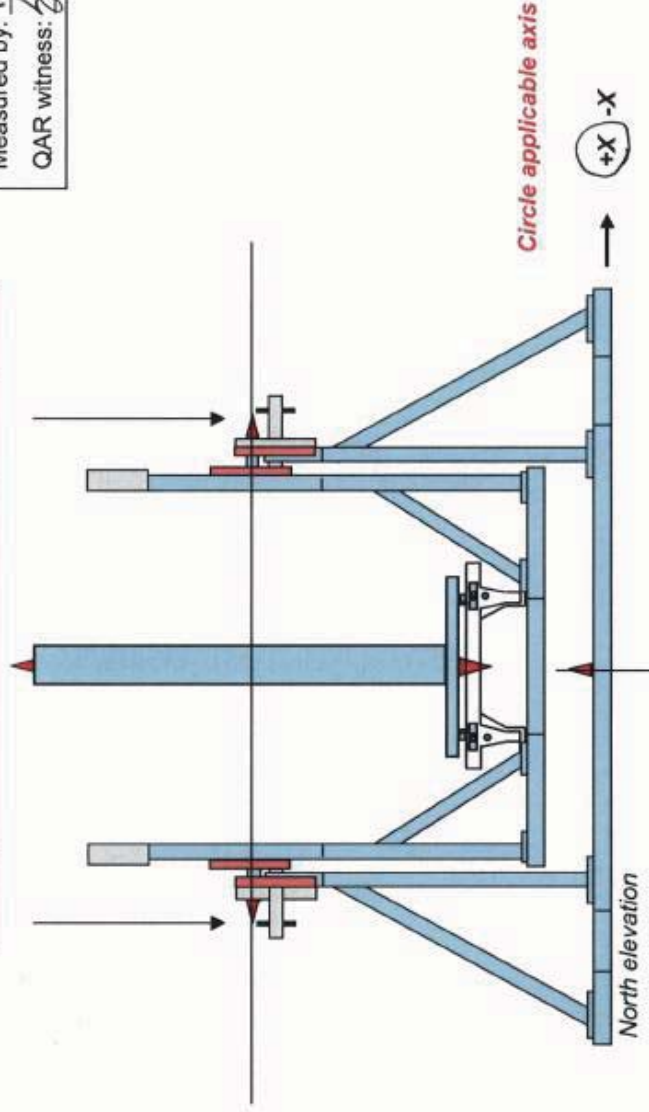
Data Sheet - Fixtures Alignment Checks

Mounting Fixtures Level

Rel. Elev.	Circle applicable direction	Rel. Elev.	Ave.
.000	← →	.000	
.000	← →	.000	
	← →		
	← →		
	← →		
	← →		
	← →		
	← →		
	← →		

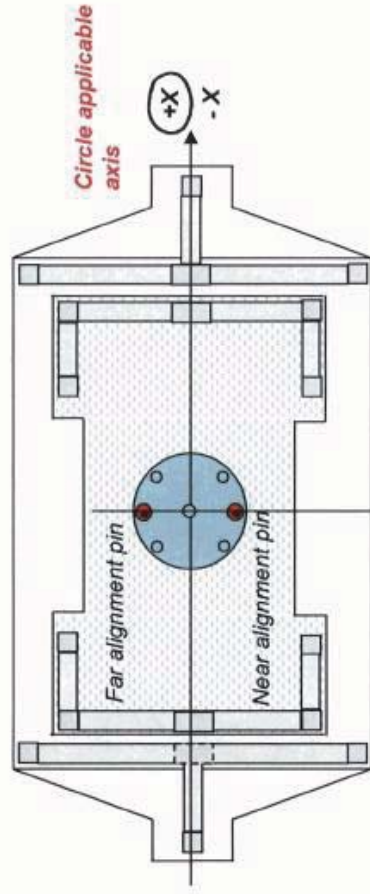
Measurement Equipment:
 Type Brunson Instruments Model 76RH s/
Model 160 optical micrometer
 ID Number 815060
 Calibration Due Date: calibrate prior to use

Measurements:
 Date: 04/22/2009
 Measured by: Michael D. Coates
 QAR witness: Gulann Keller



Data Sheet - Fixtures Alignment Checks

Auxiliary Flange Angular Offset from Cradle Axes



<i>Measurement Equipment:</i>	
Type _____	
ID Number _____	
Calibration Due Date: _____	

<i>Measurements:</i>	
Date: _____	
Measured by: _____	
QAR witness: _____	

Overhead view

Aux. flange far alignment pin

Aux. flange near alignment pin

Cradle centerline pin

Cradle peripheral pin

Circle applicable pin: (Near) Far

Circle applicable pin: (Near) Far

Circle applicable pin: (Near) Far

Circle applicable pin: (Near) Far

Circle applicable pin: (Near) Far

Ave.

0.000

0.000

0.000

0.000

0.000

Side view

New data form. These measurements were transcribed from the original, ad-hoc measurement form (attached) for better clarity. ²⁰

02/06/2009

5/2 7/6/09

Metrology Data Reduction
All Measurements Performed 4/23/2009

Notes: (1) See Data Sheets, Appendix G.
(2) Geometric constructions are provided in Appendix B
(3) All non-angular values are in inches.

ΔX Measurement

View No. (per Figure 14)		View Angle		Offsets			N	$\Sigma \Delta P_i$	$\Delta X (= \Delta P\text{-ave})$	Direction
X ₁		NA		ΔP_1	ΔP_2	ΔP_3				
Pin	Upper	0.000		0.000	0.000	0.000	2	0.000	0.00000	NA
	Lower	0.003					2	0.006	0.00300	toward -X

ΔY Indirect Determination No. 1

View No. (per Figure 14)		View Angle, Φ		Offsets			N	$\Sigma \Delta P_i$	Average ΔP	Direction
V ₃ (+)		[deg]	[rad]	ΔP_1	ΔP_2	ΔP_3				
Pin	Upper	19	0.3316	0.00700	0.00550	0.00550	3	0.01800	0.00600	toward +Y
	Lower						3	0.00750	0.00250	toward +Y

Upper-Pin Analysis

View No.: V₃(+)
 ΔP Scale: Red
Cradle-pin position: Neither Near nor Away
Implied geometric construction: F or G (both are applicable)

Using Construction F B A ΔY

		$\{\Delta P/\sin(\Phi)\}$	$\{B+ \Delta X \}$	ΔP_0	$\Delta P > \Delta P_0 ?$	i	$\{i^*A*\tan(\Phi)\}$
		0.01843	0.01843	NA	NA	1	0.00635
Check: Using Construction G		A	B	ΔP_0			ΔY
		$\{\Delta P/\sin(\Phi)\}$	$\{A- \Delta X \}$	$\{ \Delta X *\sin(\Phi)\}$	$\Delta P > \Delta P_0 ?$	i	$\{i^* B *\tan(\Phi)\}$
		0.01843	0.01843	0.0000	TRUE	1	0.00635

Lower-Pin Analysis
View No.: V3(+)
 ΔP Scale: Red
Cradle-pin position: Away
Implied geometric construction: G

Using Construction G		A	B	ΔP_0			ΔY
		$\{\Delta P/\sin(\Phi)\}$	$\{A- \Delta X \}$	$\{ \Delta X *\sin(\Phi)\}$	$\Delta P > \Delta P_0 ?$	i	$\{i^* B *\tan(\Phi)\}$
		0.00768	0.00468	0.00098	TRUE	1	0.00161

ΔY Indirect Determination No. 2

View No. (per Figure 14)		View Angle, Φ		Tan (Φ)			
V ₄ (-)		[deg]	[rad]	Sin (Φ)			
		17	0.29671	0.29237	0.30573		
		Offsets				Average	
Pin	ΔP_1	ΔP_2	ΔP_3	ΔP_4	N	$\Sigma \Delta P_i$	Direction
Upper	0.00250	0.00250			2	0.00500	toward +Y
Lower	0.00300	0.00250			2	0.00550	toward +Y

Upper-Pin Analysis
View No.: V₄(-)
 ΔP Scale: Black
Cradle-pin position: Neither Near nor Away
Implied geometric construction: B or C (both are applicable)

Using Construction B		B		A		ΔY	
		{ $\Delta P/\sin(\Phi)$ }		{ $B+ \Delta X $ }		{ $i^*A*\tan(\Phi)$ }	
		0.00855		0.00855		NA	
		1		NA		0.00261	
Check: Using Construction C		A		B		ΔY	
		{ $\Delta P/\sin(\Phi)$ }		{ $A- \Delta X $ }		{ $i^*B*\tan(\Phi)$ }	
		0.00855		0.00855		0.0000	
		1		TRUE		0.00261	

Lower-Pin Analysis

View No.: $V_4(-)$
 ΔP Scale: Black
Cradle-pin position: Near
Implied geometric construction: B

Using Construction B		B		A		ΔY	
		{ $\Delta P/\sin(\Phi)$ }		{ $B+ \Delta X $ }		{ $i^*A*\tan(\Phi)$ }	
		0.00941		0.01241		NA	
		1		NA		0.00379	

ΔY Indirect Determination No. 3

View No. (per Figure 14)		View Angle, Φ		Sin (Φ)		Tan (Φ)	
$V_1(-)$		[deg]	[rad]				
		16.5	0.2880	0.2840		0.2962	
		Offsets		Average		Direction	
Pin	ΔP_1	ΔP_2	ΔP_3	ΔP_4	$\Sigma \Delta P_i$	ΔP	
Upper	0.00400	0.00250	0.00400		0.01050	0.00350	toward +Y
Lower	0.00350	0.00350	0.00250		0.00950	0.00317	toward +Y

Upper-Pin Analysis

View No.: $V_1(-)$

ΔP Scale:	Black				
Cradle-pin position:	Neither Near nor Away				
Implied geometric construction:	E or H (both are applicable)				
Using Construction E	A	B	ΔP_0		ΔY
	$\{\Delta P/\sin(\Phi)\}$	$\{A- AX \}$	$\{ AX *\sin(\Phi)\}$	$\Delta P > \Delta P_0 ?$	$\{i* B *\tan(\Phi)\}$
	0.01232	0.01232	0.00000	TRUE	1
					0.00365
Check: Using Construction H	B	A	ΔP_0		ΔY
	$\{\Delta P/\sin(\Phi)\}$	$\{B+ AX \}$	ΔP_0	$\Delta P > \Delta P_0 ?$	$\{i*A*\tan(\Phi)\}$
	0.01232	0.01232	NA	NA	1
					0.00365
Lower-Pin Analysis					
View No.:	$V_1(-)$				
ΔP Scale:	Black				
Cradle-pin position:	Near				
Implied geometric construction:	E				
Using Construction G	A	B	ΔP_0		ΔY
	$\{\Delta P/\sin(\Phi)\}$	$\{A- AX \}$	$\{ AX *\sin(\Phi)\}$	$\Delta P > \Delta P_0 ?$	$\{i* B *\tan(\Phi)\}$
	0.01115	0.00815	0.00085	TRUE	1
					0.00241
ΔY Calculations Summary					
			ΔY		
	View:	$V_3(+)$	$V_4(-)$	Average	Direction
	Upper Pin:	0.00635	0.00261	0.00365	toward +Y
	Lower Pin:	0.00161	0.00379	0.00241	toward +Y

INTENTIONALLY BLANK

Appendix H

Data Sheet – Weigh Scale Calibration Check

Appendix H

Data Sheet – Weigh Scale Calibration Check

Data Sheet—Weigh Scale Calibration Check

Calibration control No.:	722950		
Expiration date:	6/16/09		
QAR verification:	Z Reed	Date:	4/30/09

Drawing # AYE 850018

Weight (lb)	Dwg. No./Calibration Expiration Date	Actual Calibration Weight (lb)	Actual Calibration Weight Summation (lb)	Loading		Unloading	
				Measured Scale Reading (lb)	Deviation (Actual - Measured) (lb)	Measured Scale Reading (lb)	Deviation (Actual - Measured) (lb)
0	-/ N/A R ^W	0	0	0.000	0	0.000	0
50	3/ 5/25/2010	50.0022	50.0022	50.000	0.0022	50.000	0.002
50	6/ 5/25/2010	50.0016	100.0038	99.996	0.008	99.998	0.006
25	1/ 5/20/2010	24.99829	125.00209	124.994	0.008	124.994	0.008
25	2/ 5/20/2010	24.99885	150.00194	149.994	0.008	149.994	0.008
25	3/ 5/20/2010	24.99829	175.00023	174.992	0.008	174.992	0.008
25	4/ 5/20/2010	24.99906	199.99983	199.992	0.008	199.992	0.008

The weigh-scale check has been satisfactorily completed.

SME/TL:	B. W. W.	Date:	4/30/09
QAR:	Z Reed	Date:	4/30/09

Place a completed copy of this table in the Weigh-Scale Data binder.

Appendix I

Measurement System Output – MMRTG

Appendix I

Measurement System Output – MMRTG



Model : KSR1320-1500 **RunNumber : 001550**
Version : 4.2.3 **Date : April 30, 2009**
Serial : 2938/72818 **Time : 11:31**
 Operator : Jon Bradley

Part ID : Mass Simulator
Part Serial : Position 1.
Comments : Mass simulator calculations for MMRTG test.
 : Step 5.8.1

Calculation Data

CG Tare : 001544 **April 30, 2009** **09:29** **Fixture Tare after simulator removed**
CG Part : 001538 **April 29, 2009** **16:33** **Mass Simulator**

Part Weight : 97.1980 lb **Part Estimated CG Height : 26.1000 in**

Machine Angle at Part 0 Degrees : 0.000 deg
User Angle System Polarity : Positive (CCW INCREASING ANGLE)
User Datums Offset below are in Machine Angle System
User Datum Offset X : -0.0030 in **User Datum Offset Y : 0.0030 in**

Calculation Results

Calculated Static CG (see Note 1)

Machine Referenced	CG Offset (in)	CG Moment (lb-in)	User Referenced	CG Offset (in)	CG Moment (lb-in)
Static CG X :	0.0002	0.015	Static CG X :	0.0032	0.307
Static CG Y :	0.0031	0.298	Static CG Y :	0.0001	0.007
Static CG Mag :	0.0031	0.299	Static CG Mag :	0.0032	0.307
Static CG Angle :	87.111	87.111	Static CG Angle :	1.253	1.253

Notes

1. CG Uncertainty

CG Moment Uncertainty **0.169 lb-in**
 CG Offset Uncertainty **0.0017 in**



Model : KSR1320-1500 **RunNumber : 001627**
Version : 4.2.3 **Date : December 16, 2009**
Serial : 2938/72818 **Time : 13:53**
 Operator : Frank Felicione

Part ID : Mass Simulator
Part Serial : Position 2.
Comments : Revised calculations with corrected Z-datum offset
 : Step 5.8.2

Calculation Data

CG Tare : 001547 April 30, 2009 10:19 Fixture Tare after simulator removed
CG Part : 001541 April 29, 2009 17:29 Mass Simulator

Part Weight : 97.1980 lb Part Estimated CG Height : 26.0000 in

Machine Angle at Part 0 Degrees : 359.998 deg
 User Angle System Polarity : Positive (CCW INCREASING ANGLE)
User Datums Offset below are in Machine Angle System

User Datum Offset X : -0.0140 in User Datum Offset Z : -11.0960 in

Calculation Results

Calculated Static CG (see Note 1)

Machine Referenced	CG Offset (in)	CG Moment (lb-in)
Static CG X :	-0.0073	-0.709
Static CG Y :	0.1298	12.614
Static CG Mag :	0.1300	12.634
Static CG Angle :	93.216	93.216

User Referenced	CG Offset (in)	CG Moment (lb-in)
Static CG X :	0.0063	0.614
Static CG Z :	11.2258	1091.123
Static CG Mag :	11.2258	1091.123
Static CG Angle :	89.968	89.968

Notes

1. CG Uncertainty

CG Moment Uncertainty **0.186 lb-in**
 CG Offset Uncertainty **0.0019 in**



Model : **KSR1320-1500** RunNumber : **001562**
 Version : **4.2.3** Date : **May 2, 2009**
 Serial : **2938/72818** Time : **16:41**
 Operator : **Jon Bradley**
 Part ID : **MMRTG Flight Unit Testing (F1)**
 Part Serial : **Test position 1.**
 Comments : **Step Number 5.13.1.1**
 :

Calculation Data

CG Tare : **001560** **May 2, 2009** **11:57** **Post Test Fixture Tare**
 CG Part : **001553** **May 1, 2009** **18:02** **MMRTG Flight Unit Testing (F1)**
 Part Weight : **100.1170** lb Part Estimated CG Height : **26.1000** in
 Machine Angle at Part 0 Degrees : **0.000** deg
 User Angle System Polarity : **Positive (CCW INCREASING ANGLE)**
 User Datums Offset below are in **Machine Angle System**
 User Datum Offset X : **-0.0030** in User Datum Offset Y : **0.0030** in

Calculation Results

Calculated Static CG (see Note 1)

Machine Referenced	CG Offset (in)	CG Moment (lb-in)
Static CG X :	0.0938	9.387
Static CG Y :	0.0306	3.062
Static CG Mag :	0.0986	9.874
Static CG Angle :	18.065	18.065

User Referenced	CG Offset (in)	CG Moment (lb-in)
Static CG X :	0.0968	9.687
Static CG Y :	0.0276	2.762
Static CG Mag :	0.1006	10.073
Static CG Angle :	15.911	15.911

Notes

1. CG Uncertainty

CG Moment Uncertainty **0.180 lb-in**
 CG Offset Uncertainty **0.0018 in**

Calculation Data

User Datum Offset X : **-0.0140** in User Datum Offset Z : **-11.0960** in

Calculation Results

Calculated Static CG (see Note 1)

Notes

1. CG Uncertainty

133

INTENTIONALLY BLANK

Appendix J

MMRTG Weighing Record

Appendix J

MMRTG Weighing Record

Note: The pages in this appendix were copied from the actual MMRTG test procedure, RPS/HS-OI-28220. The header information and appendix designator (D) shown on these pages pertain to the test procedure document, not to the present document.

Idaho National Laboratory

Form 412 09 (Rev. 10)

MMRTG MASS PROPERTIES TEST	Identifier:	RPS/HS-OI-28220
	Revision:	0
	Effective Date:	04/28/09
		Page: 129 of 167

Appendix D

Data Sheet — Equipment and Fixtures Attached to MMRTG During Weighing or Testing

1. Measured MMRTG gross weight (Subsection 5.9.3.3): 162.776 lb [N1].
2. Ancillary items present during MMRTG weighing but removed during testing:

Item
Hoist plate (with swivel ring and (3) attachment pins and lanyards)
Lifting ring (with (3) attachment pins and lanyards)
Connector saver cable (without shorting plug)
Lockwire (if applicable) <u>N/A Bw</u>
Mounting screws, washers, and locking nuts used to attach the MMRTG to the PWR (stainless steel) adapter ring
PWR (stainless steel) adapter ring assembly
Cable or Varglas ties (if applicable)

- a. Aggregate weight of ancillary items listed above (Subsection 5.9.8): 63.664 lb [N2]
- b. Weight of the shorting plug present during weighing (not necessarily the same one used for testing):
S/N 28680100902 0.1942 lb [N3]
- c. Weight of all ancillary items present during weighing but absent during testing [N2] + [N3]: 63.858 lb [N4]
3. Gross weight less ancillary items removed for testing [N1] – [N4]: 98.918 lb [N5]

Appendix D

Idaho National Laboratory

MMRTG MASS PROPERTIES TEST

Identifier: RPS/HS-OI-28220

Revision: 0

Effective Date: 04/28/09

Page: 130 of 167

4. Additional hardware attached during testing but not present when weighed -CCY-cable, bracket, fasteners, connector caps, and shorting plug (all items in their physically correct positions). The information in this section is supplied by the Design Agency.

- a. Serial numbers/or ID part numbers:

CCY-cable: 299 70400 902 331.54 g = 0.7309 lb
 Shorting plug: 28680100902 88.0903g = 0.1942 lb
 Fasteners + Bracket: MM 1300 85-001 Rev - 1 124.0842g = 0.2736 lb
 Aggregate weight (including fasteners and connector protective caps): 0.2736 lb

1.1987 lb [N6]

As-tested MMRTG weight [N5] + [N6]: 100.117 lb [N7]

The as-tested MMRTG weight has been determined and recorded for use in the CG-location calculations.

SME/TL:	<u>Byron W. Lee</u>	Date:	<u>05/01/09</u>
QAR:	<u>Edward Brock</u>	Date:	<u>5/1/09</u>
PWR Representative:	<u>Greg Hard</u>	Date:	<u>5/1/09</u>
DOE/NE-34 QAR:	<u>Jeffrey</u>	Date:	<u>5/1/09</u>

NOTE: The data in Lines 4(b) and 5, below, are not required to determine the as-tested weight and CG location in this procedure. Those steps may be completed by the design agency later.

- b. Aggregate center of gravity (CG) location:

X-direction datum: _____

CG offset from datum: _____ in.

Y-direction datum: _____

CG offset from datum: _____ in.

Z-direction datum: _____

CG offset from datum: _____ in.

Appendix D